

**STRUCTURAL FIRE PERFORMANCE OF BOLTED GLULAM
BEAM-TO-COLUMN CONCEALED CONNECTIONS**

by

Adam Petrycki

A thesis

submitted to the Faculty of Graduate Studies
in partial fulfilment of the requirements for the
Degree of Master of Science

in

Civil Engineering

Supervisor

Dr. O. Salem, Ph.D., P. Eng.

Associate Professor – Dept. of Civil Engineering

Lakehead University

Thunder Bay, Ontario

November 2017

© Adam Petrycki, 2017

Author's Declaration Page

I hereby declare that I am the sole author of this thesis. This is a true copy of the thesis, including any required final revisions, as accepted by my examiners. I understand that my thesis may be made electronically available to the public.

Abstract

Recent increased interest in the application of engineered-wood products, such as glued-laminated (glulam) timber and cross-laminated timber (CLT), in the Canadian building construction market has prompted amendments to be made to the building codes of several provinces. Until recently, the National Building Code of Canada (NBCC) restricted the use of wood as the primary building structural systems' material by limiting its application to buildings up to only four storeys. The current version of the National Building Code of Canada, NBCC 2015, increased the height restriction to six storeys. The experimental research study detailed in this thesis has been carried out to investigate the behaviour of concealed steel-glulam bolted connections subjected to monotonic loading at both ambient and elevated temperatures. At ambient temperature, sixteen full-size test assemblies were examined, representing a total of thirty-two tested beam-to-column glulam bolted connections. The connections in eight of the test assemblies were strengthened perpendicular to the wood grain with long self-tapping screws (STS). For both unstrengthened and strengthened connections, increasing the number of bolt rows, each row having two bolts, from two to three rows increased the connection's moment capacity with increments more than that obtained by increasing the bolt's end distance from four to five-times bolt diameters. STS-strengthened connections failed in a relatively ductile manner in contrast to the unstrengthened connections. Increasing the number of bolts to six bolts in three rows in strengthened connections reduced the occurrence of brittle failure modes compared to connections with four bolts in two rows. Critically, STS-strengthened connections experienced increased moment-resisting capacity between 1.3 and 2.4 folds. The results of the ambient tests were used to verify the calculated moment capacities of the test assemblies in order to determine the full-service design load of the connection exposed to CAN/ULC-S101 standard fire in the large-size fire testing furnace accommodated at Lakehead University's Fire Testing and Research Laboratory (LUFTRL). Outcomes of the fire resistance tests revealed that increasing the number of bolt rows from two to three, each of two bolts, increased the glulam beam-to-column connection's fire resistance time by greater increments than those achieved by increasing the bolt's end distance from four to five-times bolt diameter. Strengthened connections were found to have an increased fire resistance time compared to unstrengthened connections. Also, the STS strengthening increased the fire resistance time of the glulam connections by greater increments than those obtained by increasing the number of bolt rows and the bolt's end distance.

Acknowledgements

This thesis research project was funded using NSERC Discovery Grant and a Research Development Fund awarded by Lakehead University to Dr. Salem, as well as a partial in-kind contribution provided by Nordic Structures Inc. Any opinions, findings, conclusions or recommendations are those of the authors and do not necessarily reflect the views of the sponsoring parties.

The author would like to thank undergraduate students; B. Vasconcelos, C. Tomiuck, C. Hubbard, I. Grant, N. Lepoudre and J. Kruse for their assistance in preparing test specimens and in conducting a number of this research project's experiments. Special thanks go to Dr. M. Leitch from the Faculty of Natural Resources Management at Lakehead University for his kind assistance in preparing the slotted cuts in all the glulam beams tested in this project using his portable band-saw mill, and to Conrad Hagstrom and Rob Timoon for their help in the civil structures laboratory.

This thesis could not have been written without the support of Dr. Salem whose understanding and belief in seeing me succeed, helped me stay motivated. Thanks for letting me bend when I felt like breaking and for pushing me when I felt like bending but you knew I would not break. Thank you.

Without my partner, Alex Malachowski, and beautiful son Mikolaj Petrycki, I would have given up long ago and gone to live in a cabin in the woods, eating rabbits, beans and chips. Thank you for keeping me going.

Table of Contents

Abstract	iii
Acknowledgements	iv
List of Tables	ix
List of Equations	x
List of Figures	xi
Nomenclature	xvi
Chapter 1 Introduction	1
1.1 Background	1
1.2 Behaviour of Timber Structures at Ambient Temperature	2
1.3 Behaviour of Timber Structures at Elevated Temperatures	4
1.4 Scope and Objectives	4
Chapter 2 Literature Review and Background Research	6
2.1 Glulam Manufacturing and Grading	7
2.1.1 Finger Joints	9
2.1.2 Adhesives	10
2.1.3 Wood Species	10
2.1.4 Mechanical Properties	15
2.2 Background Research on Black Spruce Glulam	16
2.2.1 Mechanical Properties	17
2.2.2 Microscopic Study	27
2.3 Glulam Behaviour at Ambient Temperature	31

2.3.1 Testing at Ambient Temperature	32
2.4 Moment Connections	34
2.5 Glulam Behaviour at Elevated Temperatures	39
2.5.1 Testing at Elevated Temperatures	39
2.5.2 Fire Safety Engineering Design	51
2.6 Enhancing Structural Performance.....	54
2.6.1 Ambient Temperature Strengthening	54
2.6.2 Elevated Temperature Strengthening	55
2.7 Fire Protection Options	57
Chapter 3 Research Methodology	58
3.1 Experimental Program.....	59
3.1.1 Ambient Temperature Testing.....	59
3.1.2 Elevated Temperatures Testing	60
3.2 Data Collection.....	63
3.2.1 At Ambient Temperature.....	63
3.2.2 At Elevated Temperatures	64
3.3 Experimental Testing at Ambient Temperature	65
3.3.1 Materials	66
3.3.2 Test assembly Details and Fabrication Process.....	68
3.3.3 Test Setup and Procedure	72

3.4 Experimental Testing at Elevated Temperatures	73
3.4.1 Test Assembly Details and Fabrication Process.....	76
3.4.2 Elevated Temperature Test Setup and Procedure.....	77
Chapter 4 Ambient Temperature Experimental Testing Results.....	80
4.1 Effect of Bolt’s End Distance.....	82
4.2 Effect of Number of Bolts.....	86
4.3 Effect of STS Strengthening	89
4.4 Observed Failure Modes	93
Chapter 5 Fire Resistance Experimental Testing Results	101
5.1 Effect of Bolt’s End Distance.....	102
5.2 Effect of Number of Bolts.....	105
5.3 Effect of STS Strengthening	108
5.4 Time-temperature Curves.....	111
5.5 Observed Failure Modes	117
5.5.1 Unstrengthened Connections.....	117
5.5.2 Strengthened Connections	119
5.6 Charring Rate	124
Chapter 6 Conclusions and Recommendations for Future Work.....	125
6.1 At Ambient Temperature	125
6.2 At Elevated Temperatures.....	126
6.3 Recommendations for Future Work.....	128

References 130

List of Tables

Table 2.1	Nordic glulam design properties	16
Table 2.2	MOE and MOR test results against published values.....	22
Table 2.3	MOE and MOR results of interest.....	22
Table 2.4	Side hardness and compression test results against published values.....	25
Table 2.5	Compression test, samples of interest.....	25
Table 2.6	Density for 12% and oven-dry test results against published data.....	27
Table 3.1	Specified strengths and modulus of elasticity of glulam beams.....	66
Table 3.2	End distance and numbers of bolts used in test assemblies.....	72
Table 3.3	Fire resistance tests matrix.....	77
Table 4.1	Summary of results for ambient temperature testing.....	81
Table 5.1	Summary of fire resistance experimental testing results.....	102
Table 5.2	Charring rates of all tested connections.....	124

List of Equations

Equation 2.1	Time to failure formula	45
Equation 3.1	Sum of factored row shear resistance for joint.....	74
Equation 3.2	Factored row shear resistance of fasteners in a wood member i	74
Equation 3.3	Minimum row shear resistance of any row in the connection of member i	74
Equation 3.4	Four bolt, four-times bolt diameter end distance connection.....	75

List of Figures

Figure 2.1	Nordic Lam, glulam cross-section.....	6
Figure 2.2	Typical glulam manufacturing process.....	7
Figure 2.3	Finger joint: (A) feather, (B) male-female, (C) reverse.....	9
Figure 2.4	Mean MOR results for finger joint samples.....	10
Figure 2.5	Black spruce distribution.....	11
Figure 2.6	An upland black spruce forest.....	12
Figure 2.7	A black spruce bog in Lake County, MN.....	12
Figure 2.8	Black spruce sample sites.....	14
Figure 2.9	Black spruce sample sites	14
Figure 2.10	MOE and MOR Testing.....	17
Figure 2.11	Wood failure modes in static bending.....	18
Figure 2.12	Janka-ball hardness Test.....	19
Figure 2.13	Sample glue line orientation for groups A and B.....	20
Figure 2.14	All mechanically tested sample pieces.....	21
Figure 2.15	Group A: MOE/MOR test sticks.....	23
Figure 2.16	Group B: MOE/MOR test sticks.....	24
Figure 2.17	Group C: MOE/MOR test sticks.....	24
Figure 2.18	Compression stick samples from Groups A, B and C.....	26
Figure 2.19	Hitachi Su-70 Schottky Field Emission SEM.....	28
Figure 2.20	Gold-covered samples mounted on pegs.....	28
Figure 2.21	Glulam SEM cross section overview.....	29

Figure 2.22	Glulam SEM cross section with glue line details.....	30
Figure 2.23	Glulam SEM cross section with glue-wood line details.....	30
Figure 2.24	Glulam SEM cross section, glue-wood bond and interface details.....	31
Figure 2.25	Steel-timber connection (a) without and (b) with glued-in steel plate	35
Figure 2.26	Failure modes observed: (a) Complete yielding in flange; (b) bar failure and flange yielding; (c) bar failure.....	36
Figure 2.27	Potential application of studied joints	37
Figure 2.28	Test Group 6F (left) and 8F (right).....	40
Figure 2.29	Shear strength reduction with respect to change in temperature.....	41
Figure 2.30	Failure Modes: timber outside of bond line (left), failure between wood and bond line (center), and failure of glue cohesion (right).....	42
Figure 2.31	(a) Test specimen, finger joint (1), testing board (2), external lamellas (3) and insulating material (4). (b) Three-sided exposure of finger joint	43
Figure 2.32	Test furnace at Carleton University (above), Test set-up (below).....	44
Figure 2.33	FEM model used to validate previous experimental results: bolted connection (top), doweled connection (center), wood between dowels (bottom).....	46
Figure 2.34	Geometric configuration W-S-W.....	48
Figure 2.35	Comparing FEM and experimental temperatures of steel plate over time.....	48
Figure 2.36	FEM verifying temperature distribution observed during experimental trials.....	49
Figure 2.37	Increasing complexity of performance model with introduction of additional options.....	52
Figure 2.38	Three fire scenarios developed from for fire testing.....	53
Figure 2.39	Concealed moment-resisting connection strengthening methods.....	55
Figure 3.1	Lakehead University UTM with glulam sample being loaded	60

Figure 3.2	Lakehead University Fire Testing and Research Laboratory (LUFTRL).....	61
Figure 3.3	Large fire testing furnace accommodated at LUFTRL	61
Figure 3.4	Fire testing furnace and steel loading frame.....	62
Figure 3.5	Furnace bottom vents allowing the insertion of steel supports through the furnace floor.....	62
Figure 3.6	Human-Machine Interface (HMI) touch screen of furnace’s control panel.....	65
Figure 3.7	Dimensions of steel connector plates used for four both six bolt connections.....	69
Figure 3.8	Steel connector with four-times bolt diameter end distance, six bolts, and installation placement of STS strengthening.....	71
Figure 3.9	A general beam-to-column test assembly with six steel bolts in three rows.....	71
Figure 3.10	Test setup and dimensions of a general glulam beam-to-column test assembly...	73
Figure 3.11	General beam-to-column test assembly inside the furnace with thermocouples and instrumentation installed.....	77
Figure 3.12	Thermocouples layout, steel plate left, wood beam right.....	78
Figure 3.13	Beam-column test assembly with six bolts in three rows exposed to a standard fire.....	79
Figure 4.1	Moment-rotation relationships of test assemblies 1 and 3.....	83
Figure 4.2	Moment-rotation relationships of test assemblies 2 and 4.....	83
Figure 4.3	Moment-rotation relationships of test assemblies 1S and 3S.....	84
Figure 4.4	Moment-rotation relationships of test assemblies 2S and 4S.....	85
Figure 4.5	Moment-rotation relationships of test assemblies 1 and 2.....	87
Figure 4.6	Moment-rotation relationships of test assemblies 3 and 4.....	87
Figure 4.7	Moment-rotation relationships of test assemblies 1S and 2S.....	88
Figure 4.8	Moment-rotation relationships of test assemblies 3S and 4S.....	89

Figure 4.9	Moment-rotation relationships for assemblies in test groups 1 and 1S.....	91
Figure 4.10	Moment-rotation relationships for assemblies in test groups 2 and 2S.....	91
Figure 4.11	Moment-rotation relationships for assemblies in test groups 3 and 3S.....	92
Figure 4.12	Moment-rotation relationships for assemblies in test groups 4 and 4S.....	92
Figure 4.13	Typical observed glulam connection failure modes.....	93
Figure 4.14	Brittle failure mode in Test 1B	94
Figure 4.15	Brittle failure mode in Test 3B	95
Figure 4.16	Brittle failure mode in Test 2B.....	96
Figure 4.17	Brittle failure mode in Test 4B.....	96
Figure 4.18	Brittle failure modes in Test 1S and 3S.....	98
Figure 4.19	Brittle failure modes in Tests 2S and 4S.....	100
Figure 5.1	Elevated temperature time-rotation curves, Tests 1F and 3F.....	103
Figure 5.2	Elevated temperature time-rotation curves, Tests 2F and 4F.....	103
Figure 5.3	Elevated temperature time-rotation curves, Tests 1FS and 3FS.....	104
Figure 5.4	Elevated temperature time-rotation curves, Tests 2FS and 4FS.....	105
Figure 5.5	Elevated temperature time-rotation curves, Tests 1F and 2F.....	106
Figure 5.6	Elevated temperature time-rotation curves, Tests 3F and 4F.....	106
Figure 5.7	Elevated temperature time-rotation curves, Tests 1FS and 2FS.....	107
Figure 5.8	Elevated temperature time-rotation curves, Tests 3FS and 4FS.....	108
Figure 5.9	Elevated temperature time-rotation curves, Tests 1F and 1FS.....	109
Figure 5.10	Elevated temperature time-rotation curves, Tests 2F and 2FS.....	109
Figure 5.11	Elevated temperature time-rotation curves, Tests 3F and 3FS.....	110
Figure 5.12	Elevated temperature time-rotation curves, Tests 4F and 4FS.....	110

Figure 5.13	Actual time-temperature curves of all thermal measurements taken in fire resistance Tests 1F through 4F.....	113
Figure 5.14	Actual time-temperature curves of all thermal measurements taken in fire resistance Tests 1FS through 4FS.....	115
Figure 5.15	Hydrostatic behaviour on steel concealed plates.....	116
Figure 5.16	Glulam beam sections with the char layer removed, Test 1F.....	117
Figure 5.17	Row shear-out and splitting failure modes experienced in Test 1 and Test 1F assemblies at ambient, and elevated temperatures respectively.....	118
Figure 5.18	Strengthened connection with four bolts and 5D end distance, increased hole elongation, reduced brittle failure modes, complete combustion of almost all wood between the face and the first column of bolts.....	119
Figure 5.19	Strengthened connection with six bolts and 4D end distance, increased hole elongation, reduced brittle failure modes	120
Figure 5.20	Thermally degraded cross section of concealed slot cut.....	121
Figures 5.21	Residual wood sections of all strengthened connections after removal of charred layer.....	123

Nomenclature

Roman

t_f	time to failure in minutes
t_l	thickness of wood side member (mm)
d	fastener diameter (mm)
R_0	ultimate capacity at normal temperature
R_f	ultimate capacity at elevated temperature
n_r	number of fastener rows in wood connection
K_d	duration factor for wood design
K_{sf}	service factor for wood design
K_T	treatment factor for wood design
f_v	specified shear strength of wood
K_{ls}	area reduction factor for wood side members in connections
t	wood member side thickness
n_c	number of connectors in row in wood connections
a_{ci}	loaded end distance in wood connections
PR_{rT}	sum of factored row shear resistance for joint
PR_{ri}	total factored row shear resistance of fasteners in wood member i
L	moment arm between top and bottom rows of connectors
M_i	couple moment at connection

Greek

Φ_w	factor for brittle failure in wood
----------	------------------------------------

Chapter 1 Introduction

1.1 Background

Glued-laminated timber (glulam) members are structural mass timber members manufactured from smaller sections of wood known as laminations that are glued together to form a final product with a greater length, cross section and mechanical properties than those of the individual laminations. This manufacturing process is notably advantageous because it utilizes trees that were previously unusable as building materials due to their small size and/or low mechanical properties. Recent increased interest in the application of glulam as a primary building material in the Canadian construction market has prompted amendments to be made to the building codes of several provinces. Starting in 2009, 2013 and 2015, the provinces of British Columbia, Quebec and Ontario, respectively, made amendments to their provincial building codes facilitating the use of timber as the primary building system for construction of up to six storeys. Prior editions of the National Building Code of Canada (NBCC) restricted the use of wood as the primary building system by limiting its application to buildings with a maximum height of four storeys. The current version of the National Building Code of Canada, developed by the Canadian Commission on Building and Fire Codes (CCBFC), increased the height restriction to include buildings up to six storeys (Canadian Commission on Building and Fire Codes, 2015). As mid and high-rise buildings can be expected to undergo loading beyond that which can be carried by sawn timber, this presents an ideal application of large glulam structural components, as they are capable of sustaining considerable straining actions when compared to commercially available sawn lumber. Current technical documentations and guidelines in Canada provide little supporting framework to design timber beam-to-column connections especially in the context of moment resistance, a key requirement for buildings expected to resist heavy vertical and horizontal loads. In this context, the primary concern of using timber moment-resisting frames is their capability to resist moments without undergoing brittle failure modes. In terms of designing for elevated temperatures, there is no supporting framework for determining the fire resistance rating of moment-resisting connections, and extremely limited research on the behaviour of moment-resisting connections at elevated temperatures. The fire performance of wood structures is a primary concern of the public and regulatory bodies overseeing building codes, especially in the context of safety and designing buildings to withstand fire and needs to be addressed in order to further the use of wood as a

primary building system in mid and high-rise buildings. This thesis presents the results of an experimental study that evaluated the maximum moment capacity, stiffness and failure modes of glulam beam-to-column moment-resisting connections. The research also studied the effect of self-tapping screws (STS) strengthening on the glulam connections' moment capacity and stiffness at both normal and elevated temperatures. A comprehensive experimental testing program consisted of thirty-two full-size beam-to-column test connections subjected to static loading at normal temperature, and sixteen test connections at elevated temperature. Test variables investigated in this research project included bolt's end distance, number of bolt rows and STS strengthening, and the effect of these variables on the normal and elevated temperature performance of the bolted beam-to-column moment-resisting glulam-steel concealed connections.

1.2 Behaviour of Timber Structures at Ambient Temperature

At normal temperature, the primary concern of using timber in structural applications is the formation of brittle failure modes. This concern is important in the design of mid and high-rise timber buildings due to the increased vertical height carrying a wind load when compared to low-rise buildings, as well as the increased load expected during an earthquake. Heavy-timber connections that have been studied show that it is achievable to eliminate or at least reduce brittle failure modes when an adequate end distance to metal fasteners has been provided (Hampson et al., 2003). Specifically, metal connectors promote heavy timber connections to behave in a relatively ductile manner by providing a source of energy dissipation and designing the connection to fail in the steel instead of the wood (Murty et al., 2008; Andreolli et al., 2011). Brittle failure modes can be developed before the connection can experience any possible ductile behaviour (Humbert et al., 2014). An additional consideration for optimizing glulam for practical construction use, is its behaviour as a rotationally-restrained member in framed structures. Such studies have been conducted on the behaviour of heavy-timber connections used in frames subjected to axially-applied compressive and tensile loads (Gattesco, 2004). Very few research projects, such as the work done by (Quenneville, 2014; Xu et al., 2015), have been undertaken to study the behaviour and moment resistance of heavy-timber connections as part of a frame, especially in the context of frames lateral resistance (Xiong et al., 2016). Columns and beams made from glulam under axial or bending loads can be strengthened via a wide variety of strengthening option; both for the members and connections. One popular option for perpendicular-to-the grain

strengthening is the use of self-tapping screws (STS). This type of strengthening is also a very effective method to retrofit damaged glulam columns and beams with considerable longitudinal cracks and restore their axial capacity (Song et al., 2017). Self-tapping screws such as the SWG ASSY™ VG Plus are approved for the use as fasteners for structural timber connections when installed in compliance with the National Building Code according to the Canadian Construction Materials Centre (CCMC) (Canadian Construction Materials Centre, 2014). However, they have not been approved yet for use as strengthening in connections. The research to investigate the performance of strengthened concealed wood-steel-wood connections has focused on using carbon fibre-strengthened polymers (CFRP), steel plates and localized cross-laminated timber (CLT) sections strengthening around or inside the connection (Song et al., 2016). Limited research have been carried out on timber connections strengthened with self-tapping screws (Lam et al., 2008), and almost none on the effect of bolt's end distance in concealed T-stub connectors (Gehloff et al., 2010).

In general, brittle failure modes in timber connections can be avoided by selecting adequate bolt diameter and sufficient end distance. Currently, design guidelines in CSA-086-14 state that connections loaded in either tension or compression shall use a minimum end distance of five and four-times bolt diameter, respectively (Canadian Standards Association, 2014). However, no specifications are present with respect to moment-resisting connections. In Eurocode 5, a minimum end distance of seven-times bolt diameter is required for loaded end distance in bolted connections resisting a moment (European Committee for Standardization and British Standards Institution, 1995). However, previous edition of the CSA-086-14 also recommended an end distance of seven-times bolt diameter to avoid brittle failure modes in axially loaded connections. Since moment connections undergo both compression and tension concurrently, this thesis deliberately selected a reduced end distance of four-times bolt diameter in order to observe and compare the failure modes of STS-strengthened connections having either a reduced or code-specified minimum end distance of five-times bolt diameter.

1.3 Behaviour of Timber Structures at Elevated Temperatures

While most guidelines in North America for fire design are prescriptive, the general trend has been to adopt a performance-based methodology for structural fire design (Hadjisophocleous and Benichou, 1999). The trend has been supported by extensive testing of building materials as: individual components, sub-assemblies, assemblies and even entire structures. However, the focus of the fire safety field has predominantly been on steel and concrete components, not glulam or other timber products (Bisby et al., 2013). Specifically, there is no available literature on the fire behaviour of heavy-timber moment-resisting connections either as individual components or as part of a structural frame. Primarily, the focus has been on axially loaded connections (Racher et al., 2010), under compressive or tensile loading, parallel to the grain (Peng. et al., 2010) or perpendicular to the grain (Audebert et al., 2012). At elevated temperatures, the studies showed that timber connections either fail due to brittle failure modes in the wood, such as hole elongation, splitting, row shear-out, crushing or due to ductile failure modes caused by yielding in the steel components at elevated temperatures. Concealed steel components in wood-steel-wood (WSW) connections in these studies were observed to be partially insulated from the effects of fire by the wood section(s) when compared to steel-wood-steel (SWS) connections. Not only was the wood shown to act as an insulating layer around the steel components, but the concealed components benefited from a thermo-hydric transfer that occurs when water vapors escaping the wood condense on the steel components and increase the time increment at which the concealed steel components maintain a temperature of 100°C (Samake et al., 2014) before increasing due to the fire effect.

1.4 Scope and Objectives

The experimental research study detailed in this thesis has been carried out to investigate the behaviour of concealed steel-glulam bolted connections subjected to monotonic loading at both ambient and elevated temperatures. At ambient temperature, sixteen full-size test assemblies were examined, representing a total of thirty-two tested beam-to-column glulam bolted connections. The connections in eight of the test assemblies were strengthened perpendicular to the wood grain with long self-tapping screws (STS). The results of the ambient tests were used to verify the calculated moment capacities of the test assemblies so they all can be loaded to the full-service design load of the weakest connection assembly before being

exposed to CAN/ULC-S101 standard fire in the large-size fire testing furnace accommodated at Lakehead University's Fire Testing and Research Laboratory (LUFTRL).

A number of objectives of this research are listed below:

1. Design a wood-steel-wood (WSW) concealed steel moment-resisting connection;
2. Study the effects of two variables that are well documented in the Canadian Wood Design Handbook for axially-loaded connections: bolt's end distance and number of bolts;
3. Observe the failure modes of test specimens at ambient temperature, and adapt guidelines from the Canadian Wood Design Handbook to determine the design capacity of the connections;
4. Observe the effect of bolt's end distance and number of bolts on the behaviour of the connection at elevated temperatures.

Chapter 2 Literature Review and Background Research

Glued-laminated timber (glulam) is an engineered-wood product that is composed of pieces of dimensioned timber end jointed by being placed in horizontal layers and held together by an adhesive agent to form a final product with a greater length and cross-sectional dimensions, and with more desirable mechanical properties than the individual lamina. A typical cross section of Nordic Lam glulam is shown in Figure 2.1.

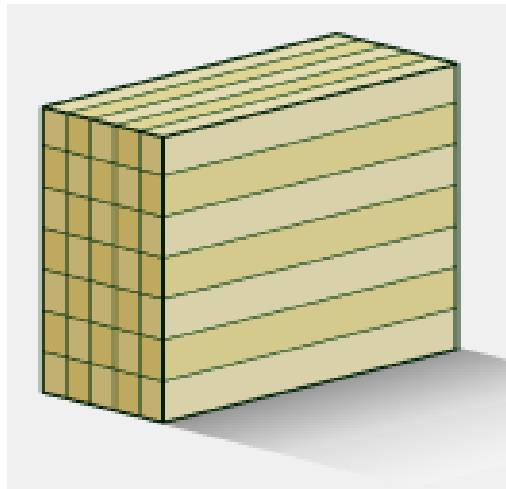


Figure 2.1 Nordic Lam, glulam cross-section (Adapted from Nordic, 2016).

Recent changes in provincial and national building codes and wood design codes stemming from a better understanding of glulam timber through experimental and analytical analyses have resulted in increase in its use as a reliable material for the construction of mid-rise residential or Industrial, Commercial, Institutional (ICI) buildings. While glulam has been used historically in many countries for centuries, research has only recently begun to focus on both the fire performance of glulam as well its ability to be utilized in moment-resisting timber framing systems. While there are almost no guidelines for the design of moment-resisting glulam connections, general design guidelines state that a 45 minute to 1.5hr fire resistance rating is required for glulam structural applications in Canada by the NBCC (CCBFC, 2015). These are two primary areas of concern that need to be investigated in order to successfully design safe mid- and high-rise buildings with mass timber as the primary component. Other areas of relevant research include the potential to strengthen heavy-timber moment-resisting connections to increase their

performance at both normal and elevated temperatures, as well as chemical and physical methods to mitigate the spread of fire and heat transfer into glulam structural members.

2.1 Glulam Manufacturing and Grading

The glued-laminated timber (glulam) manufacturing process is advantageous as it can utilize trees that were previously unusable as building materials due to their small size and/or low mechanical properties. According to a report for the Alberta Forestry Resort Institute, glulam is a value-added product of potential economic importance to the Canadian lumber and construction industries (Pirvu, 2006). Different species and grades of wood can be used in manufacturing glulam sections depending on design requirements or regional availability; however, the two most common species groups used in Canada are Douglas-Fir and Spruce-Pine (Canadian Wood Council, 2015). Lamina-stock (lamstock) is graded, trimmed and then their ends are cut to form finger joints. Afterwards, bonding agents are used to secure the lamina into the desired mass timber shape with the application of heat and pressure (Figure 2.2).

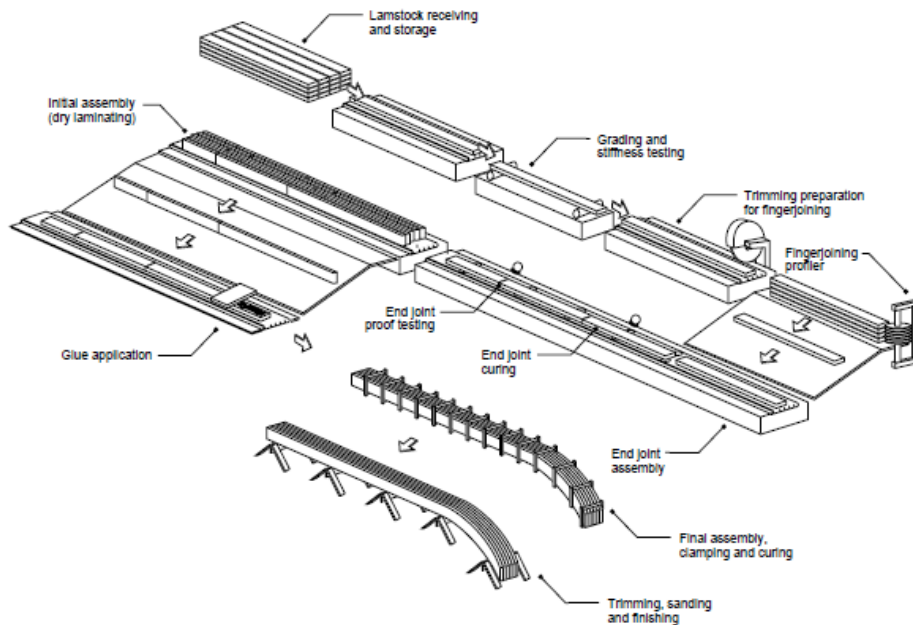


Figure 2.2 Typical glulam manufacturing process (Adapted from Canadian Wood Council, 2010).

This process meets the requirements outlined in the Canadian Wood Council's (CWC) 2015 Wood Design Manual, which defines glulam as a structural, manufactured, timber product composed of lamstock with one of four grades (B, B-F, D or C), end-jointed with finger joints, arranged in horizontal layers and glued together to form mass timber sections. Higher grade laminations, such as B and B-F, are placed in the top and bottom stress zones of beams and arches and lower-grade lamination are used closer to the neutral axis or in the beam's compression zones. All glulam sections manufactured in Canada are prepared at certified plants meeting the standards set out by the Canadian Standards Association in CSA-O122 and CSA-O177. Final products are grouped into one of three commercial species groups: Douglas-Fir-Larch, Hem-Fir and Spruce-Pine. Each product is also assigned a stress and appearance grade based on its respective application, and is provided with tabulated mechanical properties to be used during the structural design process.

According to the CWC (2015), glulam sections used as columns are given the same properties as that of a section composed of equivalently graded sawn lumber; however, the modulus of elasticity and rupture (critical for designing beams undergoing flexural bending) of glulam usually differ from that of sawn lumber of the same species. The grade of the wood used in glulam layup has been found to be consistently important in determining the mechanical properties of the final product. Extensive experimental and theoretical testing have been used to both verify the design properties published by the Canadian Wood Council and the Canadian Construction Materials Centre, and to validate reliable Finite Element models. Based on the results of an experimental and analytical study conducted at the University of British Columbia (Lam and Mohadevan, 2007), 48 Douglas-fir-larch glulam specimens with 24f-E/EX rating were examined to verify computer models developed to reflect modifications made to the design requirements with respect to the grades of the lamina layups. The outcomes of this study confirmed that the new modifications to the grades designation reduced the design modulus of elasticity of the members from 13,100 MPa to 12,800 MPa.

Similarly, the outcomes of another research study focused on confirming the validity of a finite element glulam beam computer simulation called the Ultimate Load Analysis of Glulam (ULAG), by using a series of experiments on glulam beams with different grade and layup arrangements of lamina from spruce-pine-fir trees harvested in northern Alberta, with

approximately 99% spruce species present (Timusk, 1997). In this study, glulam beams were tested on a Tinius Olsen 200-kip universal testing machine, and results were found to closely follow those predicted from the developed computer model. The average Modulus of Elasticity (MOE) for all samples was found to be approximately 9,990 MPa, and the average MOR was approximately 37.0 MPa for the Spruce-Pine-Fir glulam beams. This study also included experimentation on the finger joints in glulam sections, and the researcher found that generally, finger joints when tested specifically would fail at higher loads than solid wood samples, showing that defects in the wood usually cause the member to fail before finger joints or glue lines.

2.1.1 Finger Joints

Strength requirements for finger joints in Canada are governed by the National Lumber Grades Authority (NLGA) standards SPS 1-200 for structural lumber. In a Canadian research study (Bustos et al., 2003), tested the mechanical performance of three different finger joint configurations (Figure 2.3), that used black spruce lumber harvested from the Chibougamau region in Quebec.

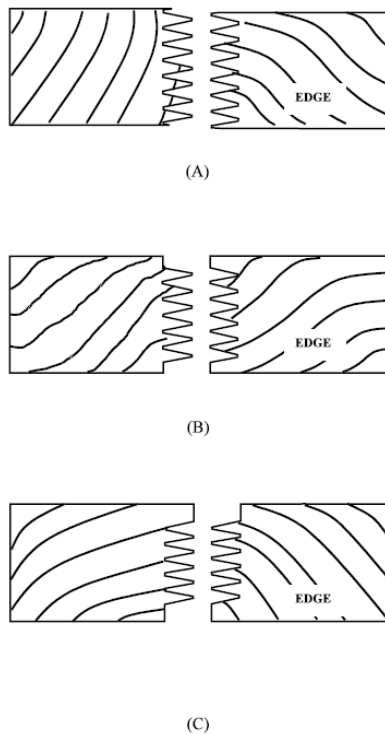


Figure 2.3 Finger joint: (A) feather, (B) male-female and (C) reverse (Adapted from Busto et al., 2003).

The outcomes of this study showed that all three joining methods met the requirements set out in the standard, with the feather joint having the best structural performance, reaching a mean MOR of almost 60.0 MPa, as seen in Figure 2.4. Also, it was observed that failure almost always occurred within the wood, with very little glue bond failure observed.

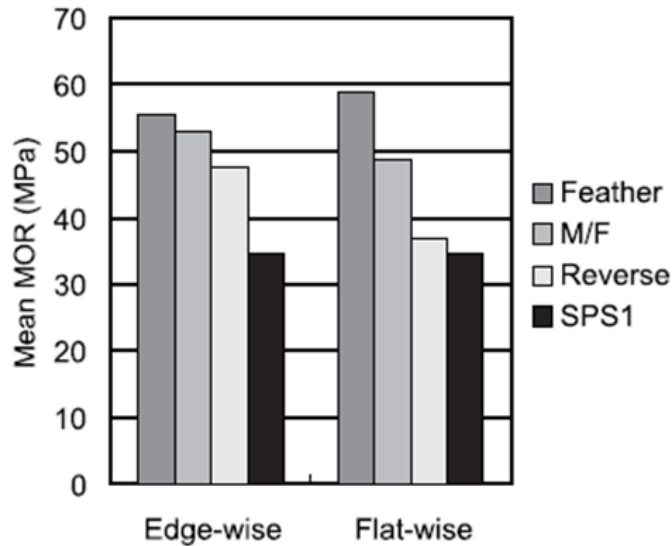


Figure 2.4 Mean MOR results for finger joint samples (Adapted from Busto et al., 2003).

2.1.2 Adhesives

The Polyurethane adhesives used in the manufacturing of Nordic glulam sections are outlined in a report by the National Research Council of Canada (NRCC, 2014): Ashland UX-100/WD3-A322 for finger-jointing and Ashland D3-A322/CX-47 for face and edge lamination. Polyurethane is a commonly used adhesive in the manufacturing of glulam, and is suitable for indoor and outdoor use. Other adhesives can be used in the manufacturing of glulam only if they meet the requirements set out in the Canadian Standards Authority document CAN/CSA-0122-06 for Structural glued-laminated timber.

2.1.3 Wood Species

Glulam members are commonly defined by their stress grade and species category: the stress grade describes the specified strengths of the material, and the species category defines what species of trees can be used individually or in combination to manufacture the glulam member. As

previously mentioned, the three categories of species combinations for glulam are: Douglas Fir-Larch (D. Fir-L), Hemlock-Fir (Hem-Fir) and Spruce-Pine-Fir. The species categories group together similar species of trees based on mechanical properties, physical characteristics and geographical considerations. The first two categories define species of trees located in the British Columbia and Rocky Mountain regions of Canada, with Hem-Fir having very limited local availability. The species defined in the S-P-F category can be found across the entire Canadian geographic region, and encompass a wide variety of spruce, pine and fir species, CWC (2015). The D. Fir-L and S-P-F species combinations are the two groups most commonly used by fabricators of glulam members. Glulam beam and column sections from Nordic Structures (Nordic Structures, 2015) are made from 90% black spruce (*Picea mariana*), this species is found only in North America and it has an extensive range across Canada and the northernmost regions of the United States, as seen in Figure 2.5 (Fryer, 2014).



Figure 2.5 Black spruce distribution (1971 USDA), Forest Service (Adapted from Fryer, 2014).

Black spruce is found growing in a variety of soil types, in both wet swampy areas and comparatively drier uplands. It grows well, and tends to dominate poorly drained sites that are underlain by permafrost; characteristic of the boreal forest in Canada (Fryer, 2014). Black spruce will mature differently depending on conditions. As species grown in swampy and cold climates, they tend to grow at a much slower pace and produce a stragglier looking tree compared to those in dryer upland conditions (Figures 2.6 and 2.7). Black spruce's structure and chemical properties promote easy ignition and forest fires, which play an important role in the species regeneration process (Fryer, 2014).



Figure 2.6 An upland black spruce forest (Photo by Steve Hillebrand, U.S. Fish and Wildlife Service - Adapted from Fryer, 2014).



Figure 2.7 A black spruce bog in Lake County, MN. (Photo by Jason J. Husveth - Adapted from Fryer, 2014).

Black spruce is widely distributed in both wet and dry climates, with some stands regenerated by fire, and some others by planting after previous logging (clear or selective cuts). It can be expected that there will be a range found within the species physical and mechanical properties dependent on harvest location. Additionally, the smaller diameter trees found growing in swampy areas may have been overlooked for property testing in the past due to the previously limited options for application of such small trees in the production of structural wood components.

Tong et al. (2009) studied the physical and mechanical properties of black spruce from both un-thinned and pre-commercially thinned farms near Beardmore, Ontario, and compared the values to both natural stands in both Ontario and those found in Quebec. In general, it was found that thinning had reduced desirable properties of the wood species, as all plantation trees were generally found to have lower values than those harvested from older natural stands in the eastern parts of Canada.

The Chibougamau-Natashquan region, approximately 400 km north of Quebec City, is the location of the manufacturing plant of Chantiers Chibougamau, which is the company responsible for harvesting the black spruce and providing Nordic Structures with timber supplies for their engineered-wood products. In a study on the black spruce harvested from this region, it has been found that natural stands regenerated through fire yielded trees with more preferable grades of wood when compared to trees harvested from previously clear or partially-cut plantations. The study showed that the resulting MOR and MOE for partial cut origin (CV1), clear cut origin (CV2 and CV3) and fire origin (FV2) stands of black spruce and compared to previously published values for natural stands, showed that the MOE and MOR for the FV2 and CV3 stands was as high or higher (Spatacean, 2008). It is worth mentioning that many of the current stands in Northern Ontario have fire or clear-cut origins.

A relatively recent research study conducted by Torquato et al. (2014), focused on comparing the mechanical properties of black spruce from natural stands that had either undergone a fire in the last 150 years or had not. Stands were located in the Abitibi, Lack St-Jean and North Shore regions of Quebec (Figure 2.8). In general, it was found that trees had more desirable mechanical properties when sampled from stands that had undergone a fire regeneration within 150 years and had regular tree growth.

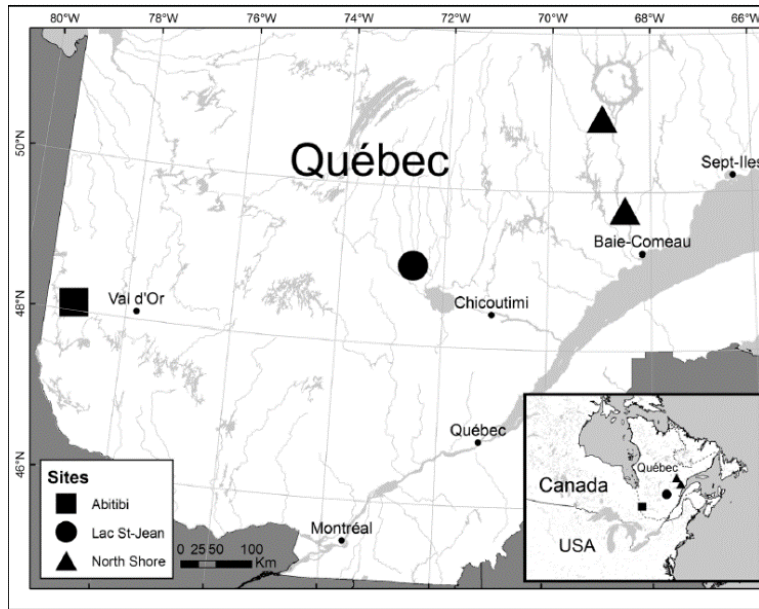


Figure 2.8 Black spruce sample sites (Adapted from Torquato et al., 2014).

This study was complemented by work published by Rossi et al. (2015) that focused on studying the growth and resulting physical and mechanical properties of black spruce at increasing latitudes in Quebec, like the five sample sites shown in Figure 2.9.

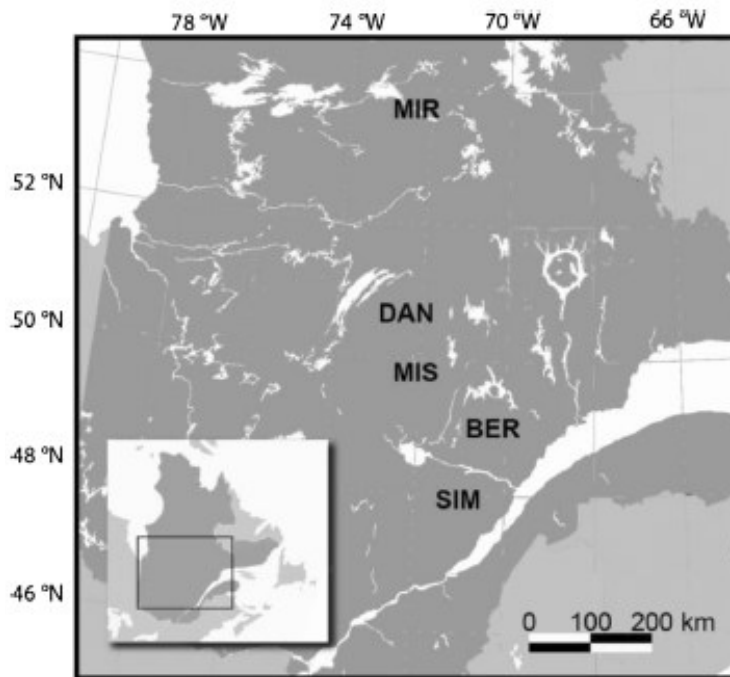


Figure 2.9 Black spruce sample sites (Adapted from Rossi et al., 2015).

The study showed that there was no beneficial increase in mechanical properties at far northern latitudes at the MIR site when compared to those grown at the other sample sites. Samples collected at approximately the same latitude as those used in Nordic's glulam members (Dan and MIS sites) had higher density and MOE values than those grown at any other latitudes, suggesting the black spruce from this region is uniquely dense and stiff when compared to other parts of Quebec and Canada in general, Rossi et al. (2015)

Currently, black spruce sees widespread commercial use for making high quality pulp and paper products and as dimensioned lumber products for light and medium construction with a variety of grades and sizes available in the spruce-pine-fir category. Current commercial applications are relatively limited due to the slow growth rate of black spruce, with many current trees coming from areas that have previously seen widespread clear or partial commercial cutting, causing a reduction in the availability and quality of larger sawn members for construction purposes. A growing value-added application of these small diameter and dense black spruce trees is in the manufacturing of composite wood construction products, especially glulam members (Pirvu, 2006). Nordic's glulam beams are made from black spruce harvested when they are between 80 and 120 years in age and can be made into 25 mm by 50 mm in rectangular strips to be used in the glulam beam and column sections. This method adds further value to the black spruce trees, as tree tops and side cuts can be used to create lamina for beams and columns (Les Chantiers Chibougamau Ltée, 2016). However, the greatest value-added benefit of using black spruce in glulam sections is that the laminating process allows for the creation of a controlled-construction product that has stronger mechanical and engineering properties than their original components, allowing for the manufacturing of both curved and straight members of very large depths and lengths to be used in the construction of mid-rise residential buildings and industrial, commercial and institutional (ICI) buildings.

2.1.4 Mechanical Properties

Using the results of experimental studies and validated computer models, the Canadian Wood Council has tabulated mechanical properties for the different glulam grades and species to be used when designing load-bearing glulam members in buildings and structures. The design values from the CWC 2015 Wood Design Handbook however, did not include the 24F-E/EX grade of spruce glulam manufactured by Nordic. The specified strength and design properties for the

Nordic Lam product are provided by Nordic structures in Technical Note S01 (2015) and presented in Table 2.1 herein. These values were recently re-evaluated and approved by the Canadian Construction Materials Council in 2015, the report states that the material properties were developed through a large sample group that included: 102 tension tests on various lamina, moment capacity on 60 beams each of 20F and 24F grades with 300 mm depth and 15 with a 600-mm depth, and compression capacity on 30 short columns, each of 89 mm x 89 mm and 140 mm x 140 mm.

Table 2.1 Nordic glulam design properties (Adapted from Nordic Structures, 2015).

Product	Nordic Lam
Applications	Beams and Columns
Appearance Grade	Architectural
Stress Grade	24F-ES/NPG
Key Design Properties	(MPa)
Comp. parallel to grain	33.0
Comp. perp. to grain	7.5
Tension parallel to grain	20.4
Modulus of elasticity	13100
Longitudinal Shear	2.5
Bending Moment	30.7

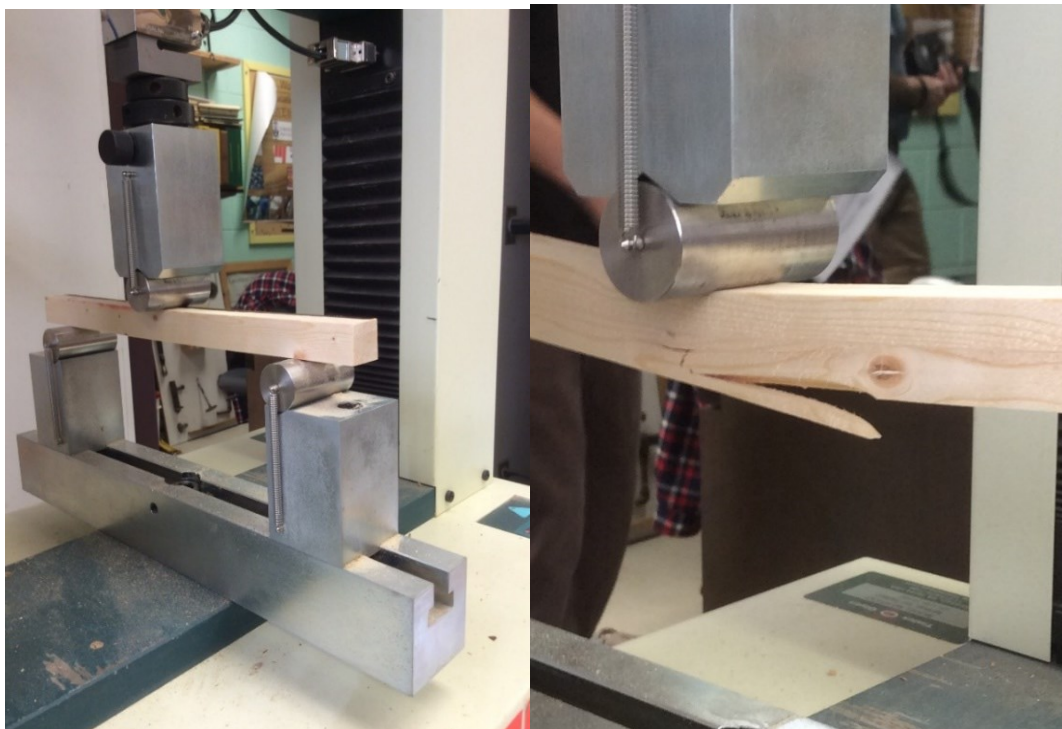
2.2 Background Research on Black Spruce Glulam

The glulam sections used in the experiments of this thesis's research project had an architectural appearance grade and a 24F-ES stress grade, and were composed of 90% black spruce and manufactured by Nordic. To gain a better understanding of this material, a limited number of samples were tested to observe the glulam mechanical and physical properties. Tests were conducted according to ASTM-143-14 specifications. In addition, microscopic imagery was taken to observe the bond between laminations at a highly-detailed level. Samples were taken from a beam section that had been previously loaded for structural testing; however, an undamaged

section of the beam near the support was cut off to provide the wood sections required for test samples.

2.2.1 Mechanical Properties

MOE and MOR tests were conducted as three-point flexural bending using the Tinius Olson H10KT testing machine (Figure 2.10(a)). The MOE is a measurement of the stress-strain relationship within a material and describes the stiffness of a material with respect to the allowable amount of elastic deformation before full recovery is no longer possible. The MOR is measurement of the maximum bending capacity of a sample before failure occurs. The sample was loaded until the machine detected a failure meeting the definitions of the test, an example failure is shown in Figure 2.10(b). These values are important in the design of both glulam products and structures. The test was conducted in accordance with ASTM-143-14 testing standards, except for the orientation of the sticks growth rings, which was limited due to the orientation of growth rings within the glulam product. Typical break patterns experienced by wood undergoing bending are showcased in Figure 2.11.



(a) Three-point flexural bending test.

(b) Computer registered sample failure.

Figure 2.10 MOE and MOR Testing.

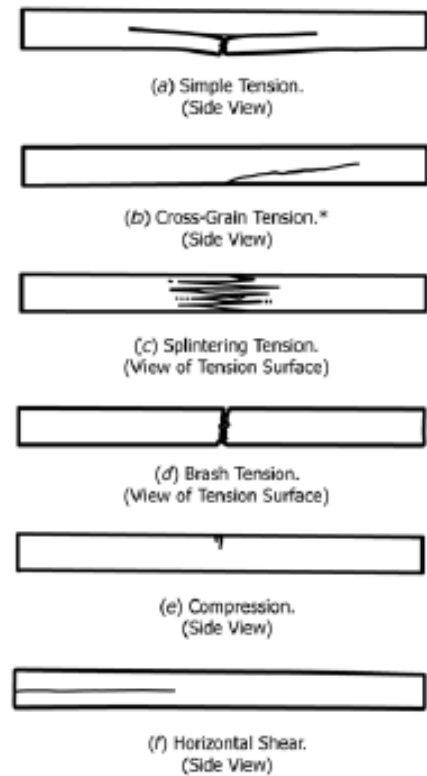


Figure 2.11 Wood failure modes in static bending (Adapted from ASTM, 2016).

The hardness test, conducted using a Janka-ball with an 11.3 mm diameter, shown in Figure 2.12, measured a samples side hardness by determining the load required to push the ball into the wood by one half of its diameter. This is an important quality in the selection of materials resistant to damage from blunt force, a desirable quality in flooring or other wood end use products. Test was conducted according to ASTM-D143-14 standards on a Tinius Olsen Universal Testing Machine H50KT; however, no buffer was used as the samples were adequately thick. Ten locations were tested, approximately 25 mm from the edge and each other, the location of the tests coincided with the glue lines between lamina, as shown in Figure 2.12. The density and moisture content of the wood were determined according to Method B of the ASTM-D4442-15; where samples were weighed then submerged in a water bath on a tared scale to determine the volume of the samples. This process is used to find both the density, given by the mass of the wood over its volume, and the moisture content of the samples.

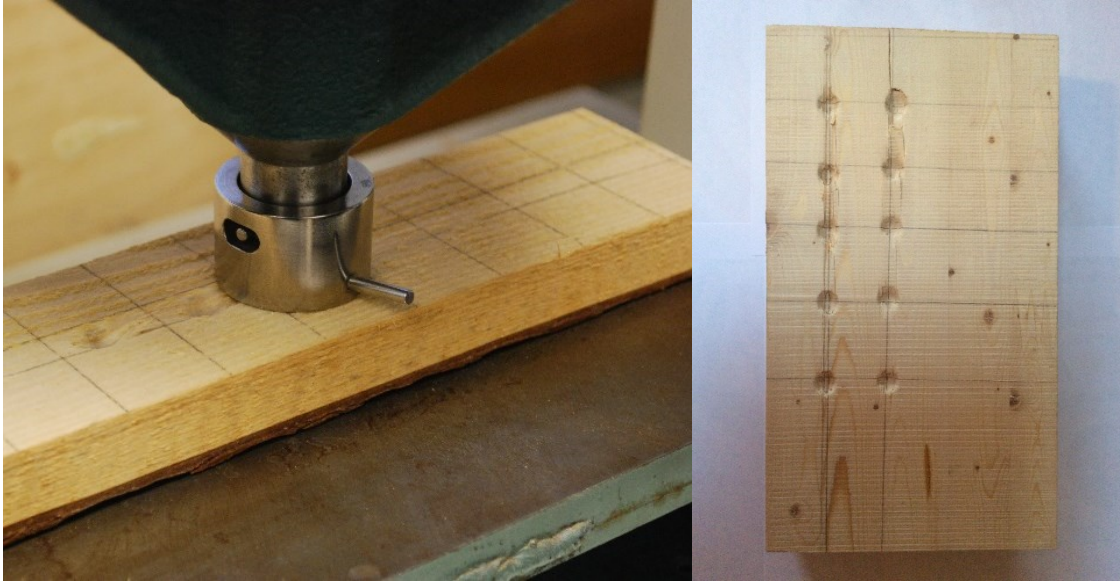
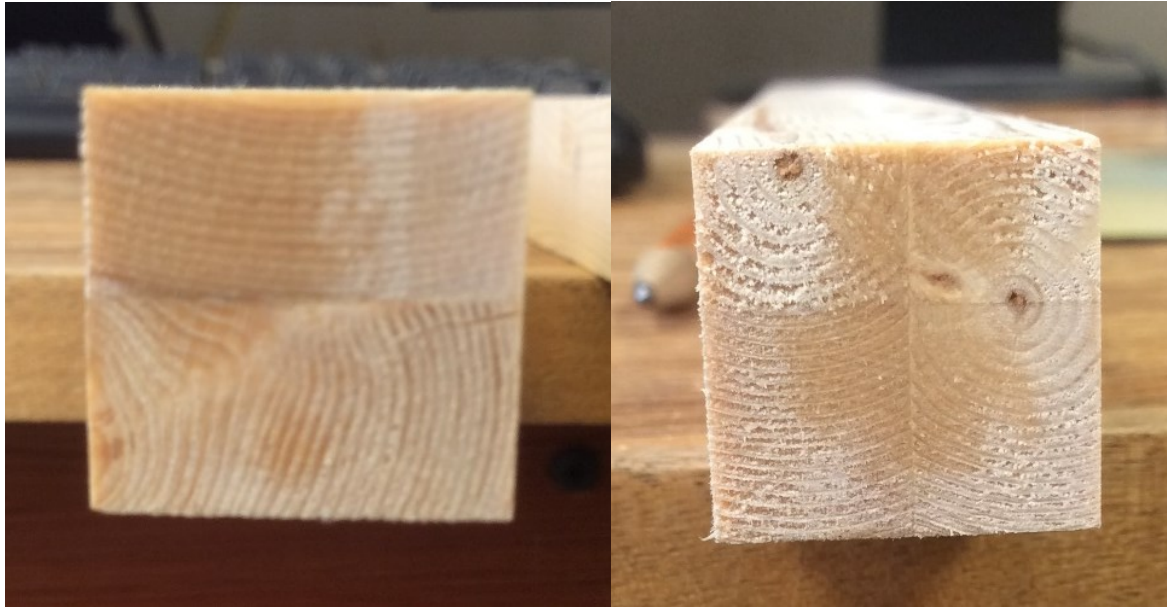


Figure 2.12 Janka-ball hardness test (Courtesy of Dr. Leitch, 2015).

The final property test was the compression resistance parallel to the grain. Compression loading parallel to the grain occurs in both axially-loaded columns, as well as the top fibers of beams undergoing bending. Samples measuring 20 mm x 20 mm x 60 mm were placed into the Tinius Olsen Universal Testing Machine H50KT so that the loading apparatus surfaces were perpendicular to the grain. Each sample was then loaded at a constant rate until failure occurs, and the measurement providing a guideline to the structural integrity of the sample when loaded in compression parallel to the grain. The raw wood source for the test samples was a previously-tested 24F-ES stress grade black spruce glulam beam of 137 mm width and 318 mm depth. However, the section that was exposed to the least amount of bending stress near the beam support was cut and transported to Lakehead University's Wood Sciences Laboratory. One cut was made approximately fifty millimetres from the side of the beam along its depth to produce a piece for the side hardness test. However, this piece was not conditioned properly, as it had a moisture content of about 8% at time of testing. This reflects the in-site moisture content of the glulam supply, which had been left in an unheated indoor area over the winter. The remainder of the sample was cut to provide samples measuring approximately 355 ± 1 mm in length and 20 ± 1 mm in thickness and width.

Thirty pieces were cut to provide the following three groups of 10 samples each: (A) vertical glue line located equally between two laminates, (B) horizontal glue line at the neutral

axis between two laminates and (C) clear spruce pieces without any glue line (Figure 2.13). Samples were placed in a conditioning chamber at 20°C and 65% relative humidity for a week, in order to bring their moisture content to 12% as required by ASTM-D4933-10.



a.) Group A.

b.) Group B.

Figure 2.13 Sample glue line orientation for groups A and B.

Once the samples were properly conditioned, they were removed and tested for their MOE and MOR. The resulting pieces were then used to provide sample pieces for the remaining tests. Using templates, two separate pieces cut from the test stick, a small piece for the density and moisture content test and a larger piece for the compression test. All mechanically tested wood sample pieces are shown in Figure 2.14. Only Group C has its density cubes displayed in the center, with Group A on the left and Group B on the right.



Figure 2.14 All mechanically tested sample pieces.

All tests were conducted on equipment that was networked to a software suite that tracked all test data and calculated the samples' mechanical and physical properties from the resulting inputs. These values were used to determine the mean values for all properties as well as the coefficient of variation (CV), where low CV values showed that results are relatively constant and therefore predictable.

The MOE and MOR values for the glulam tests are summarized below in Table 2.2, Group A had higher results for both MOE and MOR tests than Group B. Also, both Groups A and B outperformed the clear glulam sample in the MOE test having almost double the value; however, the bending capacity of all three samples groups was relatively similar. Values for Group C were slightly higher than those published by Jessome (2000), suggesting that the spruce trees used in this glulam are stronger than those historically harvested and tested. Glulam of Groups A and B results for MOE and MOR were lower than the design values supplied by Nordic. Groups A and B had different break patterns, as Group A samples would often see a tensile break across the bottom of only one lamina (half the width), while Group B samples' failure was characterized by a break across the entire singular lamina along the bottom width. Several MOE values in Group B were much lower than the others, as those values were for samples with very large defects and exclusively failed along the horizontal glue line. Table 2.3 contains specific tests' results from Groups A, B and C that were either the highest or lowest in their group for MOE, MOR, or both.

The pieces of interest are showcased in Figures 2.15, 2.16 and 2.17 for Groups A, B and C, respectively. Generally, it was noted that failures for all groups occurred around defects in the wood, including finger joints, and pieces that failed at lower values often had a greater amount of wood defects present.

Table 2.2 MOE and MOR test results against published values.

Grouping	MOE (MPa)				Species	MOR (MPa)			
	Tested		Published			Tested		Published	
	Value	CV	Value	CV		Value	CV	Value	CV
Glulam All	16,171.63	28.3%	NA	NA	Glulam All	89.70	14.3%	NA	NA
Glulam A	19,990.90	9.6%	13,000	NA	Glulam A	95.30	10.6%	30.7	NA
Glulam B	17,566.20	20.7%	13,000	NA	Glulam B	88.00	19.8%	30.7	NA
Glulam C	10,957.80	12.7%	10,400	22.3%	Glulam C	85.80	9.8%	78.3	13.3%

Table 2.3 MOE and MOR results of interest.

Sample Group	Test #	Max Load (N)	Thickness (mm)	Width (mm)	MOE (MPa)	MOR (MPa)
A	1	1,810	20.6	20.4	23,071	102.0
A	4	2,060	20.8	20.56	21,224	111.0
A	8	1,552	19.21	20.9	17,396	79.0
A	9	1,571	21.09	20.83	22,598	106.0
B	1	1,869	20.45	20.35	15,190	70.0
B	2	1,682	20.49	20.14	11,504	72.0
B	3	1,856	20.56	20.47	20,121	112.0
B	5	1,599	20.54	20.31	17,194	65.0
B	9	1,847	21.18	19.28	13,009	75.0
B	10	1,293	21.14	19.66	22,818	108.0
C	1	1,747	21.5	20.6	8,906	67.0
C	5	1,647	17.9	20.79	12,949	91.0
C	6	2430	22.09	20.41	9659	90.0
C	9	1926	20.14	18.4	13153	95.0

From Figure 2.15, it can be seen that even with the presence of finger joints and other defects, Group A samples were stiffer than those in Group B. Test 8A had much lower MOE and MOR values than other pieces in the group, as the break can be seen to have occurred across the finger joint and near a defect that would have caused stress concentrations. Lower values were seen in Group B followed by Group A for MOE and MOR. This could be due to the orientation of the glue line, with a vertical glue bind acting more similar to built up lumber. While the orientation of the glue line in Group B results in the bottom lamina having the same bending capacity as clear lumber (Figure 2.16). Sample B5 had a large knot at the middle in bottom lamina undergoing bending, where failure of this sample occurred along the glue bond line as all forces were transferred to that plane due to the presence of defects in the wood. This same failure mode was observed in samples B2 and B9 as well. Samples in Group C failed across the entire bottom section similar to the failure mode seen in Group B (Figure 2.16).



Figure 2.15 Group A: MOE/MOR test sticks (N.B. A8 below average results).



Figure 2.16 Group B: MOE/MOR test sticks.

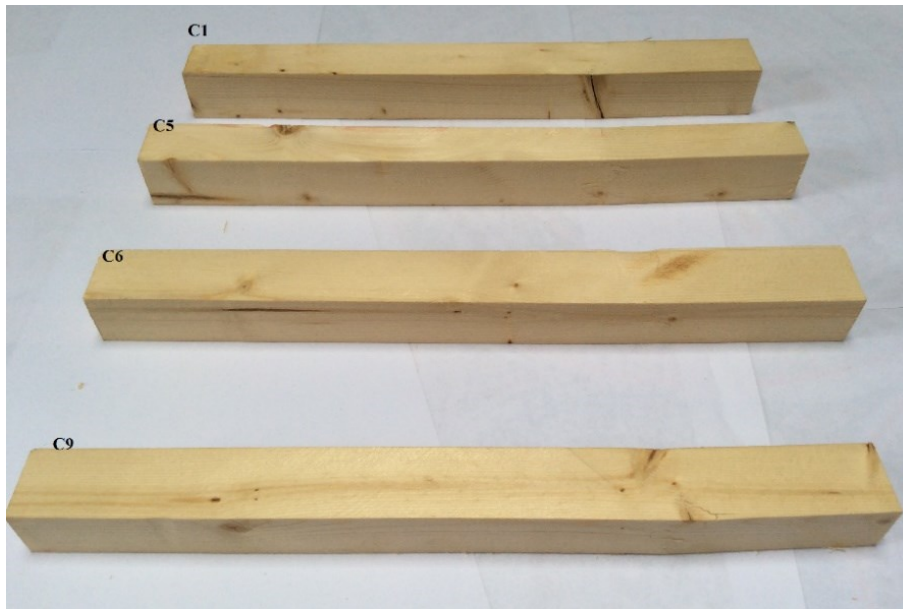


Figure 2.17 Group C MOE/MOR test sticks.

The side hardness results of the tested sample were found to be higher than those published for black spruce (Jessome, 2000), and was close to the published values for the end hardness, Table 2.4. It can be hypothesised that the slower growing and denser Quebec black spruce used in the Nordic glulam has a greater resistance to impact damage. The compression resistance parallel to the grain, highlighted in Table 2.5, for Group C was slightly higher than the published results,

Jessome (2000), and Groups A and B had much higher results than those published by Nordic (2015). Compression samples that were either the highest or lowest in their groups collected in Table 2.6. The results show that generally all three groups had similar compression resistance to loading parallel to the grain. Failures in these samples occurred quite frequently along the glue line in the presence of a defect, or around a defect causing the wood to fail before the glue.

Table 2.4 Side hardness and compression test results against published values.

	Hardness - Side (N)					Compression - Max Stress (MPa)			
	Tested		Published			Tested		Published	
Group	Value	CV	Value	CV	Group	Value	CV	Value	CV
All	3,667	13.7%	NA	NA	All	48.08	9.4%	NA	NA
A	NA	NA	NA	NA	A	48.57	5.3%	33.0	NA
B	NA	NA	NA	NA	B	49.68	11.1%	33.0	NA
C	NA	NA	2,430	16.4%	C	46.00	9.8%	41.5	14.9%

Table 2.5 Compression test, samples of interest.

Grouping	Replicate	Max Load (N)	Width (mm)	Thickness (mm)	Height (mm)	Max Stress (MPa)
A	1	20,900	20	20	60	52.2
A	9	17,680	20	20	60	44.2
B	4	17,540	20	20	60	43.8
B	5	17,860	20	20	60	44.6
B	8	22,800	20	20	60	56.9
B	9	22,600	20	20	60	56.6
B	10	20,400	20	20	60	50.9
C	9	15,880	20	20	60	39.7
C	6	20,700	20	20	60	51.7

High and low compression samples are shown in Figure 2.18 to illustrate the relationship between wood features, failure mode and ultimate capacity.



Figure 2.18 Compression stick samples from Groups A, B and C.

The increased density gained by slow-growing swampy-grown black spruce can clearly be seen in the results for 12% and oven-dry moisture conditions, as shown in Table 2.6. All glulam groups had a higher density than the published values for natural spruce by a considerable amount (Jessome, 2000). Also, the density for glulam Groups A and B was found to be close to that published by Nordic.

Table 2.6 Density for 12% and oven-dry test results against published data.

Sample Series	Density -12% (kg/m ³)				Sample Series	Density – Oven Dry (kg/m ³)			
	Tested		Published			Tested		Published	
Glulam All	613.06	8.7%	NA	NA	Glulam All	541.90	8.7%	NA	NA
Glulam A	591.75	10.7%	560	NA	Glulam A	523.07	10.7%	NA	NA
Glulam B	606.53	9.6%	560	NA	Glulam B	536.13	9.6%	NA	NA
Glulam C	640.90	2.8%	480	NA	Glulam C	566.51	2.8%	445.00	13.3%

2.2.2 Microscopic Study

It was also needed to visually capture the strong interface between wood and glue that provide glulam timber samples with an increased stiffness response matrix in comparison to clear lumber members of the same species. A microscopic study was undertaken to capture the bond between wood lamina, and to examine the resulting combined glue-wood interface. The Scanning Electron Microscope (SEM) provides high resolution images by using electrons to bombard a sample and interpret the measured results into a digital image. The SEM used in this study is a Hitachi Su-70 Schottky Field Emission that is accommodated at Lakehead University Instrumentation Laboratory (LUIL), as seen in Figure 2.19. Small 1.0 mm cubes were cut from the pieces that were used for sectioning with the microtome. The electrical nature of this type of microscope requires biological samples to be coated in gold before being placed in the machine, gold-sputtered sample sections mounted on pegs are shown in Figure 2.20.



Figure 2.19 Hitachi Su-70 Schottky Field Emission SEM (Courtesy of Dr. Leitch, 2016).



Figure 2.20 Gold-covered samples mounted on pegs (Courtesy of Dr. Leitch, 2016).

Only samples for radial and tangential view were prepared due to the orientation of the growth rings between the lamina with respect to the wood-glue interface. Both cross and radial sectional views are present on one peg that is then loaded into the SEM's chamber, which is then depressurized into a vacuum. Afterwards, the resulting images are displayed on the computer, and the view can be moved in real time. Detailed features seen in the cross-sectional plane from the SEM imagery include resin canals, early wood and latewood tracheid (the latewood cells being particular small and dense), and the wood-glue-wood interface between laminates, as seen in Figure 2.21.

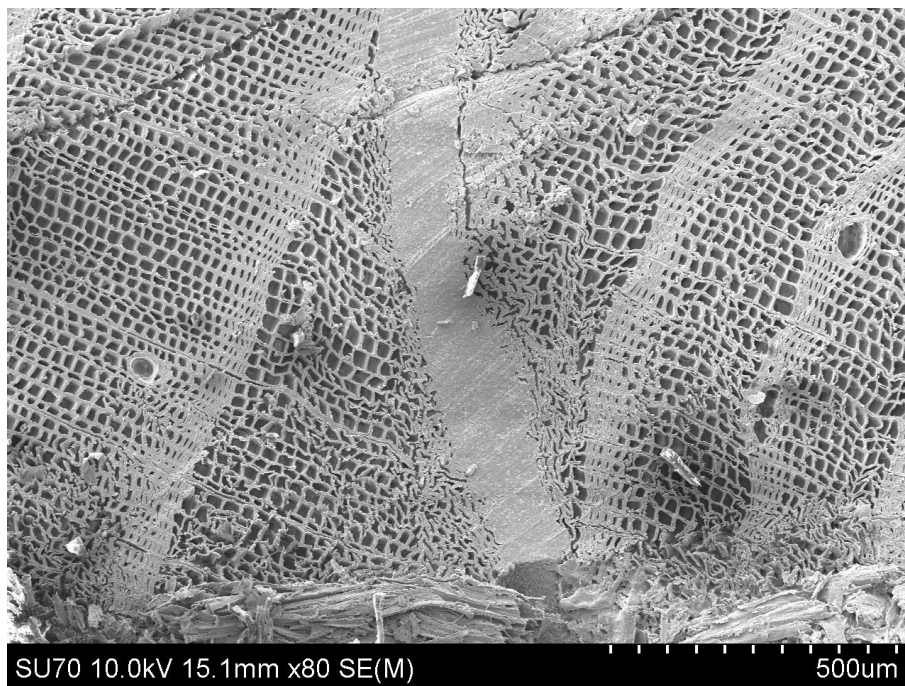


Figure 2.21 Glulam SEM cross section overview.

The SEM microscopy showed that many of the longitudinal tracheid are crushed and broken during the lamination process as can be seen in the cell walls near the glue line and within the glue shown in Figures 2.22 and 2.23.

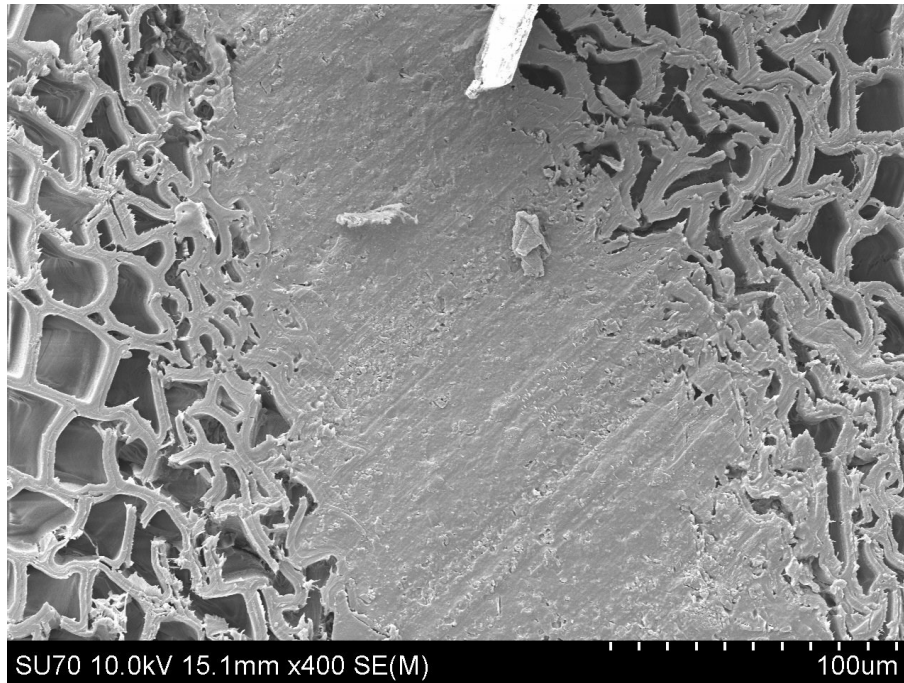


Figure 2.22 Glulam SEM cross section with glue line details.

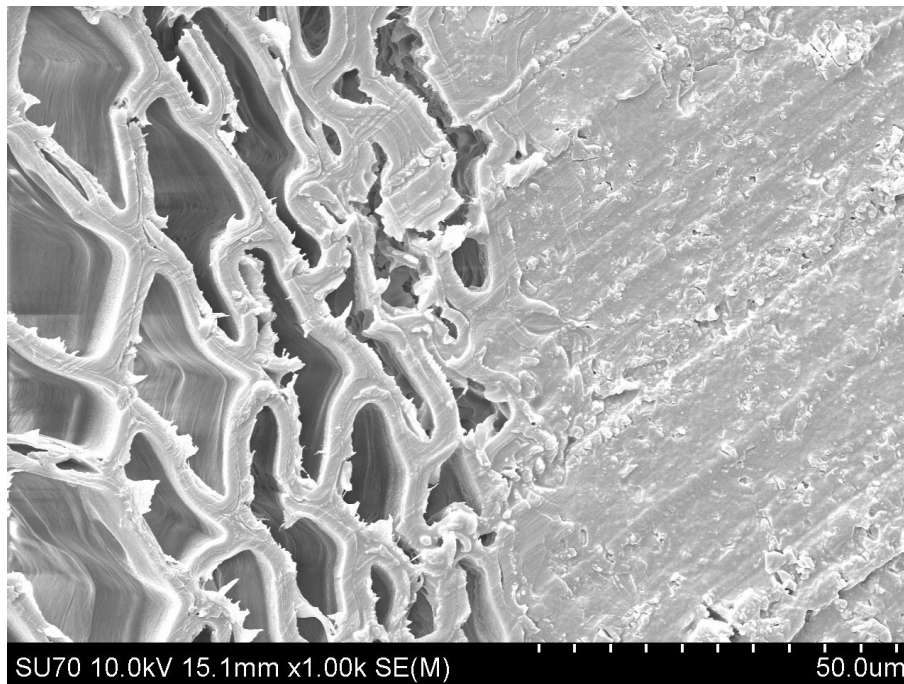


Figure 2.23 Glulam SEM cross section with glue-wood line details.

The completeness of the wood-glue bond can be seen in Figure 2.24, where the glue is shown to seamlessly be bonded along the longitudinal tracheid cell walls both between the laminates and away from the glue line.



Figure 2.24 Glulam SEM cross section, glue-wood bond and interface details.

2.3 Glulam Behaviour at Ambient Temperature

The past few decades in Canada have generally seen limited application of large glulam members in the construction of industrial, commercial and institutional buildings. In recent years, the application of glulam as a building material in the Canadian construction market has increased due to new changes in provincial building codes. The current versions of several provincial codes are now allowing the application of timber as the primary building component of mid- and high-rise buildings, which is ideal for glulam structural components that are capable of resisting heavy loads and manufactured to have desired large cross-sectional dimensions. Presently, however, the technical documentations and guidelines in Canada provide no supporting framework to design an adequate moment-resisting timber connection. This is a critical area of research if buildings are to be designed and constructed to resist lateral wind loads and earthquake loads with limited lateral

bracing systems in place. As moment-resisting connections can be expected to experience both compressive and tensile forces, the most relevant recommendations from the current Canadian Wood Design Handbook state that connections loaded axially in either tension or compression use minimum end distances of five and four-times bolt diameter, respectively (Canadian Wood Council, 2015).

2.3.1 Testing at Ambient Temperature

Historically, the primary focus on most glulam experiments has been to determine the capacity of structural members to resist various forces, in particular the behaviour of axially-loaded connections. The documentation and design guidelines provided by the Canadian Wood Council for these simple connection types have been extensively researched and newer experiments refine, re-evaluate and expand on the properties and clauses related to the design of these connections.

Mohammad and Quenneville (2001) verified design clauses that assumed the primary failure mode of connections was ductile; however, their work showed that even when minimum requirements are met, connections could still undergo brittle failure as the primary failure mode. Ultimately, their work introduced subsequent reductions in the calculation of the capacity of wood connections. The effects of number of bolts, size of bolt, end distance and the spacing of bolt columns and rows were observed on wood-steel-wood (WSW) connections and steel-wood-steel (SWS) connections loaded axially in tension. Test specimens consisted of both glulam and sawn lumber specimens broken down into 30-test groups, each group having ten replicates. The WSW connections included connections with two separate side members, while those with a slit for the concealed steel plate was cut into one solid beam section. The researchers found that a reduction was necessary for the effect of the side members due to the unequal loading exerted along the length of the connection bolts. They also found that the connections consisted of one solid member with a slit cut did not experience as drastic of a reduction in capacity as expected. Proposing a reduction factor for the effect of side members on the failure mode of the connections was found to be in better agreement with experimental results. The recommendations from the study were included in the next edition of CSA-086-14 Standard.

A similar study was carried out by Gattesco and Toffolo (2004) on the effect of the number of bolts on the failure mode of WSW connections loaded parallel or perpendicular to the grain. The experimental results were compared to Eurocode 5 at the time and additionally to the

experimental results available in literature. It was observed that increasing the number of bolts in both load cases, increased the potential for brittle failure and that Eurocode 5 analysis was in better agreement with the experimental results than those analyses proposed in literature, except in the case of perpendicular-to-the-grain loading. However, when connections loaded perpendicularly, it was found that analytical results consistently either underestimated or overestimated the capacity of the connection. The researchers highlighted that the behaviour of wood loaded in this direction is not well understood, and existing research outcomes require further refinement and validation.

With the focus on researching brittle failure modes in mind, a study conducted by Weckendorf et al. (2015) focused on beams in bending and the effect of end notches at the supports on the tension side of the member. The study consisted of fifty-eight specimens, with the focus being on how member size, notch depth, member geometry, type of glulam and load location influenced the capacity and failure modes of the glulam members. These effects were represented by grouping specimens into eleven different combinations. Specimens were loaded until failure occurred. Typically, failure occurred around the notches in the form of stable cracks, and specimens were also loaded well past the point of apparent failure to propagate the formation of visible damage to better understand the formation and effect of the failure modes in the glulam section. Surprisingly, it was found that there was no benefit observed in shear capacity when a load was applied close to the notched support based on the guidelines for members that are not notched as per CAN/CSA-086-14. Additionally, it was observed that the toughness of laminations in resisting fracture forces was related to the thickness of the mass timber members and the width of the individual laminations, specifically thicker members were tougher. Also, lamina composed of sub-lamina glued side-by-side, as in the case of Nordic Lam, were more resistant to fracture than lamina with the same width as the beam. The researchers of this study recommended that all loading on notched members be considered when determining the influence on shear forces developing in the tension side notch regions. The findings of this study were adopted into CAN/CSA-086-14.

2.4 Moment Connections

Glulam members used in the construction of mid and high-rise timber buildings as the primary material are expected to resist large loads and resulting bending moments at their end connections. Additionally, framed buildings are expected to resist lateral loading applied by wind and/or earthquake. The primary focus on research into the capacity of glulam beam-to-column moment-resisting connections is the reduction, control and prediction of brittle failure modes. Ductile failure modes are well understood and can be designed for, while brittle failure modes are often unpredictable; both in their development and effect on the capacity of the connection. To ensure the safety of occupants in taller building made of wood, every effort has to be made to either avoid brittle failure modes or ensure that failure is ductile, this reduces any chance of a catastrophic collapse.

The limited research on moment-resisting connections has focused on the effect of connections' parameters, such as type of fastener and their locations, as well as the capacity, rotational behaviour and failure modes in the glulam beams. An early study conducted by Hampson et al. (2004) suggested that the bolt's end distance had little influence on the moment capacity of fixed connections. Their study examined glulam, laminated-veneer lumber (LVL) and parallel-strand lumber (PSL) members, secured with four rivets to a 6.0 mm steel plate. While the researchers noted that adequate bolt's end distance resulted in less splitting during installation of the rivets; however, it did not predispose the connection to fail in a brittle failure mode and only reduced the capacity and stiffness of the connection by slight amount.

Murty et al. (2007) examined the applicability of the European yield model (EYM) equations to connections using small steel tube fasteners. While the connections in this experiment were loaded axially in tension, the conclusions drawn can be applied to designing moment-resistant connections. The experimental study, evaluated the effect of the diameter and number of fasteners on the behaviour of the connections in LVL and sawn lumber members. The results were found to be in good agreement with equations generated by the EYM when members were made of LVL, accuracy decreased in sawn lumber members. It was also found that increasing the number of bolts proportionally increased the capacity in LVL members' connections, regardless of the outside diameter. However, it was also seen than sawn lumber samples experienced early brittle failure before the EYM load was reached. Additionally, increasing the diameter of the fasteners in

sawn lumber members led to an inversely proportional decrease in the capacity gained by adding bolts. It was also concluded that by using fasteners with smaller diameters, connections could fail in a more ductile manner in the steel before the wood experienced brittle failure.

While most researches focus on the interaction between wood members and steel connectors, such as plates and bolts, other researchers have focused on developing novel connections to promote ductile failure modes. In an experimental study conducted by Andreolli et al. (2011), a unique connection configuration that focused on providing deformation capability and energy dissipation in the steel components of the connection to limit brittle failure in the wood was developed. This connection configuration is shown in Figure 2.25, and the observed failure modes in Figure 2.26.

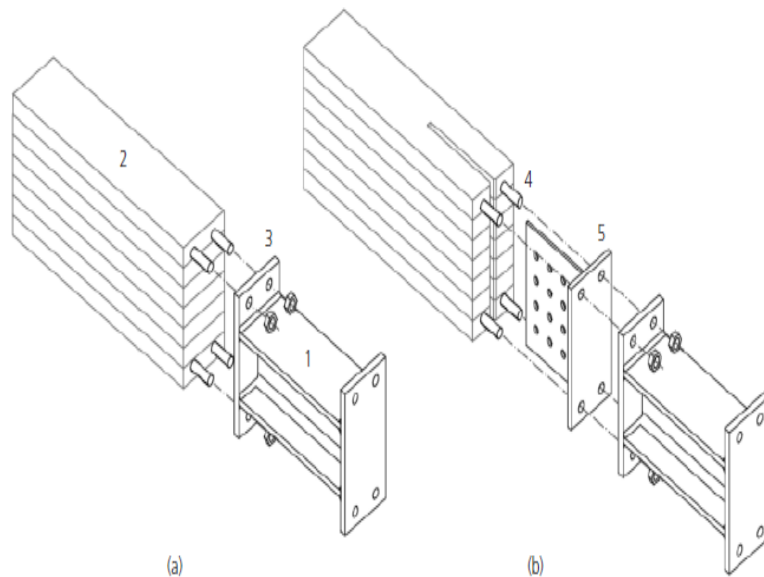


Figure 2.25 Steel-timber connection (a) without, and (b) with glued-in steel plate (Adapted from Andreolli et al., 2011)

The researchers found that the connections could be designed to behave in a semi-rigid fashion without a reduction in its moment-resisting capacity, and that it could be designed to yield in the steel components before any failure occurred in the wood section. The versatility of the connection configuration and potential for prefabricating most of the components highlighted the need to conduct further experiments on the connection in the context of a full-frame assembly, as shown in Figure 2.27, and its response to seismic forces via a non-linear analysis.

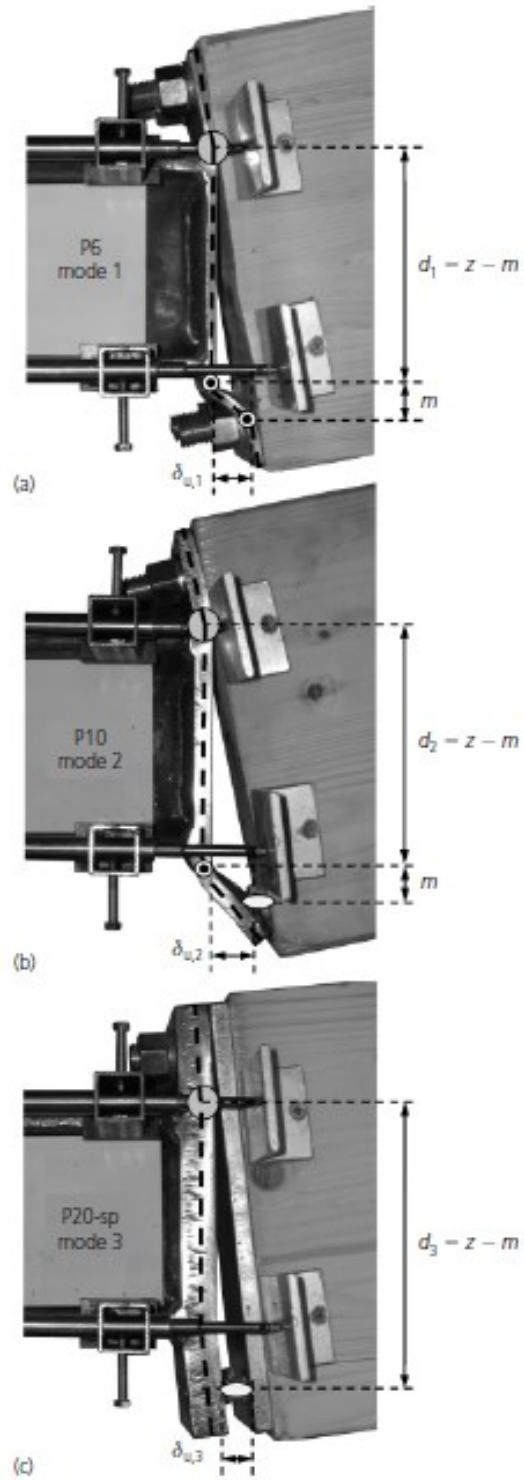


Figure 2.26 Failure modes observed: (a) Complete yielding in flange; (b) bar failure and flange yielding; (c) bar failure (Adapted from Andreolli et al., 2011).

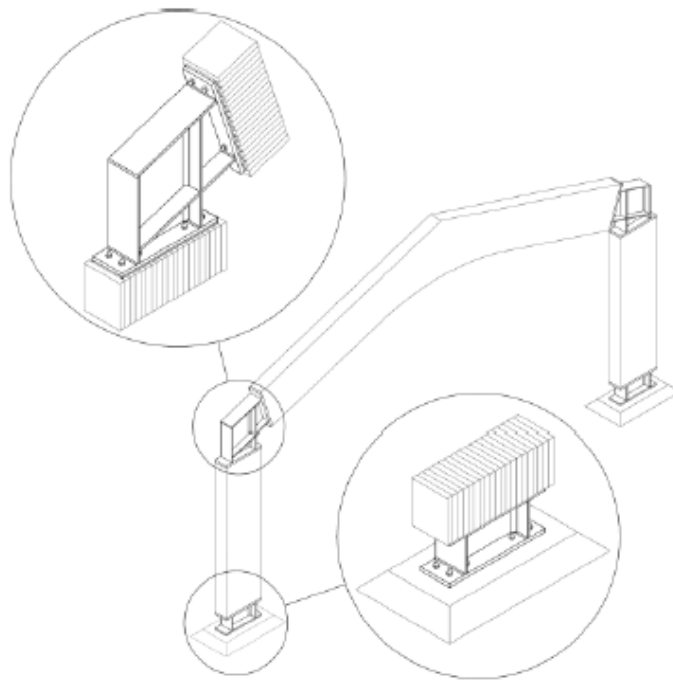


Figure 2.27 Potential application of studied joints (Adapted from Andreolli et al., 2011).

Similar conclusions were drawn by Humbert et al. (2014) during their experimental study on the mechanical behaviour of post and beam joints secured with metal fasteners. In their study, they found that although the connection capacity could be increased by increasing the stiffness in the connection steel components, this resulted in brittle failure modes in the wood section before the steel yielded in plastic failure. This requires good optimization of the connection design to increase the thickness and stiffness of the steel connecting components enough to just provide sufficient lateral resistance without promoting the formation of brittle failure in the wood section before failure occurs in the steel components.

Only a few research projects have been conducted to investigate the actual behaviour and moment-resisting capability of heavy-timber connections or to build analytical models that can be used to predict the behaviour of heavy-timber connections with steel components, similar to the model developed by Xu et al. (2015). Their test connection configuration consisted of a steel plate installed in the centre of a glulam beam section, perpendicularly to the grain with two different bolt configurations. A load was applied to the end of the steel plate in a direction parallel to the grain of the glulam section. The fabricated connection underwent both compression and tension

forces parallel to the grain in the wood section at the steel plate interface. The experimental results were used to validate the developed finite element model, where Hoffman criteria was used to account for the two different directions that axial forces were working in within the wood section at the connection. The model was able to predict with fair accuracy the global moment response, moment capacity and failure modes observed in the experimentally tested connections.

While some advances have been made in using FE models to predict the response of individual glulam members and connections, there is very little literature available with respect to the lateral resistance of heavy-timber structures. In a study carried out by Xiong and Liu (2014), two monotonic tests and eight cyclic tests were conducted on ten full-scale, one-story, one-bay glulam frames, each composed of two posts and one beam. Frame connections were developed to feature slots in the wood, to insert the steel platers making the connection configuration. Concealed steel T-plates were used at the base of the columns, and the column and beam sections were connected via a concealed steel plate inserted in the top of a post and adjacent glulam beam section. Test assemblies included simple frames and frames with various lateral strengthening: X-brace, K-brace, knee-brace and shear wall infill. The researchers found that due to the semi-rigid connections nature, the lateral stiffness of unbraced frames was unreliable, with splitting and other brittle failure modes observed at the joints. Additionally, the bracing in the X-braced and K-braced frames was found to have low ductility, promoting the formation of brittle failure, despite achieving a desired lateral stiffness in the frame. The results of those frames were found to be more desirable than those observed in the knee-braced frames, which while being elastic did not achieve a required lateral resistance. The frame which showed the ductility and a high capacity for energy dissipation, resulting in a stiffer frame that did not exhibit the same brittle failure modes observed in the other frames.

2.5 Glulam Behaviour at Elevated Temperatures

In order to fulfill the structural fire design requirements for glulam structures, the fire behaviour of the different structural components and the factors associated with their load-carrying capacities need to be well understood and studied.

2.5.1 Testing at Elevated Temperatures

In general, the strength of a glulam timber member subjected to fire comes from its residual cross-sectional area after charring due to elevated temperatures; therefore, the effect of density on internal temperatures generated during fire exposure need to be accounted for. A research program by Yang et al. (2009) involved three different experimental studies relating glulam properties at elevated temperatures to the density of the respective wood species. They studied: the effect of temperature on mechanical properties of glulam timber, charring depth and rate after standard fire exposure, and temperature distribution within glulam sections. In their research projects, the intent was to study the heat transfer rate and resulting internal temperatures of five softwoods commonly used as construction materials in Taiwan, compare the results to those derived from equations and finally produce results that can be used for estimating the applicability of different species for glulam design with respect to fire resistance. Their studies' outcomes showed that woods with higher density generally performed better in fire than those with lower densities and that the mechanical properties of all wood outside the charred zone remained unchanged after experiencing elevated temperatures. These studies also showed that an increase in density correlated with decreased charring rate and slower rate of heat flow. Their testing was conducted in a furnace where specimens were exposed to three-sided burning with CNS 12514 Standard Fire Test, which is a similar standard to the ISO-834 fire tests (Yang et al., 2009). In those fire tests, temperatures were recorded using insulated thermocouples installed within the glulam members in two different configurations depending on the size of the specimen, Figure 2.28.

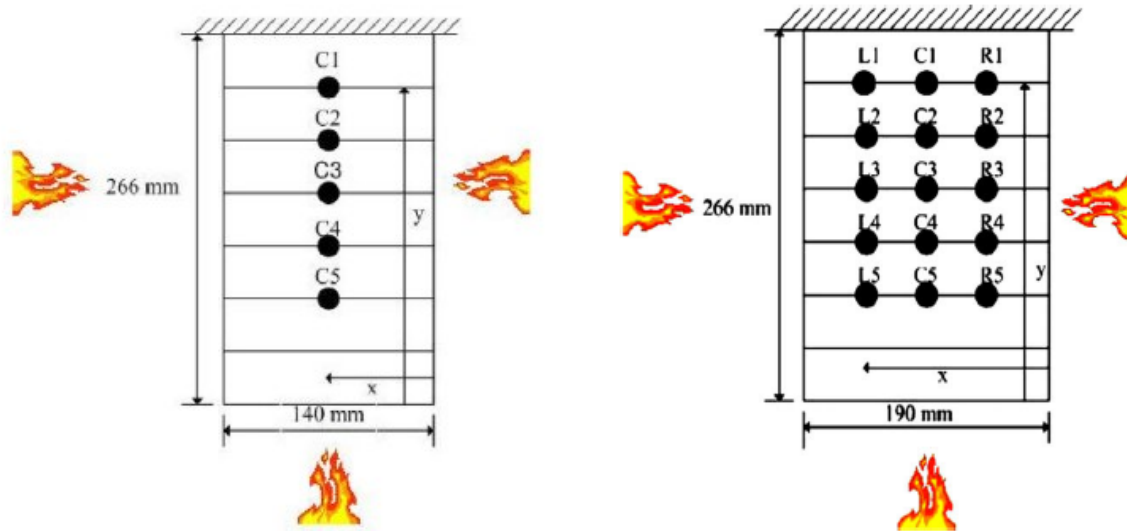


Figure 2.28 Test Group 6F (left) and 8F (right) (Adapted from Yang et al., 2009).

Yang and his research team selected five types of softwood: Japanese cedar, Taiwania, China fir, Douglas fir and Southern pine for their studies. All beams experimentally tested had a length of 1800 mm and were composed of seven laminates, each of 38 mm thick, and two different widths were studied: 140 mm and 190 mm. Thermocouples were embedded within the glulam sections during the manufacturing process and both the fire properties and temperature distribution were measured after 30, 45 and 60 min of fire exposure conducted in a large-size furnace (Yang et al., 2009).

Changing internal temperatures can affect two unique characteristics of glulam sections: the adhesive and the finger joints used to end join pieces. It is important to understand the thermo-mechanical properties of these components and their effect on the glulam building structural elements when exposed to elevated temperatures. An unexpected failure of a glulam beam due to shear along a glue line during a past fire experiment, prompted Frangi et al. (2004) to experimentally study the shear behaviour of adhesives at different elevated temperatures. The objective of this study was to determine the shear behaviour and resistance at elevated temperatures of different adhesives used in the production of glulam timber and use the results to validate a FE model to simulate the unexpected failure that occurred when a glue line sheared in a timber member loaded under fire conditions. To study the shear behaviour of glue at elevated temperatures, seven different adhesives were selected to study: one epoxy (Araldite AW 136 h

with Hardener HY 991), one resorcinol-formaldehyde (RF, Kauresin 460 with Hardener 466), and five different 1-K-PURs (Kauranat 970, Kauranat 107 TR, Balcotan 107 TR, Balcotan 60 190, Purbond HB 110 and Purbond VN 1033). The RF adhesive had been previously studied and no concerns about failure at elevated temperatures had been raised, so it was selected to be a reference point for other adhesives that are less sensitive to heat. While epoxy, known to be sensitive to heat, was selected as reference point for glues that perform poorly at elevated temperatures. Small specimens measuring 112 x 40 x 40 mm, were heated to different constant temperatures then transferred to a loading arrangement that was kept at the same temperature with an industrial air heater. Afterwards, the heated specimens were loaded to failure within 30 to 60 seconds. The authors conducted 74 fire tests on each adhesive with temperatures ranged from 20°C to 170°C, and documented the samples shear strengths and failure modes. Studying the behaviour of bond lines at elevated temperatures produced three very interesting results. First, as Figure 2.29 is showing the reduction of shear strengths of the glues and timber with respect to time, all five 1-K-PUR adhesives had different behaviour at elevated temperatures, this group of glues is most commonly used in glulam manufacturing in Canada. Secondly, it was shown that generally, the shear strength of the glue decreases at a greater rate than the shear strength of the wood with temperature increase. Thirdly, as seen in Figure 2.30, three different failure modes were observed: shear failure in the timber outside the bond line, shear failure between the wood and bond line and loss of cohesion in the glue.

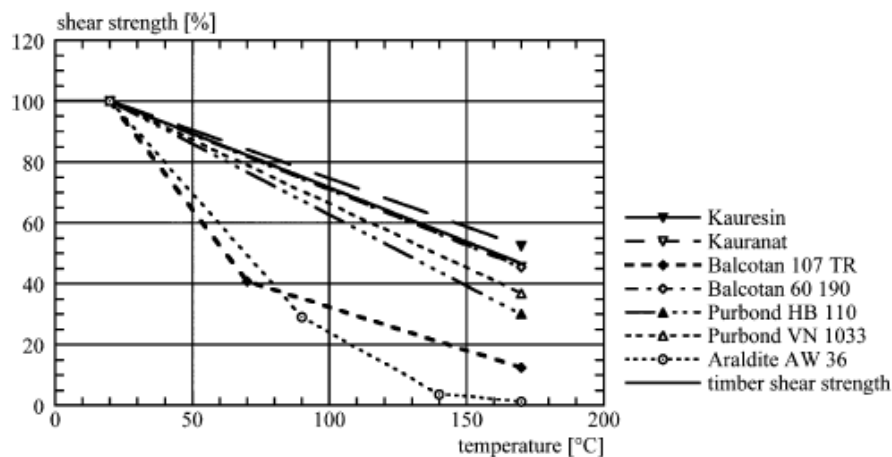


Figure 2.29 Shear strength reduction with respect to change in temperature (Adapted from Frangi et al., 2004).

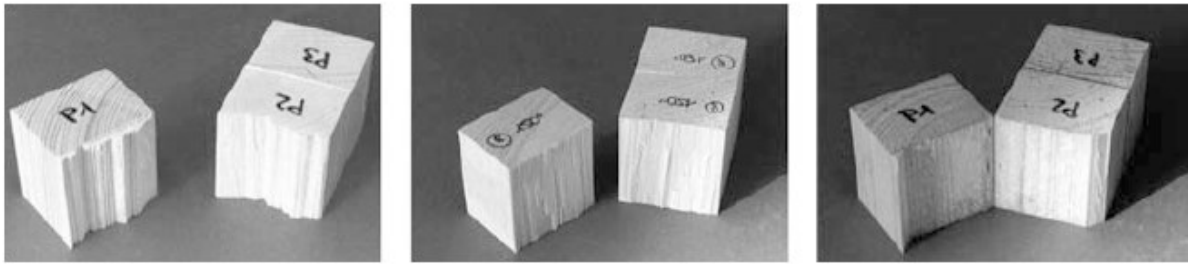


Figure 2.30 Failure Modes: timber outside of bond line (left), failure between wood and bond line (center), and failure of glue cohesion (right) (Adapted from Frangi et al., 2004).

As part of a larger research project being conducted at the Swiss Federal Institute of Technology, Klippel et al. (2013) performed an experimental analysis on the fire behaviour of finger joints in timber members. The main purpose of this project was to study the structural behaviour of finger joints under fire loading and explore whether a relationship exists between the location of the finger joint, its adhesive and the tensile capacity of the glulam component under fire exposure. In order to study the behaviour of finger joints under fire exposure, Klippel and his research team carried out an experimental analysis on testing boards. All lamellas used were of 40 mm thick, approximately 3.50 m long and widths varied from 80 mm to 200 mm. Also, beam depth was 280 mm for all tests except one, which had 200 mm depth. The location of the finger joint was either in the middle of the beam or one lamella above the bottom. Tensile loads and fire exposure were applied according to EN 1363-1 standard fire tests. Experimental data included displacements and temperatures that were collected using LVDTs and thermocouples, respectively, as well as time to failure. The research study also showed that the fire resistance of their specimens strongly correlated with the type of failure observed: failure in or along the finger joint, tensile failure in solid wood or a mixed type failure. Their results showed the followings: the adhesives tested had no discernable impact on the fire resistance as charring governs the load bearing capacity of the member, finger-jointed lamellas exposed to three-sided fires failed sooner than those where the finger joint was exposed to two-sided fire by approximately 10 to 15 minutes. A general test setup and a three-sided fire failure are shown in Figures 2.31(a) and (b), respectively.

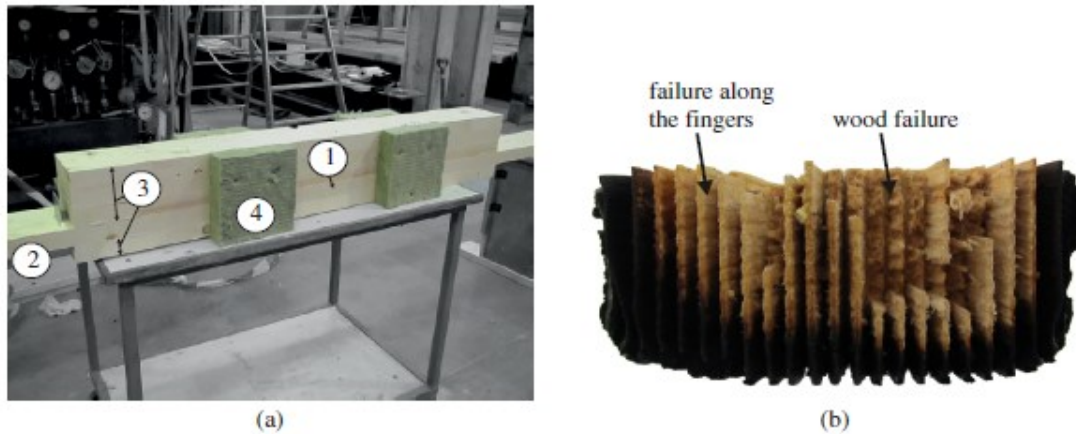


Figure 2.31 (a) Test specimen, finger joint (1), testing board (2), external lamellas (3) and insulating material (4); (b) Three-sided exposure of finger joint (Adapted from Klippel et al., 2013).

The most difficult components of a timber structure to design for fire resistance are the connections; their critical nature is highlighted by Peng et al. (2011; 2012) who studied, modelled and experimentally tested WSW and SWS heavy-timber connections under tensile loads. In both papers, primary objective was to study and model the fire behaviour and performance of wood-steel-wood connections in glulam assemblies and develop a framework for the fire resistance design of heavy-timber connections to address the lack of design guidance on this topic. To predict the fire resistance of WSW timber connections, a FE model was developed using ABAQUS/Standard software to simulate the resulting temperature profile and heat transfer during exposure to CAN/ULC-S101-07 standard fire. The thermal model used temperature related properties of wood and steel presented in literature to account for: the rate of heat conduction within the specimen, the rate of both convection and radiation heat transfer between the fire and test specimen and the rate of heat exchange between connected members. The model's timber properties were checked against experimental results for a timber member exposed to same standard fire. Once the timber properties were validated, a WSW connection from the experimental study was modelled and the FE model outcomes were compared against the published experimental results (Peng et al., 2011). In a further study, their FE model was validated by conducting fire tests on both SWS connections and WSW at Carleton University's Fire Lab, Figure 2.32.

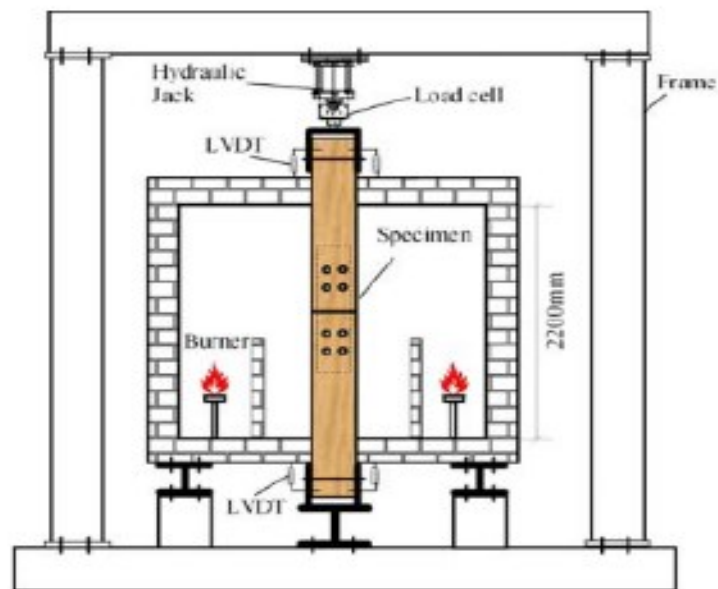


Figure 2.32 Test furnace at Carleton University's Fire Lab (above), Test set-up (below).
(Adapted from Peng et al., 2012).

The connection configurations tested under fire had previously been studied at normal temperatures and therefore provided a reference point for assigning load ratios of 10%, 20% and 30% to the specimens. Other factors studied in the experiment and their impact on the fire resistance of the assemblies was the number and size of bolts and effect of fire protection, such as

gypsum boards, plywood and intumescent coating, on the connection's fire performance. From their 2011 study, Peng et al. found their FE model to be in good agreement with previously published test results, and that the resulting data was used to develop an empirical equation to predict the time to failure of WSW connections as shown in Equation 2.1. They also found that the WSW connections had a comparable fire resistance to wood-wood-wood (WWW) connections due to the failure generally beginning in the external members and fasteners, with the outside member wood thickness playing a greater role in the fire strength than the fastener diameter.

Equation 2.1 Time to failure formula (Adapted from Peng et al., 2011).

$$t_f = -0.0042 \ln\left(\frac{R_f}{R_0}\right)(t_1^2 + 2d^2)$$

Where:

t_f = time to failure in minutes

t_1 = thickness of wood side member (mm)

d = fastener diameter (mm)

R_0 = ultimate capacity at normal temperature

R_f = ultimate capacity at elevated temperature

Peng et al. (2012) continued to validate their FE model, Figure 2.33, by carrying out a series of experiments on WSW and SWS connections. The results showed that thicker wood members performed better, reductions in load ratios increased fire performance, larger diameter bolts increased the fire performance of the connections but the number of bolts did not, edge distances should account for the rate of charring when considering normal design loads and finally, the protection from gypsum boards and plywood increased the fire performance of the connections; however, the intumescent paint applied to steel components did not improve fire resistance by a significant amount and was difficult to apply.

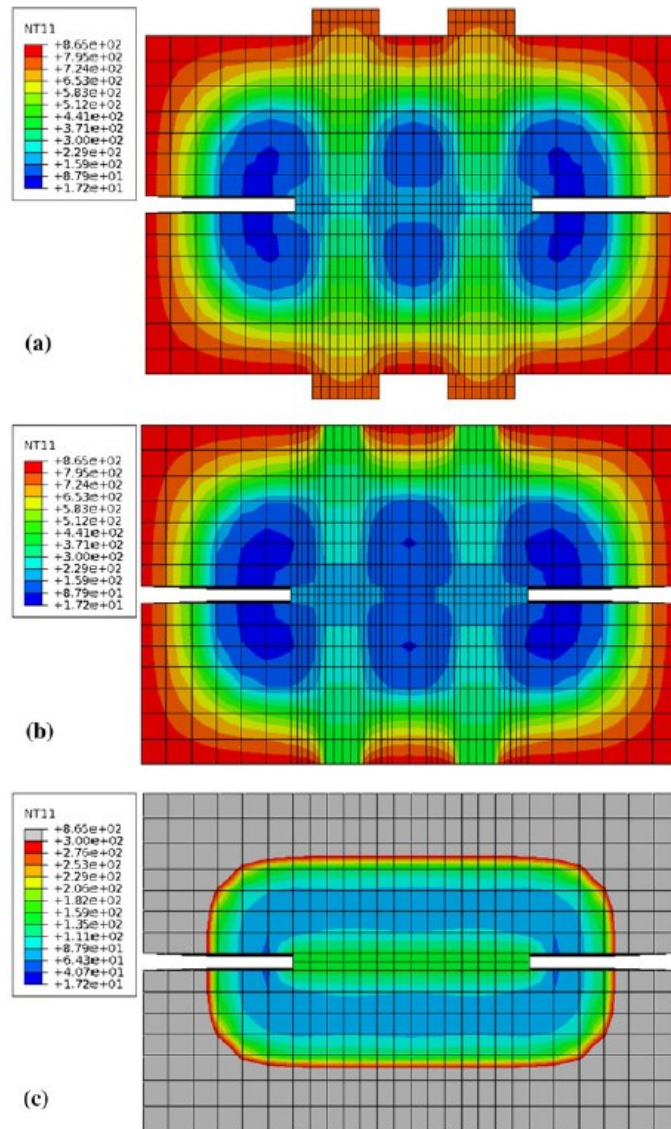


Figure 2.33 FE model validated by previous experimental results: bolted connection (top), doweled connection (center), wood between dowels (bottom) (Adapted from Peng et al., 2011).

Audebert et al. (2014) identify that in real timber connections, some tension loading occurs perpendicular to the grain; however, the authors highlighted that only a few publications have studied perpendicular loading in timber under normal temperatures, and almost no research has been conducted on this loading case at elevated temperatures. The aim of Audebert et al.'s (2014) research paper was to study the normal-temperature and fire behaviour of glulam members loaded perpendicular to the grain via WSW connections. Also, the research team looked at whether a

previously developed FE model for connections subjected to tension parallel to grain could be adapted to accurately predict the results and therefore validate the model for other applications.

Audebert et al. (2014) modified a previously-developed FE model to predict the capacity of a connection in tension perpendicular to the grain. The modifications were made to the material property meshes, primarily to take into account the failure mode and behaviour of wood loaded in a perpendicular-to-the-grain direction. Also, the resulting model was validated by conducting tests on six specimens under normal conditions and four under ISO 834 standard fire exposure. Thermocouples, wire displacement sensors and pyrometer plates were used to collect relevant data. The two different configurations of timber connections, summarized in Figure 2.34, were loaded in tension perpendicular to the grain. The observed load carrying capacities of the connections under normal conditions, were a mean 82.6 kN for configuration A16 and a mean of 128.8 kN for configuration A20, both values were approximately 10% higher than those calculated using the Eurocode 5. For the fire tests, samples were loaded to 10% and 30% percent of ultimate capacity for sample A16 and 30% and 45% of ultimate capacity for sample A20. This resulted in fire resistance times of 71 minutes, 48 minutes, 69 minutes and 62 minutes, respectively and agreed with their FEM results, which predicted failure time of 58 minutes, 45 minutes, 55 minutes and 52 minutes respectively. Of particular interest in their results was that a fire resistance of more than an hour could be reached for this type of connection and that their FEM successfully showed that the steel plate acting as a surface for the water escaping the heated wood to condense on, increasing the time over which the steel plate stayed at a temperature of around 100°C, as seen in the time-temperature curve of two thermocouples attached to the concealed steel plate within the glulam member in Figure 2.35, and the FEM temperature model in Figure 2.36.

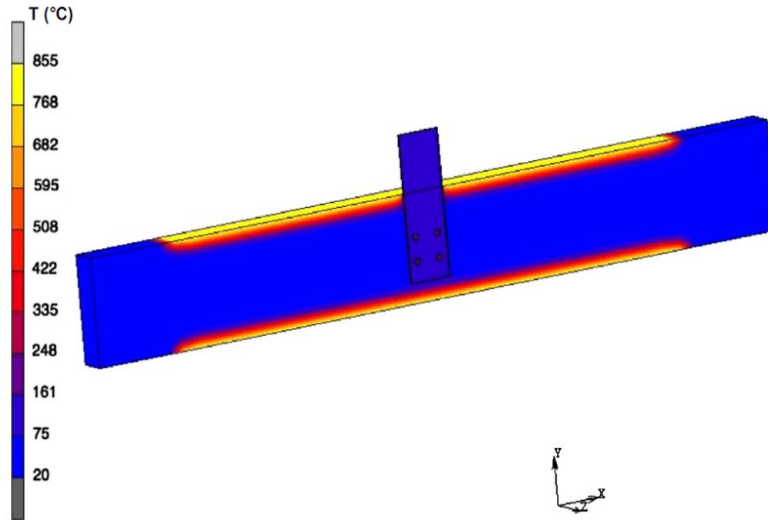


Figure 2.36 FEM verifying temperature distribution observed during experimental trials.
(Adapted from Martin and Tingley, 2000).

The literature reviewed provides a good deal of insight on the behaviour of glulam timber building components exposed to fire conditions, and provides a solid framework for developing further studies and potentially in providing guidance and documentation with respect to designing for fire resistance using a performance-based methodology instead of a prescriptive-based approach.

From (Frangi et al., 2004) research, it is shown that there is a relationship between elevated temperature and shear strength of both wood and bonding agents. The most critical aspect of their results was the broad range of performance seen in 1-K-PUR glues, as the fire behaviour of the chosen adhesive should be well known before selecting it as a bonding agent in glued-laminated timber as there is potential for a loss of cohesion and a resulting shear failure between laminates. However, the results also showed that many of the glues follow similar trend of shear strength reduction as solid timber, and since the experiment used samples of wood free of knots or other similar defects, real timber sections would always fail in wood first before glue due to the additional reduction in strength from knots and other defects. The data from these experiments has the potential to be incorporated into FE models as it shows a well-defined numerical relationship between elevated temperatures and the shear strength properties of the bonding agents. Also, glues that lose shear strength at very low temperatures should be avoided at all costs when considering

fire design, such as epoxy or the 1-K-PUR called *Balcotan 60 190*, both lost about 20% of their strength at only 40°C, far below the reductions seen in the other glues.

From the available literature, it is clear that knowing the internal temperature of the wood at different distances from the outside surfaces during a fire can be very useful for designing glulam members with respect to glue lines, finger joints and Fibre-Strengthened Polymers (FRP) strengthening. This data is also critical for two reasons: it provides better information for the FE modelling of glulam with respect to the heat transferring behaviour of the timber and the resulting reduction in the wood cross section from charring. From (Yang et al., 2009) research results, it can be seen that some equations are available to predict and calculate the internal temperatures of fire-exposed timber with some success; however, almost all their results were higher than the calculated values, highlighting the need to develop a relationship between some physical property of the timber and its rate of heat transfer. In general, there is a fair relationship between increased density and lower internal temperatures for comparably-sized timber members. More importantly, it has been shown that the China fir with the lowest density sees lower internal temperatures than both Japanese cedar and Taiwania which have higher densities but also higher internal temperatures than both southern pine and Douglas fir, the two densest softwoods tested. From the two densest woods, it can be seen that the fir with a lower density actually sees lower internal temperatures than the denser southern pine. Considering that both the China fir and Douglas fir seem to conduct less heat than the comparable softwoods in their density range. Also, it was concluded that the critical factor deciding the rate of internal heat transfer in wood sections is the cellular structure of the wood and the arrangement of the vessels and pores within that make up the microscopic structure of tree.

2.5.2 Fire Safety Engineering Design

Historically, most countries around the world have used prescriptive codes to determine the Fire Safety Engineering (FSE) requirements of buildings, both in respect to the design of the structural integrity of the building under fire loading and to the safety of the occupants with respect to egress from the fire (Hadjisophocleous and Benichou, 1999). Over the last two decades, countries have begun to shift their codes to a performance-based framework, where design of the building is approved if it can be shown to perform as safely as if it had been constructed according to the prescriptive code. The reasons for this change are technical, economical and social.

The two critical components of FSE are designing a structure that can withstand fire condition while also providing the occupants with means of safe egress to prevent any fatalities. Performance-based design approach is especially critical when applied to the structural integrity of steel structures, as steel is a commonly used building component and particularly susceptible to losing strength and stiffness during a fire (Bailey, 2006). However, following prescriptive codes by fire-protecting all steel structural elements costs time, money and has in some cases been shown to be either redundant or unnecessary (Bailey, 2006). However, as shown in Figure 2.37, using a performance-based framework for a structural fire design can result in increasingly complex models and interactions as one attempts to fully account for all variables and prove the fire safety design of the structure is adequate. The increasing complexity involved in a performance-based design, both with respect to designing the structural integrity of a building and the safety of its occupants provide an opportunity for a greater integration of computers into the design, planning, testing and improvement of a building's fire safety. Computer programs can be developed to model the effects of a fire on both the structural performance of a building and the evacuation of its occupants. In addition, many of the articles reviewed showcased how computer models can be used in other beneficial ways, such as providing assistance to occupants and first responders during fire, improving maintenance of safety equipment in buildings, training of occupants to handle fires or to further study the effects of fires on structures and their occupants.

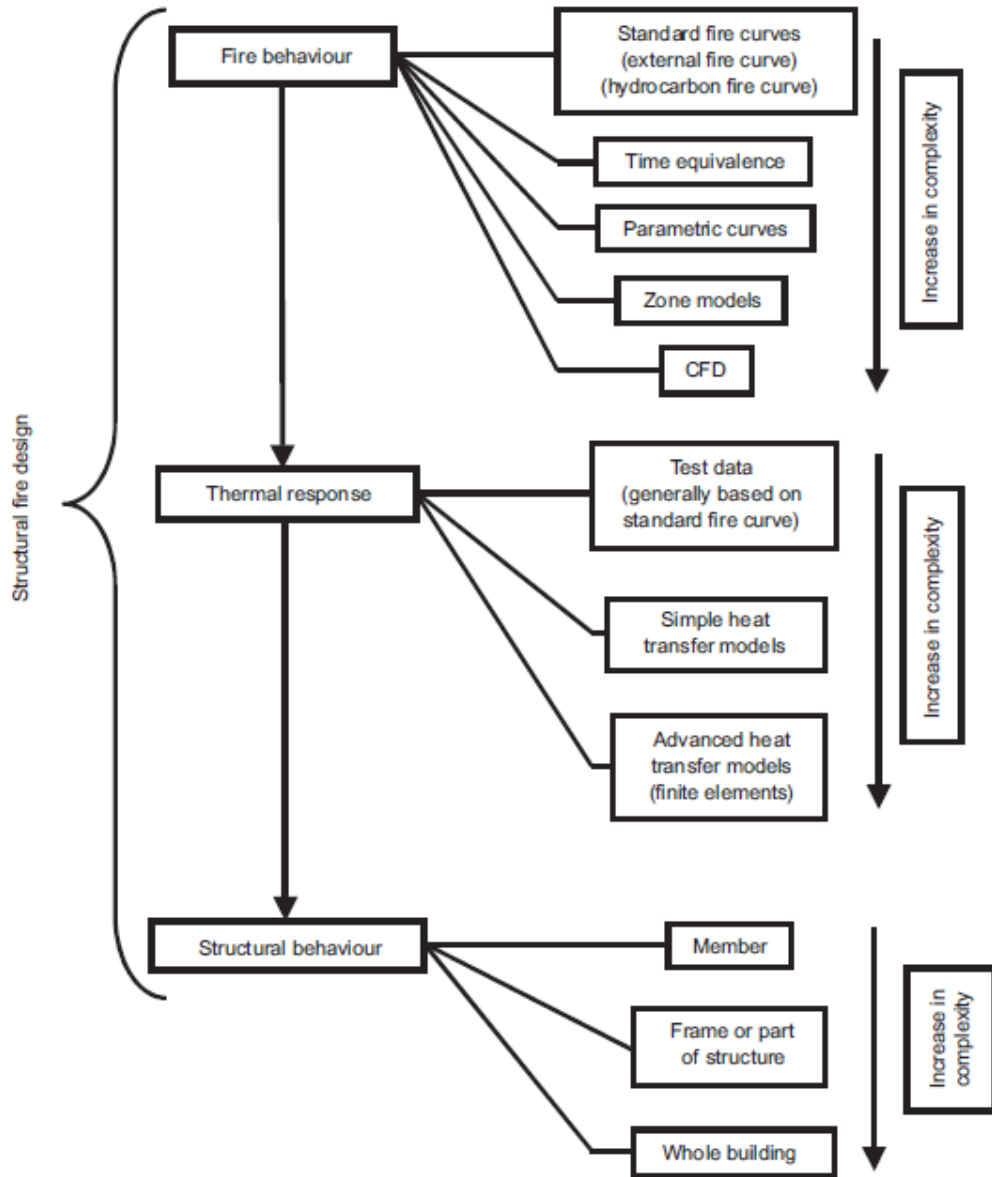


Figure 2.37 Increasing complexity of performance model with introduction of additional options (Adapted from Bailey, 2006).

Lamont et al. (2006) used a FE software to study the structural behaviour of an eleven-storey office building in London, England, using both the prescribed code and a performance-based approach. Citing the wealth of knowledge that has been developed since the Cardington frame fire tests carried out in the UK in 1990s, where a steel frame successfully carried a load despite having no fire protection in most iterations of the fire test, the authors proposes there is now a better understanding of the behaviour of whole steel-concrete composite frame structures

subjected to fire. Working with a regulatory body, the authors modeled three different fire scenarios as seen in Figure 2.38. The fire models were applied to two different building cases: the first with all prescribed fire protection present, and in the second case all secondary beams were left without fire protection. The detailed Finite Element Analysis of the examined structure determined that the deflection and strain patterns were similar for both cases in the composite slab, and therefore would result in similar structural damage. The paper showcases the ability of an engineer to remove redundant fire protection by determining the performance of the structural integrity of the building exposed to fire following both prescribed and performance-based design approaches.

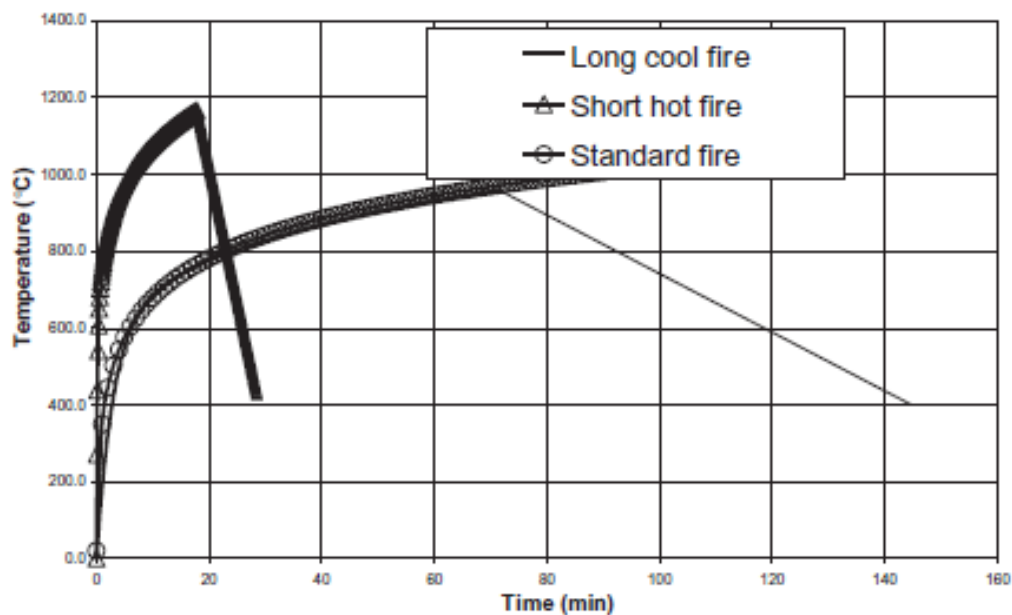


Figure 2.38 Three fire scenarios developed for fire testing (Adapted from Lamont et al., 2006).

Bisby et al. (2013) highlighted the increase in large-scale non-standard structural fire testing using real fires to demonstrate the structural performance of building systems under a certain fire load can meet the safety standards determined by a prescriptive code. They also summarized previous reviews and assessed what research needs to be pursued. The different fire testing methods outlined in the literature are summarized in a comprehensive chart. The chart categorized test methods based on the complexity of both, the fire model and structural model. It also showed that the majority of fire tests either use complex assemblies and simple fires, or simple structural models and complex fire models, with only a few fire tests incorporated both a complex

structure and complex fire that accurately represents in situation conditions. These tests are critical in validating computer models of fires and structural assemblies under fire loading, so their fire performance can be accurately compared to that of a real building designed according to a prescriptive code. Bisby et al. (2013) identified a wide range of knowledge gaps including: modelling of natural fires, failure localizations and lack of modelling of timber structures. The study also highlighted that the material of focus in literature was mainly steel, and despite the number of sub-frame assemblies tested in standard fires, no studies with wood as the primary structural component were identified in that category.

Gaps of knowledge exist in several areas of fire safety engineering, especially in the application of wood as a primary or secondary component in mid or high-rise buildings. More large scale non-traditional fire testing is required to further develop and validate computer models of this complex interactive system. Most prescriptive fire protection codes rely on standard fires that either underestimate or overestimate a real fire behaviour. In order to accurately design a building for adequate fire resistance, more natural fire curves need to be evaluated and modeled to simulate true fire conditions. Although there are many computer-integrated solutions for calculating the structural performance of a building under fire condition, the flow of data is one directional and does not represent the interconnected nature of a fire. For example, once a fire is modeled, the fire data is then applied to a single element of the structure, and eventually the interactions of that element are then compared to the global structure and the resulting effects of fire exposure are determined. There are no provisions for interactions in the other direction, such as a floor collapsing, changing the nature of the fire, the forces flowing through the member under inspection and the structure as a whole.

2.6 Enhancing Structural Performance

2.6.1 Ambient Temperature Strengthening

Most research conducted on moment-resisting timber connections was focused on using self-tapping screws (STS), or other steel components that were installed perpendicular to the grain to provide increased connection resistance and reduce brittle failure modes (Gehloff et al. 2010; Song et al. 2016). This method has been proven to reduce the formation of brittle failure modes by reducing the formation of failure around defects in the wood by allowing for the transfer of forces

through the reinforcing screws rather than through the damaged or defective sections of wood. Some strengthening techniques can be applied to damaged timber sections, as the reinforcing mechanisms can help transferring the load through the damaged sections. Song et al. (2016) showed that both FRP sheets and self-tapping screws were able to restore cracked columns to full compressive capacity, or even to a higher load-carrying capacity, Figure 2.39.

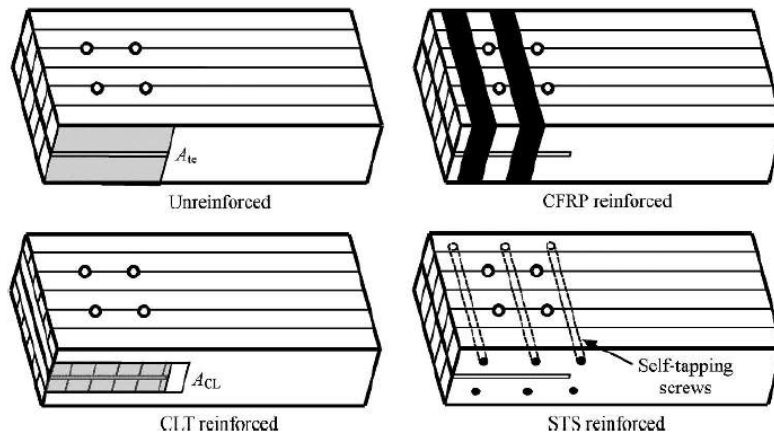


Figure 2.39 Concealed moment-resisting connection strengthening methods (Adapted from Song et al., 2016).

2.6.2 Elevated Temperature Strengthening

Glulam beams can be strengthened with Fiber-strengthened Polymer (FRP) laminates to increase their flexural bending capacity. Martin and Tingley (2000) investigated the fire performance of this strengthening method and the behaviour of the FRP in conjunction with timber. The main objective of their study was to examine the behaviour of loaded FRP-strengthened glulam beams under fire conditions, as well as the relationships between FRP type, FRP location and beam width and depth on the fire resistance of the tested beams. In their experiments, glulam beams were exposed to three-sided ASTM E-119-88 standard fire, and the top side of the beams were insulated with ceramic fiber blankets to simulate the existence of a slab or floor assembly. In total, thirty full-size glulam beams were tested, four with no strengthening and the rest with FRP sheets. The following parameters were varied between tests: beam width, beam depth, interior or exterior placement of FRP, number of FRP laminates and type of FRP sheets. Once test specimens were loaded, the beams were exposed to standard fire, and the resulting

time to failure measured and compared to the calculated results obtained from two different design methods. The results showed that the fire resistance of FRP-strengthened glulam beams comes primarily from the wood cross-section unaffected by charring or elevated temperatures. No noticeable effect was noticed on the fire endurance of the glulam beams due to the FRP laminates. Also, the different types of FRP and their qualities had no impact on the results. Interior placement of FRP was found to provide better fire performance of the strengthened member due to the insulating nature of the wood. An empirical adjustment was formulated showing that the calculated time to failure of FRP-strengthened glulam beams should be reduced by half as the design load of the FRP-strengthened glulam members is twice that of the conventional glulam members; however, this factor is only valid for members with a width less than 79.4 mm. In addition to the study of the structural behaviour of FRP-strengthened glulam beams exposed to fire, the authors actually have raised some concern about using FRP sheets and its potential hazards when exposed to fire. For instance, when designing a FRP-strengthened beam, it needs to be understood that the flexural bending capacity can be doubled at normal temperature; however, this can result in a beam that will quickly go back to its original strength once the external FRP-laminate is exposed to temperatures just over 100°C, resulting in a beam that could theoretically have its load ratio doubled once the FRP lamellas weakened enough. If FRP lamellas can be developed with higher tolerances for elevated temperatures, the possibility of installing them on the external surface of glulam beams and retaining their strength can exist. In conclusion, there is need for additional research on the benefits of adding fire protection layers such as gypsum board or plywood over the FRP lamellas to increase the fire resistance of FRP-strengthened glulam specimens. FRP lamina placed internally inside a glulam beam section, one or two layers from the bottom, could potentially increase the fire resistance of FRP-strengthened glulam beams, as the bottom wood layer chars, the load is transferred to an internal FRP layer which theoretically would then slightly increase the capacity of the residual wood section, depending on the internal temperature and its effect on the FRP strengthening.

2.7 Fire Protection Options

While some allowances are made for the application of fire protection sprays and chemicals in the Canadian Wood Design Handbook, it has generally been found that the application of fire retardant chemicals negatively effects the fire performance of timber, Levan and Winandy (1989). Levan and Winandy found that during a fire, the chemicals while slowing the rate at which flames spread, the heat transfers through occurred in the wood members. Also, the released acidic chemicals reduce the mechanical properties of wood members after temperatures were reduced. Results also showed that in certain applications, wood members coated with fire retardant spray would also see their mechanical properties degrade due to the interaction between the wood fibers and the applied chemicals.

Typically, most experimental studies on the fire resistance of timber components concluded that the addition of protective layers of gypsum board or plywood can considerably reduce the rate of fire spread, heat transfer and charring. In general, minimum research has been carried out since these findings on alternative chemicals or methods that increase the fire resistance of timber structural components.

Chapter 3 Research Methodology

Construction materials and products undergo extensive testing, verification and codification before their use is permitted in Canada. Similarly, the design and construction of structures in Canada must meet prescriptive or performance-based guidelines as mandated by respective national and provincial building codes. These requirements are developed through extensive experimental testing programs, computer models and mathematical analyses. The results of these experimental programs provide critical information that can be used to study the physical and mechanical properties of construction materials and assemblies and observe their structural behaviour. The analysed results of an experimental program can be used to develop guidelines for the use of specific materials or components in the construction of buildings or other structures. Additionally, experimental results can be used to validate computer models that can be later used to design and predict the behaviour of construction components and/or assemblies subjected to loading under different conditions. The reviewed literature highlighted the lack of research on the behaviour of moment-resisting heavy-timber connections both at normal and elevated temperatures. Based on the reviewed literature, it was observed that many of the experimental programs for steel and concrete at elevated temperatures focused on testing components as part of a sub-assembly or entire assembly to better replicate in-situ conditions of a connection that forms one part of the structural response of a structure or frame to loading. Therefore, to study the behaviour of concealed beam-to-column moment-resisting connections at elevated temperatures, an experimental program methodology was developed. The research work carried out in this thesis was part of larger research effort led by Dr. Salem at Lakehead University to study the behaviour of value-added wood products, such as glued-laminated timber (glulam) and cross-laminated timber (CLT), at normal and elevated temperatures.

3.1 Experimental Program

Recent trends in fire safety design have seen specimens loaded at 100% of their design capacity under normal loading conditions and exposed to a standard fire until failure occurs. In Canada, a minimum fire resistance rating of 45 minutes is required for structural timber components. Additionally, there are no guidelines for the design, or strengthening of heavy-timber moment-resisting connections, only for axially-loaded simple connections. Therefore, to accomplish the research of this thesis, the following objectives have been identified:

1. Design a wood-steel-wood (WSW) concealed steel moment-resisting connection;
2. Study the effects of two variables that are well documented in the Canadian Wood Design Handbook for axially-loaded connections: bolt's end distance and number of bolts;
3. Observe the failure modes of test specimens at ambient temperature, and adapt guidelines from the Canadian Wood Design Handbook to determine the design capacity of the connections;
4. Observe the effect of bolt's end distance and number of bolts on the behaviour of the connection at elevated temperatures.

3.1.1 Ambient Temperature Testing

Normal temperature testing was conducted at Lakehead University's Civil Engineering Structures Laboratory. The laboratory has a large Universal Testing Machine (UTM), based on previous experimental studies conducted with the equipment, it was determined that full-size assemblies would be placed within and supported on a large steel I-Beam placed along the bottom of the machine, Figure 3.1. Each test was duplicated to verify the experimental results.

To focus the study on the moment-resisting connections, an inversely loaded test set-up was selected, this allowed for the force to be applied through the center of the UTM, in close proximity to the moment-resisting connections and ensured that the sample would not have its movement constrained before failure occurred. To evaluate the rotational behaviour and moment-resisting capacity of the connections, the assembly was simply supported where the connection was not present to ensure that the applied moment was entirely transferred to the connections, left and right to the column in the middle of the test assembly, and was also easily quantified.



Figure 3.1 Lakehead University's UTM with glulam sample being loaded.

3.1.2 Elevated Temperatures Testing

Elevated temperature testing was conducted at Lakehead University's Fire Testing and Research Laboratory (LUFTRL) at Thunder Bay campus, Ontario. The state-of-the-art facility, shown in Figure 3.2, accommodates a large custom-designed furnace with two natural-gas fed burners that can raise the furnace' environment temperature up to 1500 °C. The furnace compartment is housed within a large steel loading frame (Figure 3.3). The furnace is made from strengthened heavy-steel plated walls that are lined from inside with thick Fiberfrax blankets (Figure 3.4). The furnace large door and the roof can be removed using the 1-ton jib crane installed in the facility. Additional vents on the furnace's floor and roof are present to facilitate the access of instrumentation and set up of experimental assemblies (Figure 3.5). These features of the furnace allowed for tests conducted at elevated temperatures to follow a similar experimental setup and methodology as that used during ambient temperature testing.



Figure 3.2 Lakehead University Fire Testing and Research Laboratory (LUFTRL).



Figure 3.3 Large fire testing furnace accommodated at LUFTRL.



Figure 3.4 Fire testing furnace and steel loading frame.



Figure 3.5 Furnace bottom vents allowing the insertion of steel supports through the furnace floor.

3.2 Data Collection

In order to accomplish the objectives of this experimental study, measurements and experimental data is required to study the behaviour of the WSW connections under both normal and elevated temperatures. Also, it was very important to provide reference and insight into recorded visual observations of the connections' response to loading and failure modes as the test assemblies were loaded above its ultimate capacity. The critical data points that needed to be captured in both ambient and elevated temperatures are the load applied to the test specimen and the resulting deflections of the assembly. Additionally, to study the behaviour of moment-resisting connections exposed to fire, thermal measurements were collected, including furnace temperatures, external wood temperatures and internal wood temperatures.

3.2.1 At Ambient Temperature

In normal temperature condition, each test assembly was gradually loaded following a load-controlled protocol until failure occurs. Therefore, it was critical that the loading on the specimen be recorded to develop a load-response relationship for the connections being tested. To measure the response, the deflections of the beams in response to the gradually-increased loading were captured using a number of Linear Variable Differential Transformers (LVDTs) at different locations, in such a way that the data from one sensor can be used to verify the data from other sensors, increasing the validity of the results and providing a data collection redundancy in case of sensor errors or malfunctions during experimentation. Additionally, as deflections can be expected to be relatively large over the course of the loading, sensors had the ability to be quickly adjusted or relocated to accommodate the movement of the specimen. Using the load cell data, deflections of the specimen and the geometry of test set-up, the applied moment and resulting rotations of the connection were calculated. Also, the moment-rotation relationships were plotted and analyzed. The relationship shown on the graph should validate any observations made regarding the connections' failure modes and the effects of the bolt's end distance and/or number of bolts. In particular, the moment-rotation curves should highlight whether the connection behaves in a brittle or ductile fashion depending on the bolt's end distance and number of bolt variables.

3.2.2 At Elevated Temperatures

Identical test assemblies were loaded to the full-service design load of the weakest connection assembly before being exposed to CAN/ULC-S101 standard fire in the large-size fire testing furnace accommodated at Lakehead University's Fire Testing and Research Laboratory (LUFTRL). The design capacity of each connection configuration was determined by adapting the clauses and equations in the Canadian Wood Design Handbook (2015) in conjunction with the observed progression of failure with increased load at normal temperatures. In fire resistance testing, failure criterion was determined to be achieved once the column at the middle of the test assembly had deflected a substantial amount, at which one of the connections, left or right to the column, had exerted a rotation magnitude of 0.1 radian. Therefore, it was very important that both loading data and corresponding deflection data are collected over the time of the fire resistance experiment. In addition, during fire testing, it is very crucial that the applied transverse load remains constants over the entire duration of the test. As the load was kept constant, the glulam beam-column test assembly would deflect due to the effects of fire exposure and the resulting decrease in the functional glulam cross-section. Since it is impossible to place any displacement transducer inside the fire testing furnace due to the extremely elevated temperatures that could easily reach 800 – 900°C in about 30 minutes, low-thermal elongation ceramic rods were used to measure the displacements of the test assembly at different locations.

In addition to the mechanical measurements, thermal measurements were required to be captured during fire resistance testing. Temperature data of the furnace compartment was used to control the standardized fire within the furnace and is processed and interpreted by a computer system built into the furnace control panel. Figure 3.6 shows the UI for the furnace control program, thermocouples installed in the furnace, provide temperature feedback to the computer, which in turn controls the flow of gas to the burners and regulates the temperature in the furnace compartment to follow the profiles of pre-programmed standardized fire curves.



Figure 3.6 Human-Machine Interface (HMI) touch screen of the furnace’s control panel.

While these thermocouples provide temperature readings that are used to control the furnace and reflects the temperature of the standardized fire, it does not address the specimen assembly itself or any of its components. Therefore, high-temperature insulated k-type thermocouples need to be used to gather the required thermal measurements of the wood and steel components of the test assemblies. This data provides information on the transfer of heat through the specimen, the temperature of components at a given time during the test and can be used to observe the relationship between time, temperature, rotation and failure for glulam moment-resisting connections.

3.3 Experimental Testing at Ambient Temperature

A total of thirty-two beam-column test assemblies representing four different glulam beam-to-column connection configurations with and without perpendicular-to-the-grain strengthening, were experimentally tested at normal temperatures. Using the collected load-displacement data, the connections’ strength and stiffness and failure modes were observed and documented. The capacity of each connection at ambient temperature was determined and used to load all fire test connections to 100% of the service design load of the weakest connection configuration (with four bolts and four-times bolt diameter end distance) to study the time to failure at elevated temperatures.

3.3.1 Materials

Test assembly members were made of black spruce glulam with a stress grade of 24F-ES/NPG and an architectural appearance grade (Nordic Structures, 2015). The wood material was chosen based on its similarity to that growing in the local region. Glulam members were built up from laminations measuring approximately 25 mm x 50 mm that were bonded along their edge, face and finger jointed with either phenol-resorcinol or polyurethane adhesive. The desired cross-sectional dimensions were then achieved when the outer faces were planed down to the members designed width and depth. The principal mechanical properties of the glulam sections summarized in Table 3.1 (Nordic Structures, 2015), have been provided by the manufacturer and verified by the Canadian Construction Materials Centre (CCMC) in Evaluation Report CCMC 13216-R (CCMC, 2014). The mechanical properties were used to select a cross section with a width of 137 mm and a depth of 317 mm, representing the smallest reasonable cross section found to be adequate for a typical 4.0 to 6.0 m span glulam beam carrying standard prescribed gravity loads for a mid-rise residential building.

Table 3.1 Specified strengths and modulus of elasticity of glulam sections.

Strength/Property	Units (MPa)
Comp. parallel to grain	33.0
Comp. perp. to grain	7.5
Tension parallel to grain	20.4
Modulus of elasticity	13100
Longitudinal Shear	2.5
Flexural bending	30.7

Additionally, connection components were analysed, and it was found that the governing failure mode would be row shear failure according to CSA 086-14, clause 10.4.4.4. This clause was used to estimate the maximum moment capacity that could be applied to the connection with respect to row shear in tension; however, the reduction factor for side members was not applied, as based on the research by Mohammad and Quenneville (2001). As per their study, members with

a slotted cut did not see the same reduction in row shear out capacity as those composed of two separate wood members. The test specimens of this thesis research project were stored indoors and maintained a moisture content of approximately 12% over the course of the experimental program.

The concealed T-stub connectors were fabricated from 12.7 mm (1/2 inch) thick plates of 300W grade steel. The selected grade is commonly used in steel connections and has widespread commercial availability. The thickness was chosen to ensure failure occurred in either the glulam section or the bolts, while keeping the amount of wood cut to a minimum. The T-stub steel connector was secured to the glulam beams using commonly available A325M bolts that were selected to ensure that the entire wood section of the side members was mobilized, compared to dowels or other more concealed fasteners. While the bolts and nuts ensured that the wood side members stayed parallel to the steel T-stub connector during loading.

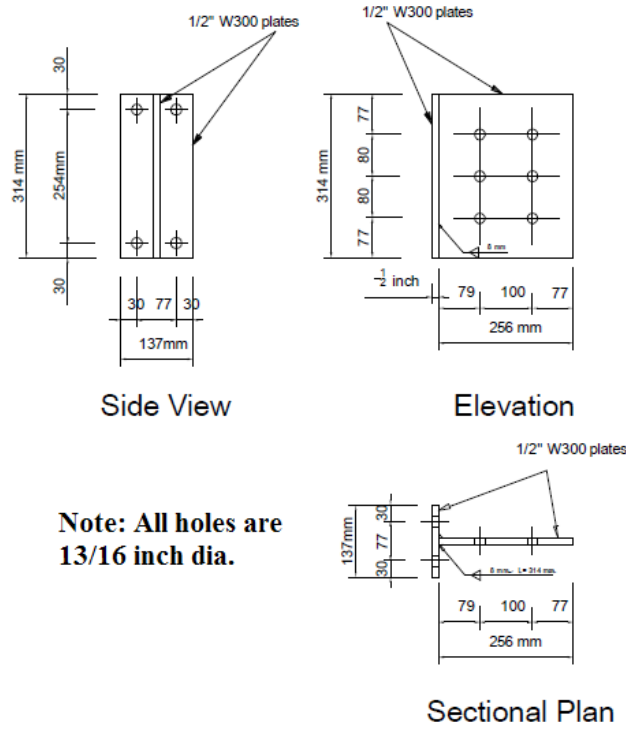
Based on the reviewed literature, it was understood that failure would occur in the wood around the connection due to brittle failure in the timber material. Therefore, any method of strengthening selected should be one that can be hypothesized to, or has been shown to, reduce the propagation of brittle failure in the wood and ideally should satisfy this requirement at both normal and elevated temperatures. The method of strengthening connections selected should also be readily available in Canada, relatively simple, and should rely on components that have been approved and codified for use in Canada as either fasteners or strengthening in axially loaded connections.

The screws selected for perpendicular-to-the-grain strengthening around the connection were SWG ASSY VG plus CSK[®] self-tapping screws measuring 300 mm in length and 8 mm in diameter. Self-tapping screws (STS) were chosen to act as effective method of strengthening as they are relatively easy and quick to install, and are also inexpensive and as previously discussed have performed well as a strengthening option for deteriorating wooden beams and columns. The screws are manufactured from carbon steel and have a bending yield strength of 1015 MPa and an un-factored shear strength of 641 MPa (CCMC, 2014). The STS length was chosen so as to provide strengthening through the majority of the beam's depth, and the smallest diameter was chosen to minimize the amount of wood material taken off the beam cross section. The yield and shear strengths of the STS were used to predict the maximum moment capacity of the strengthened sections, as based on work done on the unstrengthened sections. It was predicted that row shear

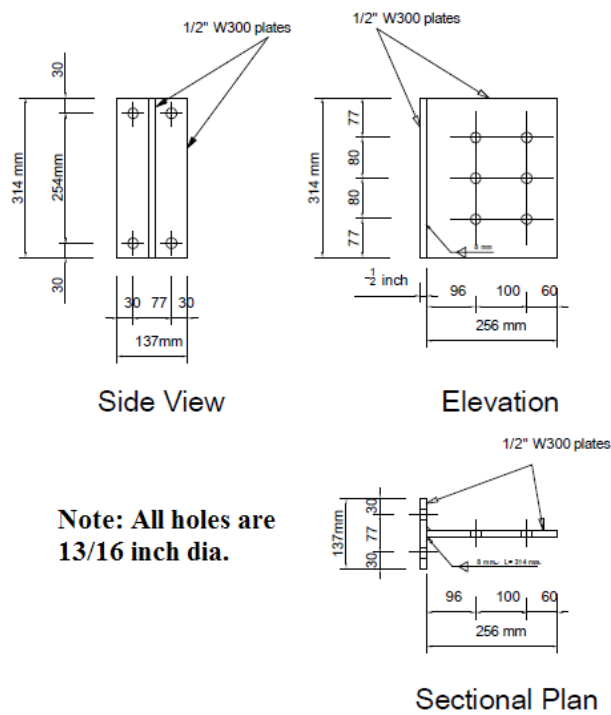
out would not occur, or would not result in moment-capacity reduction until the STSs began to yield or sheared. It was also found that the screws would yield before shearing based on the predicted failure modes; however, for the six-bolt connections the maximum moment capacity based on failure in shear was only marginally greater than that predicted by failure in bending. The capacity of the connections with STS strengthening was also calculated using CSA 086-14 clause 10.4.4.3.2 to determine the yielding capacity of the STS strengthening, where the capacity was found to be less than that of the unstrengthened connections, and so were not considered.

3.3.2 Test Assembly Details and Fabrication Process

In addition to the STS strengthening effect on the beam-to-column connections' moment-resisting capacity, two study parameters, the bolt end distance and number of bolts, were investigated in this research project. Each test specimen's beam-to column connection assembly included two beam sections, simultaneously testing two connections with the same bolt and end distance configuration. Two test groups had a bolt end distance of four-times bolt diameter, while the other two had five-times bolt diameter end distance connections. For each test assembly having the same end distance, two bolt configurations were used: four A325M bolts in two rows and six A325M bolts in three rows. The bolt's end distance is defined as the distance between the centre line of the first column of bolts and the interface of the beam end with the steel connector flange. Detailed measurements of the steel T-stub connectors used for all tests with four and five-times bolt diameter end distances are shown in Figures 3.7(a) and (b), respectively. As the bolts and wood sections were expected to fail well before the steel plate, plates with six bolt holes were used in all tests.



(a) Steel T-stub connector with four-times bolt diameter end distance.



(b) Steel T-stub connector with five-times bolt diameter end distance.

Figure 3.7 Dimensions of steel connector plates used for four both six bolt connections.

Two experiments were carried out for each connection configuration of end distance and number of bolts. Each test assembly consisted of two identical steel T-stub connectors, attached to each side of the supporting glulam column in the middle using four long 19.1 mm (3/4 inch) diameter fully-threaded steel rods. Four holes were drilled into the column section for each rod to pass through. An adequate number of holes were drilled into the beam sections to match the holes in the steel connectors' flanges. Holes in the beam sections and the steel plate were all sized to be 1 to 2 mm (1/16 inch) larger than the bolts' diameter in accordance with CSA-086-14. Also, holes in the beam were drilled with a spade bit and a vertical guide to keep the holes straight through the section, while holes in the steel plates were punched by the steel fabricator. The concealed steel-glulam beam-to-column connection configuration was accomplished by preparing a vertical slotted cut in each beam section using a portable band-saw mill, where the slot was cut to be 2 to 4 mm larger than the steel plate thickness. To accommodate the nuts attaching the steel connectors to the column via the long steel threaded rods, cylindrical notches were cut into the ends of the glulam beam sections. The locations of the notches, above and below the rows of the connecting bolts, placed them outside the potential pull-out path of the bolts in the glulam beams. The potential for slip was avoided by the tight tolerances around the bolt holes and slotted cut which ensured there was no visible gap between the beam end and the column and that all parts of the connection were in direct contact before loading occurred, bolts and nuts were hand tightened and then tightened to two thirds circumference with a wrench. In sixteen of the thirty-two tested connections, each beam section was strengthened with six self-tapping screws around the connection. Screws were installed perpendicularly to the wood grain from the tension side of the beam. Screws were installed in a row of three on both sides of the concealed steel plate, with the screws in each row located in the centre of the wood stress blocks resisting row-shear out during loading, Figure 3.8. Figure 3.9 shows a general test assembly with six bolts in three rows in each beam section. Relevant details of the eight assemblies tested and their test designations are summarized in Table 3.2.

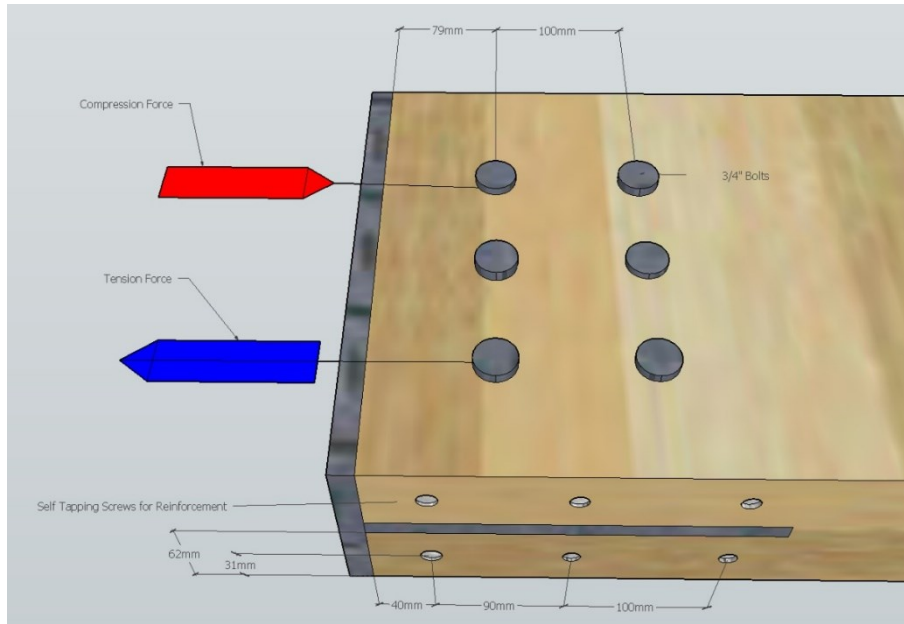


Figure 3.8 Steel connector with four-times bolt diameter end distance, six bolts and installation placement of STS strengthening.

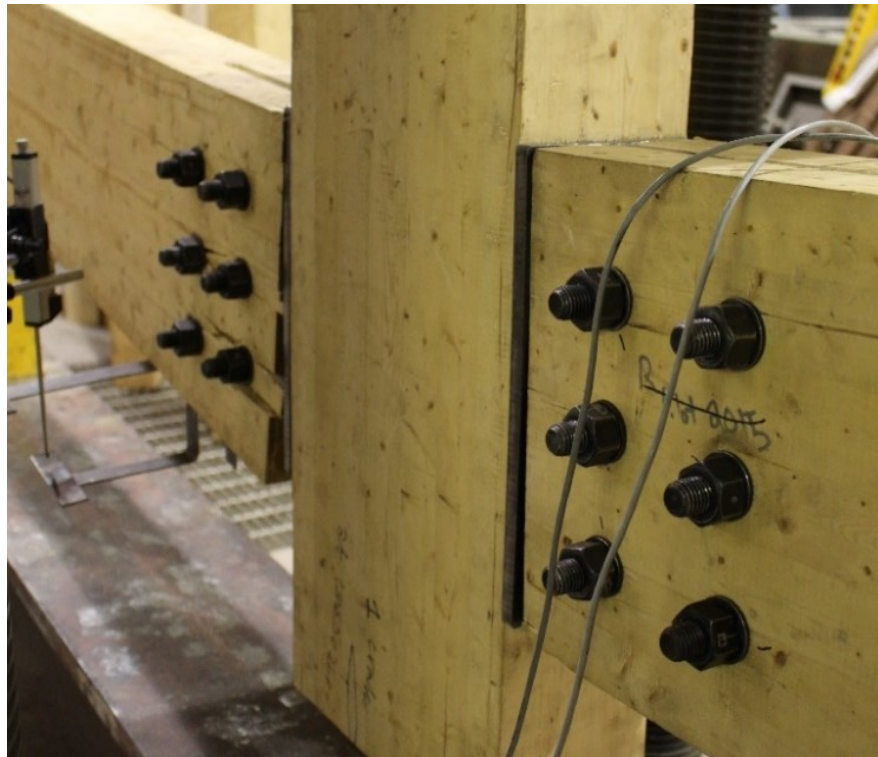


Figure 3.9 A general beam-to-column test assembly with six steel bolts in three rows.

Table 3.2 End distance and numbers of bolts used in test assemblies.

Test No.	End Distance	No. of Bolts	Use of STS
1	four-times bolt dia.	4	No
2	four-times bolt dia.	6	No
3	four-times bolt dia.	4	No
4	four-times bolt dia.	6	No
1S	five-times bolt dia.	4	Yes
2S	five-times bolt dia.	6	Yes
3S	five-times bolt dia.	4	Yes
4S	five-times bolt dia.	6	Yes

3.3.3 Test Setup and Procedure

Test assemblies were carried on two supports that were spaced 3200 mm apart and secured to a steel I-beam that had been placed within a large universal testing machine. Specimens were gradually loaded under displacement control at a rate of 2 mm/min until the beam-to-column assemblies failed. The connections' moment-resisting capacity, strength and modes of failure were evaluated, and the effects of changing test variables were observed. Vertical deflections were monitored using six linear variable differential transducers (LVDTs) and one draw-wire displacement sensor attached to each test assembly to capture the deflection at the assembly's centre point, near the supports and near the column. A layout of the installed LVDTs (T1 through T6) and the draw-wire displacement sensor (T7) on a general test setup with relevant dimensions are shown in Figure 3.10.

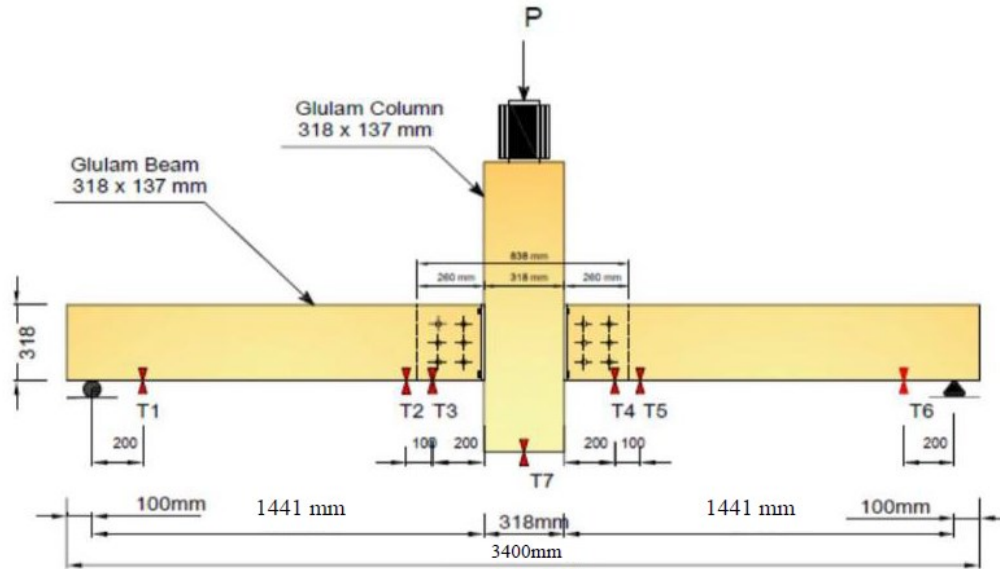


Figure 3.10 Test setup and dimensions of a general glulam beam-to-column test assembly.

LVDTs T1 and T6 measured the vertical displacements of the beams near the left and right-side supports, respectively. LVDTs T2 and T3 measured the vertical displacements of the beam on the left of the column, which later were used to calculate the left-side connection rotations; while the measurements of T4 and T5 were used to calculate the connection rotations on the right side. The draw-wire displacement sensor T7 measured the deflections at the assembly's centre point. During testing, damage to the glulam beams due to loading was marked and numbered to document the propagation and nature of the failure in the test assembly as the applied moments and the corresponding connection rotations were gradually increased. The rotation of the wood beam relative to the T-stubs was measured by the LDVTS, based on the selected design, no rotation, slip or translation was anticipated to occur between the column and steel T-stub connectors, with failure predicted to occur in the bolts or the glulam section, resulting in rotation between the horizontal plane and the beams at the steel connector.

3.4 Experimental Testing at Elevated Temperatures

A total of sixteen beam-column test specimens consisting of four different glulam beam-to-column assemblies with and without perpendicular-to-the-grain strengthening were experimentally examined. All test assemblies were loaded with a monotonic load that was calculated based on previously documented failure modes in connections loaded to their maximum

capacity at normal temperatures. It was observed in this previous experimental program that the connection failed when an initial drop in its moment-resisting capacity was recorded due to brittle failure in the wood in contact with the bottom row of bolts under tensile stresses which experienced row shear out. Based on this information, a load was applied to the test assemblies that resulted in the connections undergoing 100% of the designed row-shear out capacity determined by Cl. 10.4.4.4 from the Canadian Wood Design Handbook (2015) (Equations 3.1 to 3.3).

Equation 3.1, Sum of factored row shear resistance for joint.

$$PR_{rT} = \Sigma(PR_{ri}) \quad \text{Eqn. (3.1)}$$

Equation 3.2, Factored row shear resistance of fasteners in a wood member i .

$$PR_{ri} = \phi_w (PR_{ijmin}) n_R K_d K_{sf} K_T \quad \text{Eqn. (3.2)}$$

Where;

$\phi_w = 0.7$ (factor for brittle failure)

$n_R = 1.0$ (No. of fastener rows)

$K_d K_{sf} K_T = 1.0$ (*Duration, Service and Treatment Factors*)

Equation 3.3, Minimum row shear resistance of any row in the connection of wood member i .

$$(PR_{ijmin}) = 1.2 f_v (K_{ls})(t) n_c (a_{ci}) \quad \text{Eqn. (3.3)}$$

Where;

$f_v = 2.5$ MPa (*Specified Shear Strength*)

$K_{ls} = 1.0$ or 0.65 (*Factor for member loaded surfaces*)

$t = 62$ mm (*member thickness*)

$n_c = 2$ (*number of connectors in row*)

$a_{ci} = 3.5D$ or $4.5D = 66$ mm or 88 mm (*loaded end distance*)

As previously mentioned, and based on the performance at ambient temperature of the concealed connections, the author determined that a side member reduction factor was not necessary for the loading of the test assemblies presented in this thesis. It was also observed that slotted members did not experience as drastic of a reduction in row-shear out resistance as those connection composed of two separate timber members, as per Mohammad and Quenneville (2001). This load was maintained on the test assembly over the course of the fire exposure period until the assembly met the required failure criterion. Based on these details, the following calculations were used to determine appropriate loading for the specimens. A sample of design calculations for the beam-to-column connection of four bolts with four-times bolt diameter end distance is shown in Equation 3.4.

Equation 3.4, Four bolt, four-times bolt diameter end distance connection.

$$PR_{r1} = \phi_w (PR_{ijmin}) n_R K_d K_{sf} K_T = (0.7) (1.0) ((PR_{ijmin}) \quad \text{Eqn. (3.4)}$$

Where:

$$\begin{aligned} (PR_{ijmin}) &= 1.2 f_v (K_{ls}) (t) n_c (a_{ci}) \\ &= 1.2 (2.5) (1.0) (62 \text{ mm}) (2) (66 \text{ mm}) = 24,552 \text{ N} \end{aligned}$$

Therefore:

$$\begin{aligned} PR_{r1} &= \phi_w (PR_{ijmin}) n_R K_d K_{sf} K_T \\ &= (0.7) (1.0) (24,552 \text{ N}) = 17\,186 \text{ N} = 17.2 \text{ kN} \end{aligned}$$

$$\text{So } PR_{r2} = 17.2 \text{ kN}$$

Therefore:

$$PR_{rT} = 17.2 * 2 = 34.4 \text{ kN}$$

Once the row-shear out resistance was determined, the load required to generate a moment equivalent to the tensile force causing row-shear failure was determined as follows;

The Couple moment between compression and tension bolts is equal to the force acting along one axial direction times the moment arm between the top and bottom rows, which was 160 mm for all connections.

$$M_i = PR_{rT} * L = PR_{rT} *(160 \text{ mm})$$

Force at support taken as;

$$\begin{aligned} \text{Support Reaction} &= M_i / \text{moment arm (distance from center of support to beam-steel interface)} \\ &= M_i / 1328 \text{ mm} \end{aligned}$$

The experimental load is twice the support reaction, as it is shared equally by the supports

Therefore;

$$PR_{rT} = 34.4 \text{ kN}$$

$$\text{Couple Moment} = 34.4 * 160 = 5504 \text{ kN.mm}$$

$$\text{Force at support} = 5504 / 1328 \text{ mm} = 4.14 \text{ kN}$$

$$\text{Applied Column Load} = 8.28 \text{ kN}$$

Based on these calculations, the maximum design load that can be applied to the column to generate a moment, using the design guidelines in CSA-086-14 with respect to row-shear out resistance, is 8.28 kN.

3.4.1 Test Assembly Details and Fabrication Process

Eight full-size glulam beam-column test assemblies, representing sixteen individual beam-to-column connection test samples, each consisted of a double glulam beam-to column connection, with one wood-steel-wood connection configuration underwent experimental testing while being exposed to CAN/ULC-S101 standard fire. Two test assemblies had a bolt end distance of four-times bolt diameter, while two other assemblies had five-times bolt diameter end distance on their connections. For each two tests having the same end distance, two different bolt configurations were used: four A325M bolts in two rows and six bolts in three rows. All four test assemblies were duplicated but with the addition of self tapping screws installed as perpendicular-to-the-grain strengthening. The steps to manufacture the connections for ambient temperature testing were followed for fire resistance testing. The relevant test details of the eight assemblies tested at elevated temperatures and their test designations are summarized in Table 3.3.

Table 3.3 Fire resistance tests matrix.

Test No.	End Distance	No. of Bolts	Use of STS
1F	four-times bolt dia.	4	NO
1FS	four-times bolt dia.	4	YES
2F	four-times bolt dia.	6	NO
2FS	four-times bolt dia.	6	YES
3F	five-times bolt dia.	4	NO
3FS	five-times bolt dia.	4	YES
4F	five-times bolt dia.	6	NO
4FS	five-times bolt dia.	6	YES

3.4.2 Elevated Temperature Test Setup and Procedure

Every test assembly was inversely carried on two supports that were spaced 3000 mm apart and located within a large-size fire testing furnace that is accommodated at Lakehead University's Fire Testing and Research Laboratory (LUFTRL), Figure 3.11.



Figure 3.11 General beam-to-column test assembly inside the furnace with thermocouples and instrumentation installed.

The supports were connected to a strong steel I-beam running beneath the center of the furnace across its width and is part of the steel frame structure that is used to elevate the furnace from the floor as well as to apply the transverse loading. A hydraulic jack installed above the furnace and attached to the steel supporting structure was used to apply the calculated design load to the test assembly by transferring the load into the furnace's middle top vent via an insulated steel post. Two draw-wire displacement sensors were installed outside the furnace to the supporting steel structure and attached to two ceramic rods that were inserted through the furnace's roof. The placed ceramic rods with the sensors attached to them captured the vertical deflections of the left and right beams at a distance of 200 mm from the beams respective beam-column interface, as shown in Figure 3.12. The measured displacements were used to determine the rotations of the beam-to-column connections, in conjunction with the displacement of the column measured by a third externally installed draw-wire displacement sensor attached to the top of the column at the middle. The temperature of the wood and steel components of each test assembly were measured by twelve high-temperature insulated k-type thermocouples installed only on the right-hand side connection as detailed in Figure 3.12.

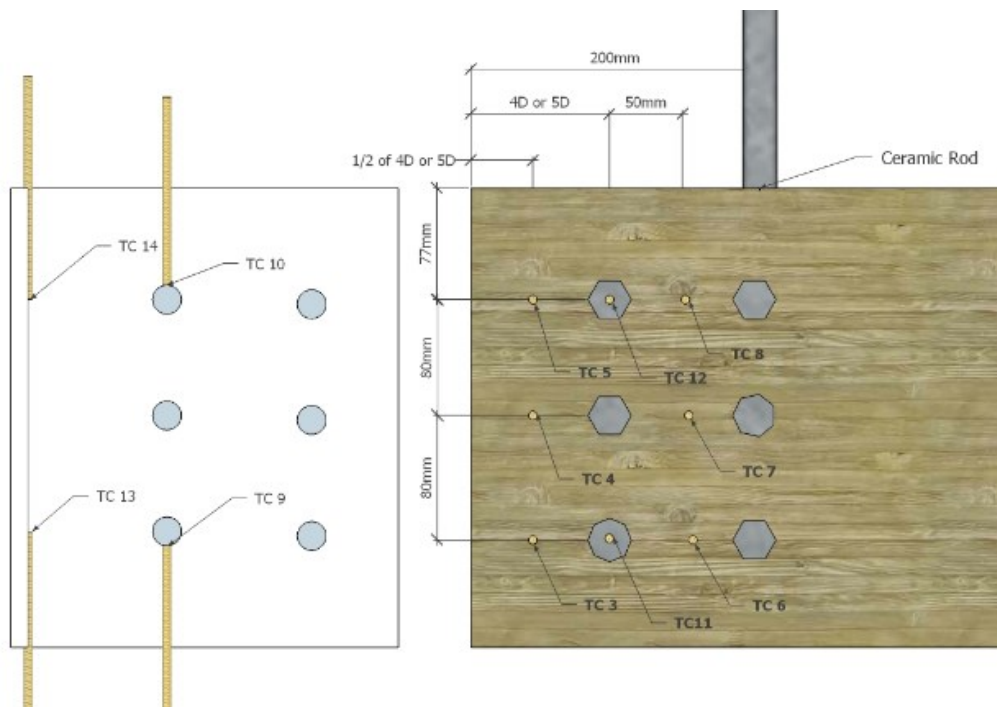


Figure 3.12 Thermocouples layout, steel plate left and wood beam right.

Six thermocouples were installed in the wood section at a depth of 30 mm, representative of the lateral midpoint of the wood sections on both side of the concealed steel plate. The other six thermocouples were used to measure the temperature of the steel components in the connection: four were installed on the plate and two on the bolt heads, providing data on the difference between the internal and external steel temperatures over the course of the fire resistance test.

The total load was applied in 25% increments and maintained for at least 30 minutes prior to test assembly undergoing fire exposure as per the CAN/CSA-S101 standard. The standard fire exposure was controlled and monitored by a built-in computer system and shielded thermocouples that are an integral component of the custom-designed fire testing furnace. An assembly with five-times bolt diameter end distance and having six bolts in three rows is shown undergoing standard fire exposure in Figure 3.13. During fire resistance testing, the relevant deflections were measured and once the sample was observed to reach a magnitude of deflection that coincided with failure at normal temperatures, the test was terminated. As post-test analysis, cross sectional cuts were made into the charred samples to determine the charring rate of the glulam assemblies, while the char layer around the connections was removed to highlight and confirm different failure modes.



Figure 3.13 Beam-column test assembly with six bolts in three rows exposed to a standard fire.

Chapter 4 Ambient Temperature Experimental Testing Results

As the monotonic load was applied on the test specimens, the vertical displacements measured by the LDVTs were used to calculate the angle of rotations between the glulam beam and the supporting column on each side. The load on the assembly was gradually increased until one of the connections reached its maximum moment capacity, after which rotations would continue increasing with no possibility of increasing the transverse load. The displacement measurements of both sides were found to be in good agreement over the test duration; however, results shown in this thesis are reflective of the connection that saw a marginally inferior performance. The moment applied to the connections was determined by using the measured values from a load cell connected to the universal testing machine which was applying the load to the specimen via the suspended glulam column. The resultant reaction calculated at each support was multiplied by the moment arm considered to be equal to the distance from the centre of the support to the end of the glulam beam at the connection. The rotation of the connections was determined from the change in displacement of the beam captured by the LDVTs located at the connections. The LDVTs at the pin supports were used to ensure that right and left-hand sides of the assembly experienced similar rotations at their respective pin supports, verifying that both connections were undergoing similar moment loads during testing.

A summary and comparison of the maximum moment-carrying capacities, yield moments, developed rotations and deformability ratios of the different beam-to-column connection configurations are shown in Table 4.1. The presented results are the average set of values based on the data gathered from four separate tested connections in each test assembly grouping.

Table 4.1 Summary of results for ambient temperature testing.

Test Assembly	No. of Bolts	Bolt's End Distance	Initial Stiffness [kN.m/rad] (kN.m/°)	M _(max) [kN.m]	Rot. at M _(max) [rad]	M _(yield) [kN.m]	Rot. at M _(yield) [rad]
1	4	4 <i>d</i>	1234.24 (21.53)	11.92	0.011	11.1	0.009
2	6	4 <i>d</i>	2138.25 (37.30)	26.51	0.016	19.1	0.009
3	4	5 <i>d</i>	1195.18 (20.85)	22.75	0.023	21.0	0.019
4	6	5 <i>d</i>	1532.24 (26.73)	34.98	0.027	31.8	0.021
1S	4	4 <i>d</i>	1260.50 (21.99)	28.78	0.025	26.2	0.021
2S	6	4 <i>d</i>	1584.25 (27.64)	35.11	0.031	28.0	0.020
3S	4	5 <i>d</i>	1676.31 (29.24)	46.21	0.032	42.0	0.025
4S	6	5 <i>d</i>	1854.66 (32.35)	53.44	0.047	48.5	0.027
Test Assembly	No. of Bolts	Bolt's End Distance	Drop in Load at Failure (%)	Est. M _(max) (kN.m)	Deformability Ratio	Ductility Ratio	
1	4	4 <i>d</i>	16	11.15	1.07	1.22	
2	6	4 <i>d</i>	10	22.3	1.39	1.77	
3	4	5 <i>d</i>	27	14.53	1.08	1.21	
4	6	5 <i>d</i>	15	28.53	1.10	1.29	
1S	4	4 <i>d</i>	8	21.22	1.10	1.19	
2S	6	4 <i>d</i>	6	42.44	1.25	1.55	
3S	4	5 <i>d</i>	20	21.22	1.10	1.28	
4S	6	5 <i>d</i>	10	42.44	1.10	1.74	

4.1 Effect of Bolt's End Distance

The moment-rotation relationships observed in Tests 1 and 3 using four bolts; with four and five-times bolt diameter end distance, respectively, are developed in Figure 4.1. When the bolt's end distance was increased from four to five-times bolt diameter, the connection moment capacity was increased by a factor of 1.90. Maximum moments observed were 11.92 kN.m in Test 1 and 22.75 kN.m in Test 3S, and the rotation values captured at these moments were 0.011 and 0.023 radians, respectively.

Tests 2 and 4 used six bolts in the connection with four and five-times bolt diameter end distances, respectively. Results for the test replicates were in good agreement, and the moment-rotation relationships developed are shown in Figure 4.2. When six bolts were used in the connection, the increase in the end distance from four to five-times bolt diameter increased the connection's maximum moment capacity by a factor of 1.32 times. A maximum moment of 26.51 kN.m was observed in Test 2 in comparison to 34.98 kN.m in Test 4. Also, the corresponding rotations observed for these moments were 0.016 and 0.027 radians, respectively. It was observed that the effect of the bolt's end distance was significant on the maximum moment capacity of the connections of both four and six bolt connections. It was also observed that connections with four-times bolt diameter end distance had a stiffer initial response than the connections with five-times bolt diameter end distance. As the end distance is reduced, it can be expected that the shorter length of wood engaged by the bolts in row shear out responds to loading sooner than that of the connections with five-times bolt diameter end distance, which may see a greater load distributed across the wood between the end of the beam and the bolts, before the connection fully responds.

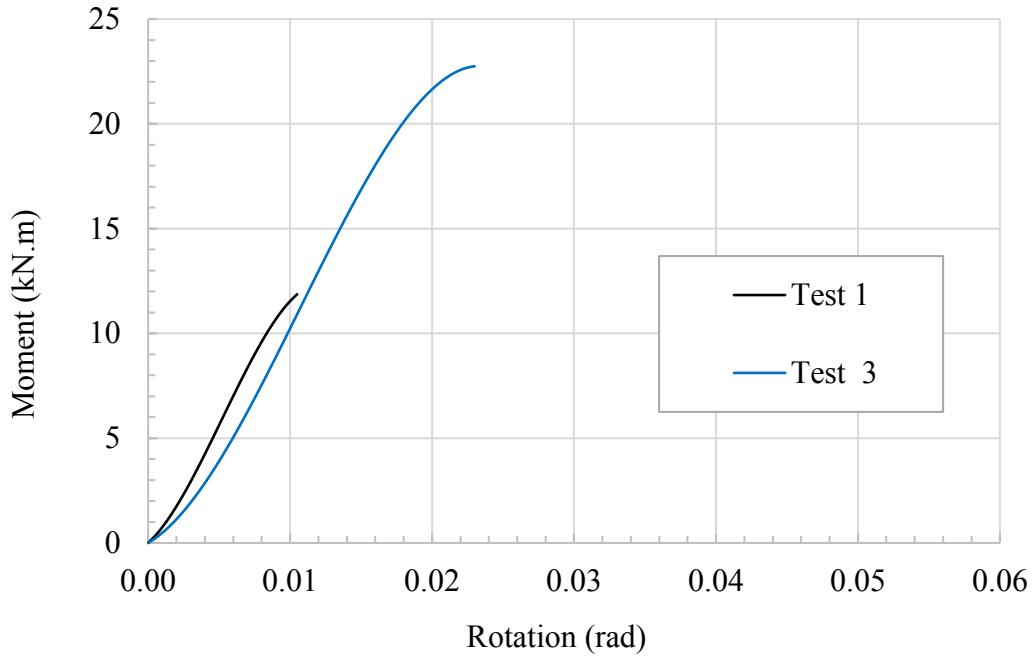


Figure 4.1 Moment-rotation relationships of test assemblies 1 and 3 using four bolts with four and five-times bolt dia. end distance, respectively.

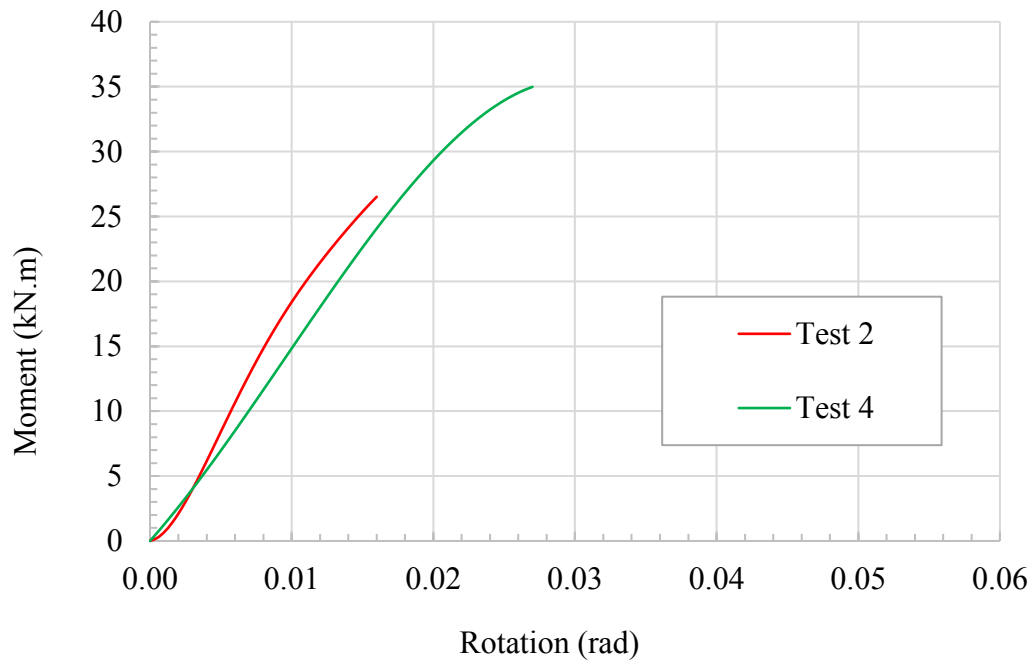


Figure 4.2 Moment-rotation relationships of test assemblies 2 and 4 using six bolts with four and five-times bolt dia. end distance, respectively.

The moment-rotation relationships observed in Tests 1S and 3S using four bolts, with four and five-times bolt diameter end distances, respectively, are developed in Figure 4.3. When the bolt's end distance was increased from four to five-times bolt diameter, the connection moment capacity was increased by a factor of 1.6. Maximum moments observed were 28.78 kN.m in Test 1S and 46.21 kN.m in Test BS, and the rotation values captured at these moments were 0.025 and 0.032 radians, respectively.

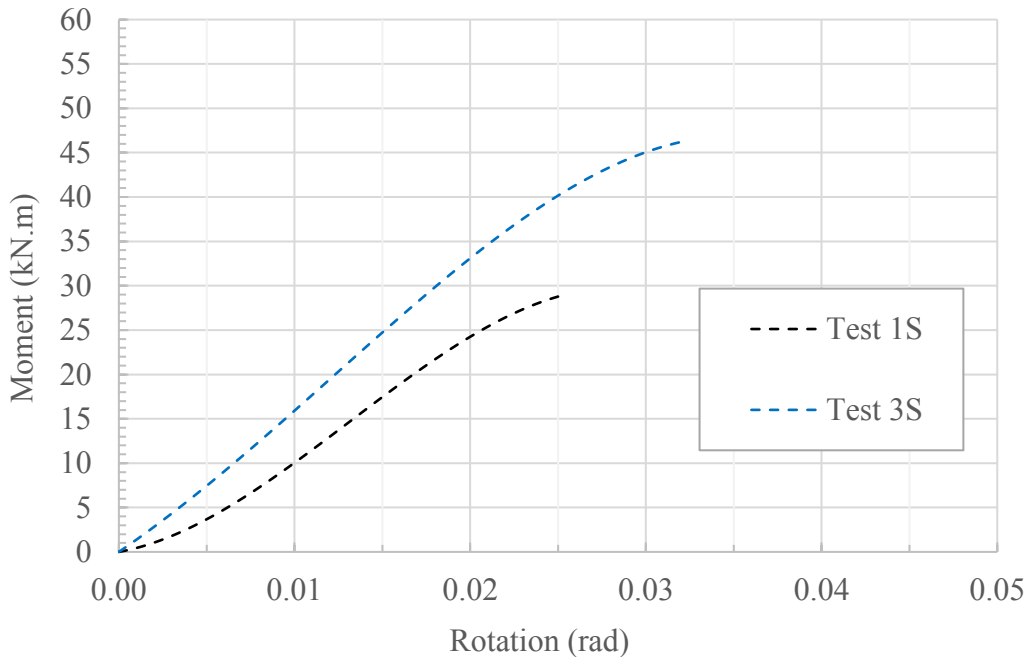


Figure 4.3 Moment-rotation relationships of test assemblies 1S and 3S using four bolts with four and five-times bolt dia. end distance, respectively.

Tests 2S and 4S used six bolts in the connections of four and five-times bolt diameter end distances, respectively. Results for the test replicates were in good agreement, and the curves developed are shown in Figure 4.4. When six bolts were used in a STS-strengthened connection, the increase in the end distance from four to five-times bolt diameter increased the connection's maximum moment capacity by a factor of 1.5. A maximum moment of 35.11 kN.m was observed in Test 2S in comparison to Test 4S with a maximum moment of 53.44 kN.m. Also, the corresponding rotations observed for these moments were 0.031 and 0.047 radians, respectively. It was observed that the effect of the bolt's end distance was considerable on the maximum moment capacity of the connections of both four and six bolt connections. It was also observed that STS-

strengthened connections having four bolts with four-times bolt diameter end distance had a reduced initial stiffness response than those with five-times bolt diameter end distance. As the end distance is reduced, it can be expected that the shorter length of wood engaged by the bolts in row shear out responds to loading sooner than the connections with five-times bolt diameter end distance. This reduced distance to the STS, sees the connections respond sooner to loading than the strengthened connection with five-times bolt diameter end distance, where the distance to the perpendicular-to-the-grain strengthening screws is greater. However, in connections with six bolts, the connections with five-times bolt diameter end distance had a stiffer initial response than those with four-times bolt end distance. This may be a result of the STS-strengthening taking up the load sooner and beginning to yield as the connections with six bolts experienced greater loading than those with only four bolts.

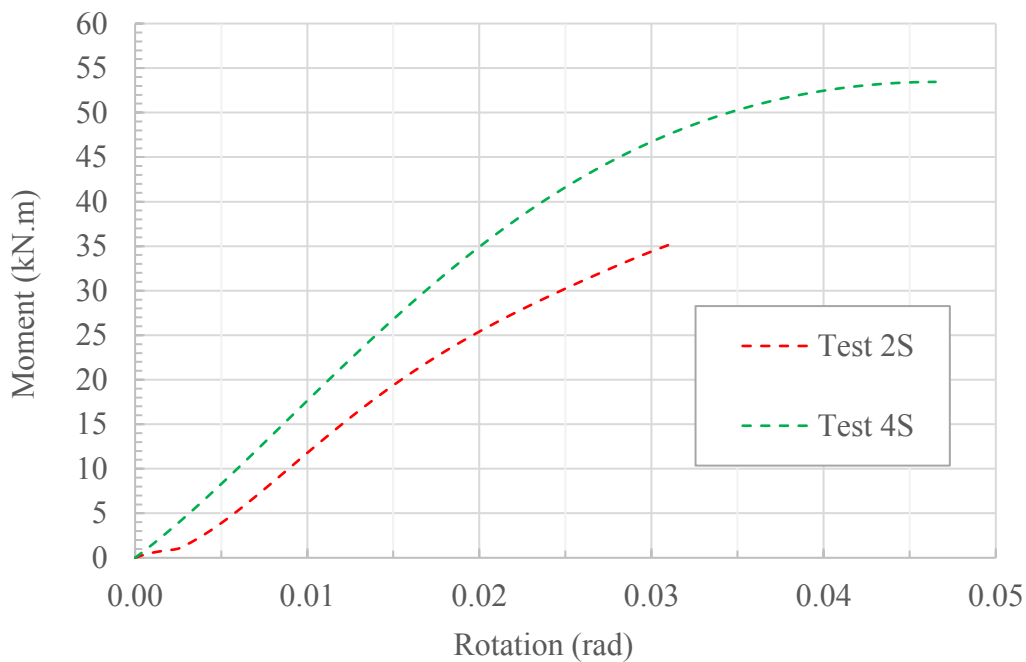


Figure 4.4 Moment-rotation relationships of test assemblies 2S and 4S using six bolts with four and five-times bolt dia. end distance, respectively.

4.2 Effect of Number of Bolts

A reduced bolt's end distance of four-times bolt diameter is featured in Tests 1 and 2, connected with four and six bolts, respectively. As illustrated by the moment-rotation relationship curves in Figure 4.5, increasing the number of bolts in the STS-strengthened connections, while keeping the end distances the same, resulted in a marginal increase in the connection's maximum moment capacity. The maximum moment sustained by the beam-to-column connection of Test 1, with four bolts, was 11.92 kN.m. In comparison, the maximum moment sustained by Test 2, with six bolts, was 26.51 kN.m, reflecting a moment increase by a factor of 2.2. An end distance of five-times bolt diameter was utilized in Tests 3 and 4, with four and six bolts, respectively. The moment-rotation relationship trends observed in this comparison were similar, as highlighted in Figure 4.6. A maximum moment of 22.75 kN.m was sustained by Test 3 connections; however, by increasing the number of bolts to six, the moment capacity of Test 4 connection was raised by a factor of 1.53, to approximately 34.98 kN.m. The respective rotations for the maximum moments for Tests 1 and 2, were 0.011 and 0.016, respectively; while Tests 3 and 4 saw rotations at their maximum moments of 0.023 and 0.027, respectively. The test assemblies with six bolts saw the promotion of brittle failure modes, predominantly wood splitting, to a greater extent than that experienced by the connections with four bolts. Also, increasing the number of bolts, increased the initial stiffness of the connections with both end distances, four and five-times bolt diameter, and it increased the connection's maximum moments substantially with only a small increase in the rotation values at failure.

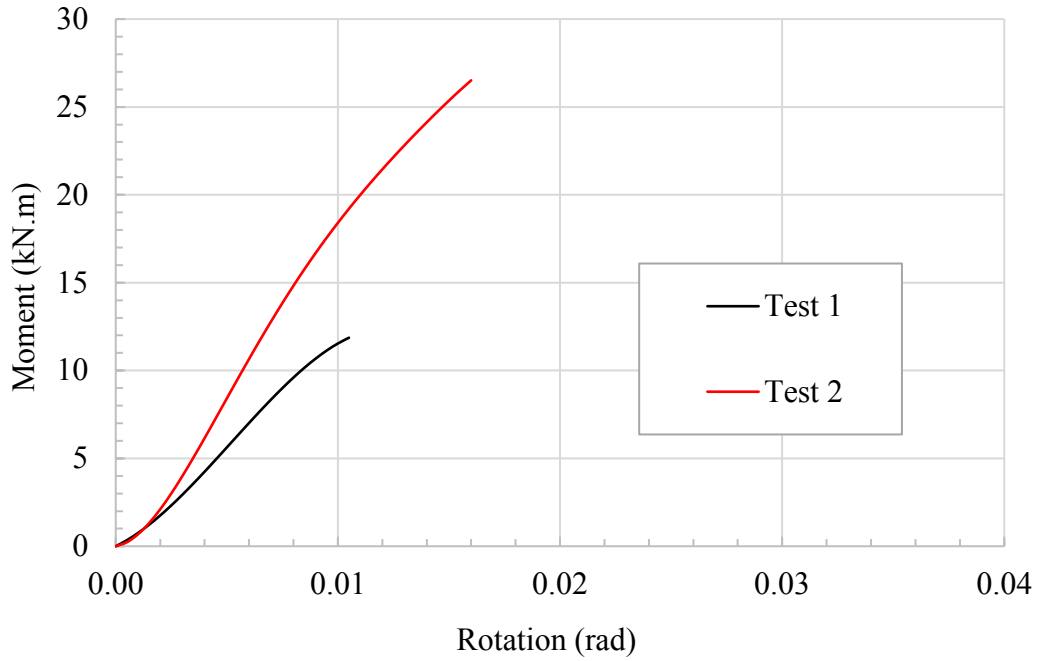


Figure 4.5 Moment-rotation relationships of test assemblies 1 and 2 using four and six bolts with four-times bolt dia. end distance, respectively.

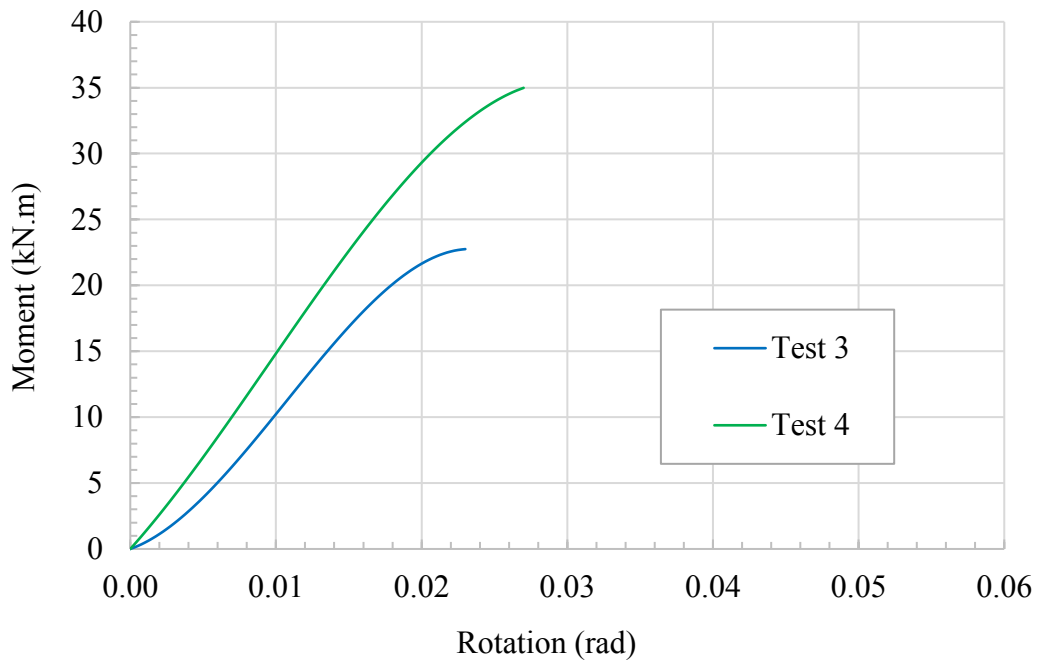


Figure 4.6 Moment-rotation relationships of test assemblies 3 and 4 using four and six bolts with five-times bolt dia. end distance, respectively.

A reduced bolt's end distance of four-times bolt diameter is featured in Tests 1S and 2S, connected with four and six bolts, respectively. As illustrated by the moment-rotation relationship curves in Figure 4.7, increasing the number of bolts in the STS-strengthened connections, while keeping the end distances the same, resulted in a marginal increase in the connection's maximum moment capacity. The maximum moment sustained by the beam-to-column connection of Test 1S, with four bolts, was 28.78 kN.m. In comparison, the maximum moment sustained by Test 2S, with six bolts, was 35.11 kN.m, reflecting a moment capacity increase by a factor of 1.2. An end distance of five-times bolt diameter was utilized in Tests 3S and 4S, with four and six bolts, respectively. The moment-rotation relationship trends observed in this comparison were similar, as highlighted in Figure 4.8. A maximum moment of 46.21 kN.m was sustained by Test 3S connections; however, by increasing the number of bolts to six, the moment capacity of Test 4S connection was raised by a factor of 1.15, to approximately 53.44 kN.m.

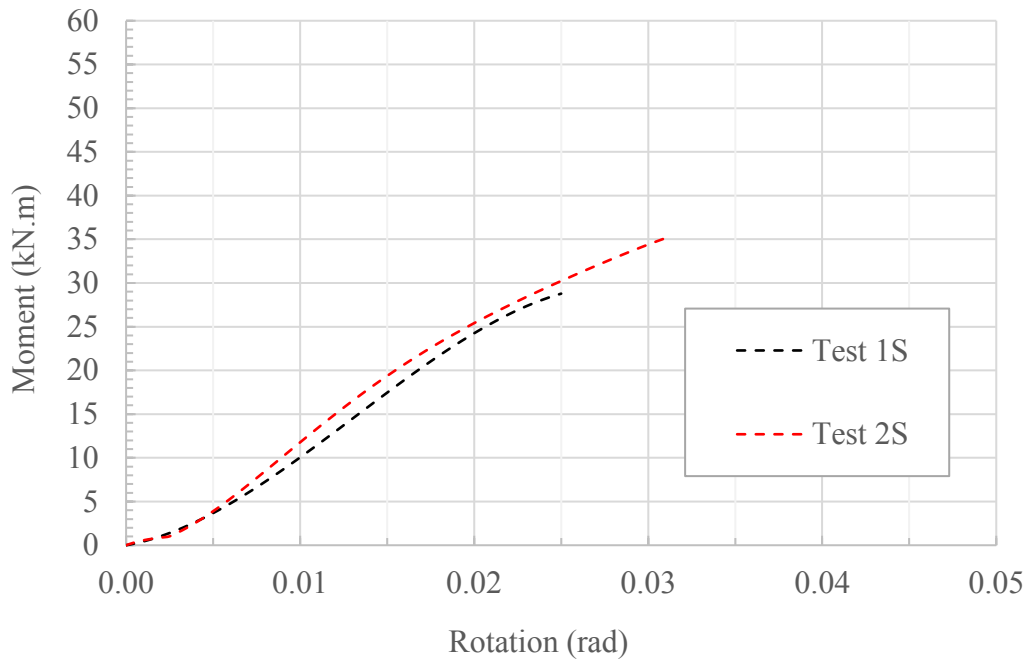


Figure 4.7 Moment-rotation relationships of test assemblies 1S and 2S using four and six bolts with four-times bolt dia. end distance, respectively (both STS-strengthened).

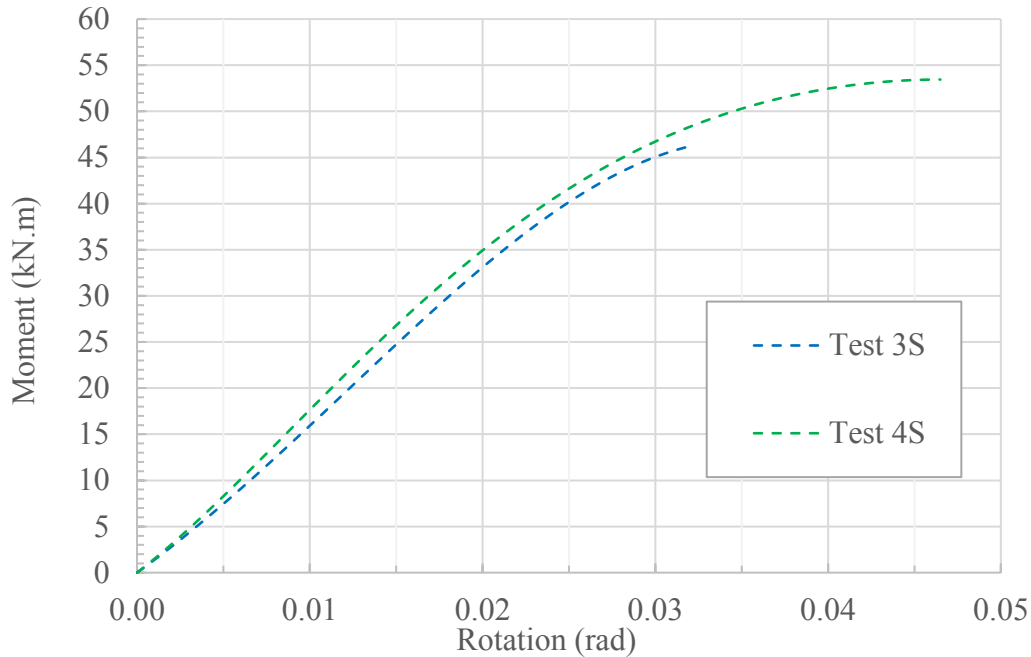


Figure 4.8 Moment-rotation relationships of test assemblies 3S and 4S using four and six bolts with five-times bolt dia. end distance, respectively (both STS-strengthened).

The strengthened test assemblies with six bolts generally achieved more ductile behaviour when compared to the test assemblies with four bolts. This was contrary to the previously-observed results for the same connection without strengthening that saw the promotion of brittle failure modes when the number of bolts was increased. This suggests that reinforcing a connection prone to brittle failure with STS provided a source of energy dissipation that eliminated the brittle failure modes that are characterized by a sudden loss in the moment-resisting capacity of the connection. In addition, increasing the number of bolts from four to six bolts, increased the connection's initial stiffness.

4.3 Effect of STS Strengthening

Figures 4.9 through 4.12 illustrate the effect of self-tapping screws (STS) strengthening on the moment-rotation relationships of all four test groups. Figures 4.9 and 4.11 show that four-bolt connections in Tests 1 and 3, with four and five-times bolt diameter end distance, respectively, saw increase in the connection's maximum moment capacity. In Figure 4.10, similar trends are showcased for connections that utilized six bolts with end distance of four-times bolt diameter; while Figure 4.12 shows the STS reinforcing effects on six-bolt connections but with end distance

of five-times bolt diameter. STS strengthening increased the moment-carrying capacity of connections of four-times bolt diameter end distance with both four and six bolts by a factor of 2.4 and 1.3, respectively. For connections of five-times bolt diameter end distance, strengthening increased the maximum moment capacity of four and six-bolt connections by a factor of 2.0 and 1.5, respectively. The incremental increase in the moment capacity was greater for connections with four bolts than those with six bolts. The increased reservoir for energy dissipation provided by strengthened connections with six bolts promoted more ductile failure modes in the connections as evidenced by comparing the shape of the curves of Tests 2S and 4S from Figures 4.10 and 4.12, respectively, with the comparable moment-rotation relationship curves. Moreover, STS strengthening increased the initial stiffness of the connections with five-times bolt diameter by a factor of 1.4 for connections with four bolts and by a factor of 1.2 for six-bolt connections. However, strengthening had no considerable effect on the initial stiffness of four-bolt connections with an end distance of four-times bolt diameter, and it actually reduced the initial stiffness substantially for those connections with six bolts and four-times bolt diameter end distance. Connections with STS strengthening also experienced greater rotation values before failure. Tests with four-times bolt diameter end distance had their rotational resistance increased by factors of 2.3 and 1.9 for four and six-bolt connections, respectively. With the addition of STS strengthening, four and six-bolt connections with an end distance of five-times bolt diameter had their rotational resistance increased by a factor of 1.4 and 1.7, respectively. Generally, unstrengthened connections failed via splitting failure through the area of wood resisting row shear out applied by the tensile forces developed in the connection resisting the moment. STS-strengthened connections did not experience any splitting failure, but always failed in row shear once the STS yielded under the stresses developed due to the applied loads. While the connections with five-times bolt diameter end distance, saw an increase in the initial stiffness compared to similar but unstrengthened connections with the same end distance.

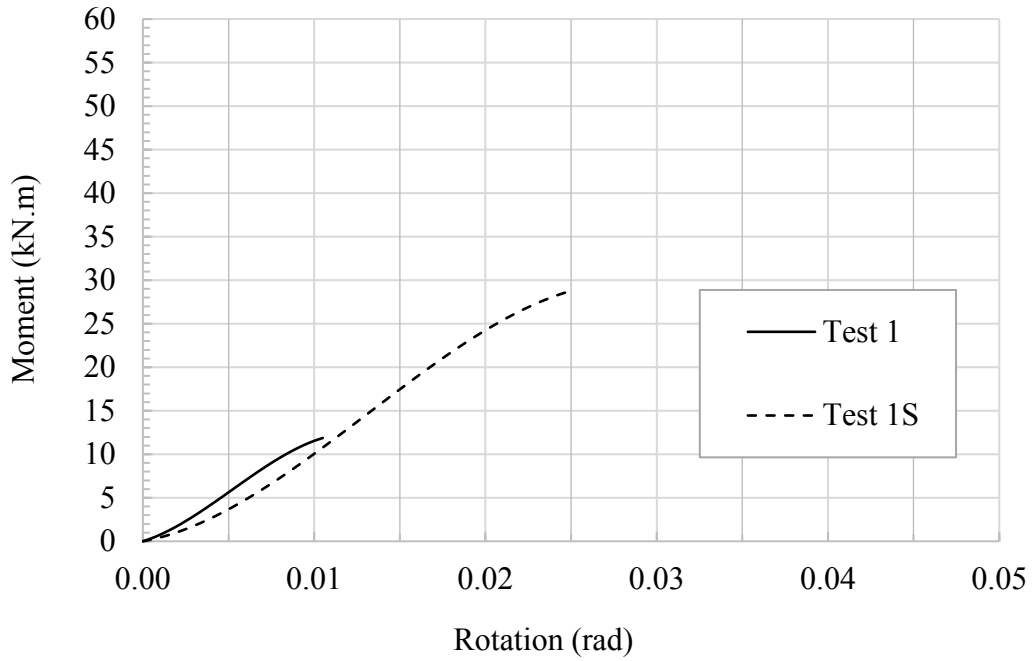


Figure 4.9 Moment-rotation relationships for assemblies in test groups 1 and 1S using four bolts and four-times bolt dia. end distance, unstrengthened vs. strengthened, respectively.

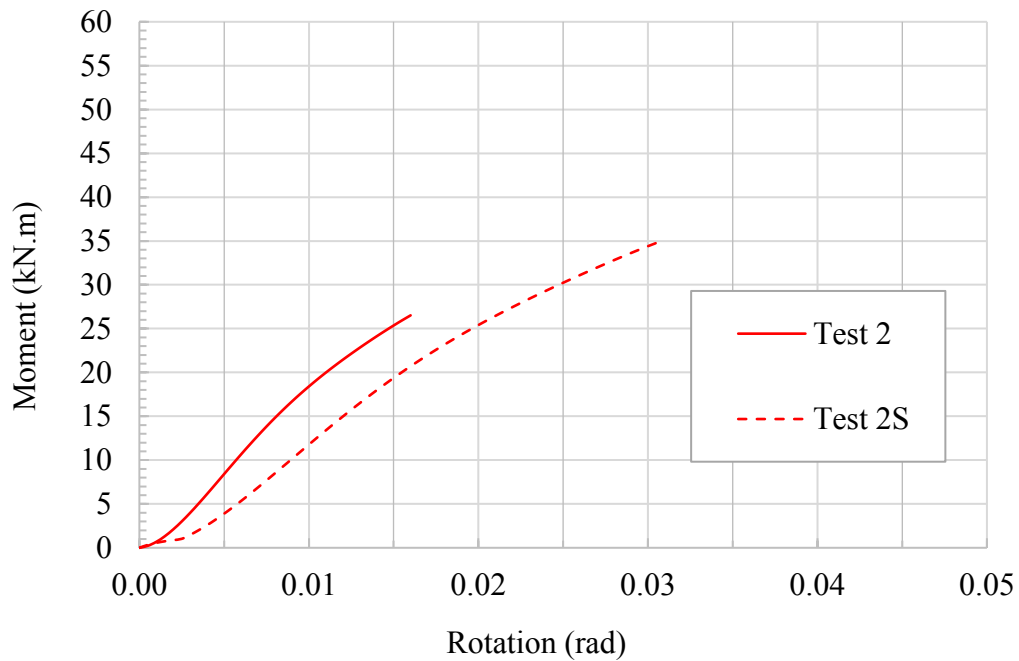


Figure 4.10 Moment-rotation relationships for assemblies in test groups 2 and 2S using six bolts and four-times bolt dia. end distance, unstrengthened vs. strengthened, respectively.

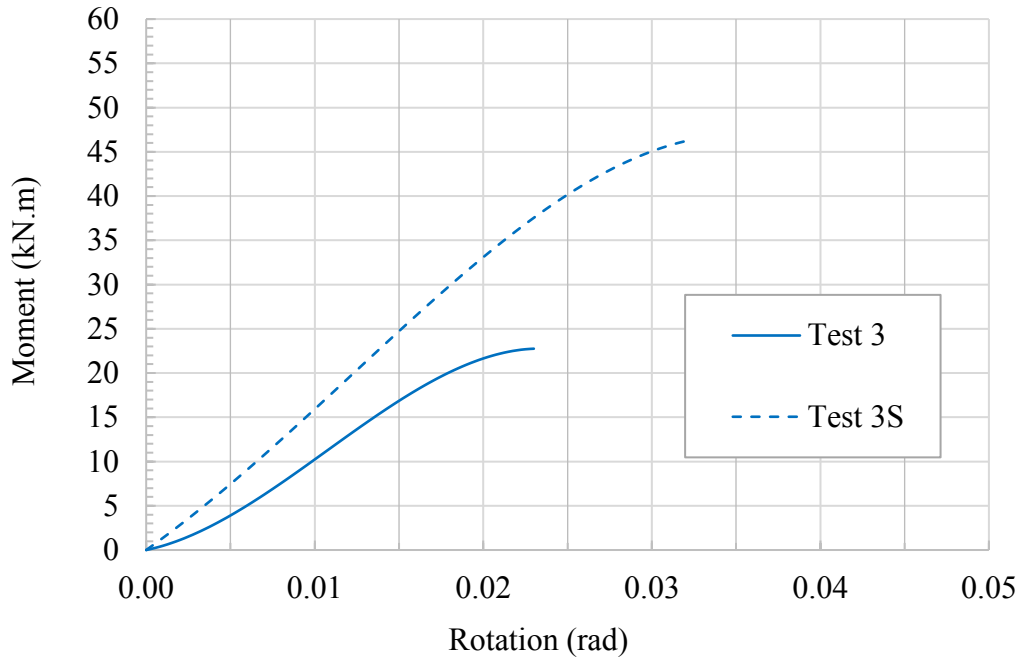


Figure 4.11 Moment-rotation relationships for assemblies in test groups 3 and 3S using four bolts and five-times bolt dia. end distance, unstrengthened vs. strengthened, respectively.

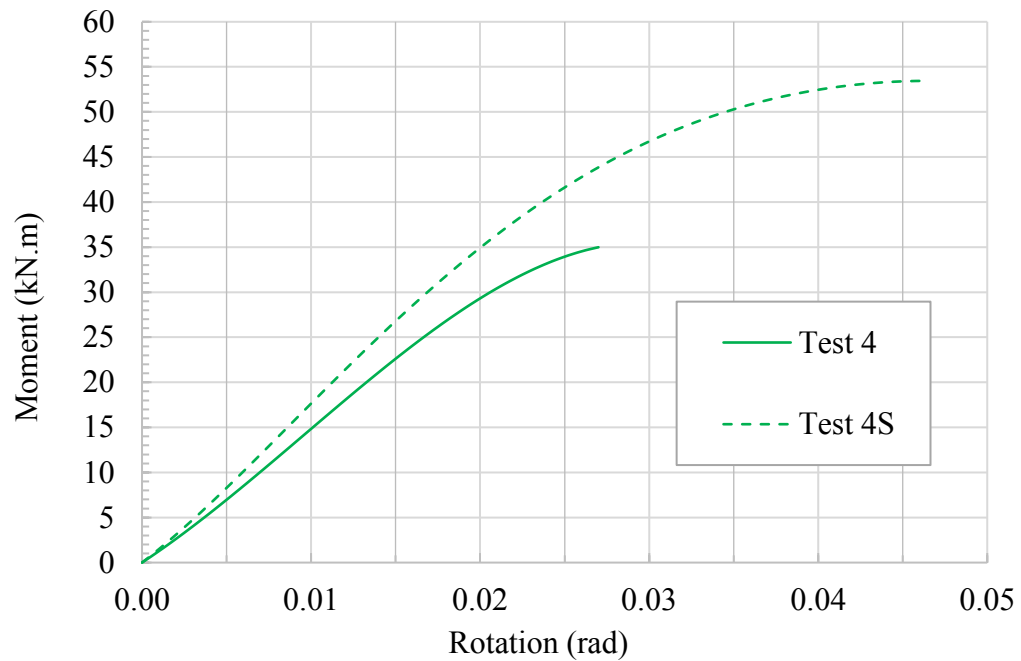


Figure 4.12 Moment-rotation relationships for assemblies in test groups 4 and 4S using six bolts and five-times bolt dia. end distance, unstrengthened vs. strengthened, respectively.

4.4 Observed Failure Modes

A number of brittle failure modes such as, row shear-out and splitting were observed in all test assemblies. A glulam beam-to-column wood-steel-wood connection loaded to failure can be seen in Figure 4.13. The steel plates experienced no deformation for all tests, while steel bolts experienced minimal deformations in some of the test assemblies, in particular those using six bolts. For all connections, failure was first observed to occur along the line of the bottom row of bolts, where the developed tensile forces are. Failure along this row resulted in splitting or pull-out of the wood between the end of the beam and the first bolt, then between the first bolt and second bolt in the row. This failure typically continued to propagate past the bolt farthest from the end of the beam as a longer split in the wood. Predominantly, all unstrengthened connections failed via splitting through the section of wood resisting row shear, before full row shear occurred. In the four-bolt connections, brittle failure modes would then begin to occur along the line of the top row of bolts, and eventually followed similar trends to the failure seen along the axis of the bottom row of bolts. Figures 4.14 and 4.15 show these failure modes for Tests 1 and 3, both connected with four bolts and having four and five-times bolt diameter end distances, respectively.



Figure 4.13 Typical observed glulam connection failure modes.

These figures also show the observed splitting failure that would occur at the interface between the wood fibres under compression and those under tension when the top row of bolts were mobilized to resist the rotation of the beam after the initial failure due to splitting at the bottom row (highlighted by the green circle numbered 5 in Figure 4.14 and along the same plane in Figure 4.15).



Figure 4.14 Brittle failure mode in Test 1B with four bolts and four-times bolt diameter end distance.



Figure 4.15 Brittle failure mode in Test 3B with four bolts and five-times bolt diameter end distance.

In the six-bolt connections, splitting or shear-out of the wood along the middle row of bolts, or splitting above the top row of bolts would precede any failure along top row of bolts. Seen in Figures 4.16 and 4.17 are samples from Tests 2 and Tests 4, both connections secured with six bolts and having four and five-times bolt diameter end distance, respectively. It was observed that the failure modes in the glulam connections secured by six bolts in three rows were more severe, as the addition of extra bolts mobilized a greater portion of the wood cross section to resist the developed rotations under the applied loads.

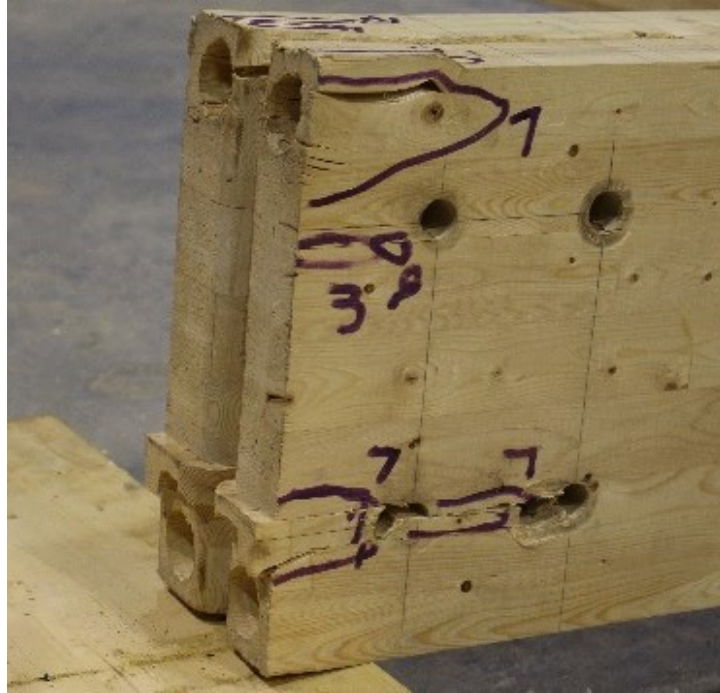


Figure 4.16 Brittle failure mode in Test 2B with six bolts and four-times bolt diameter end distance.

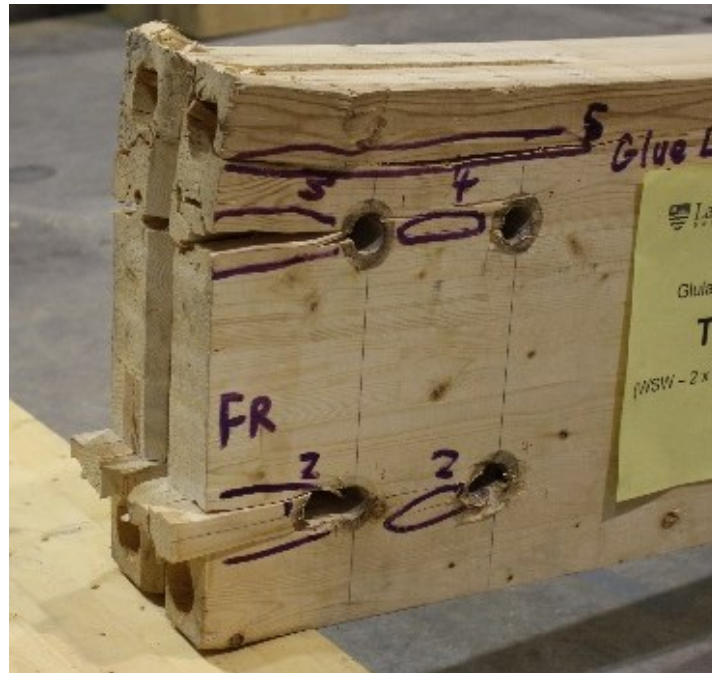


Figure 4.17 Brittle failure mode in Test 4B with six bolts and five-times bolt diameter end distance.

The strengthened connections' brittle failure modes, including row shear-out and splitting, were observed in all test assemblies, but to various extents. The steel T-stub connectors experienced no deformation in all tests, except for minimal bending in the flange away from the column of approximately two to three millimetres in some of the six-bolt connections. Several bolts were noticeably bended, as the yielded fasteners were more pronounced in the connections using six bolts, in particular the strengthened connections. Moreover, the perpendicular-to-the-grain strengthening provided by the STS resulted in increased bending in the flange of the steel connectors for all connections compared to those that had not been strengthened. Previously-observed failure modes in the unstrengthened connections did not always result in row shear, with the wood often failing by splitting, either between the bolts and the end of the beam or between the two columns of bolts. However, splitting did not occur with STS strengthening installed through the relevant wood stress blocks. This can be interpreted to the fact that the installed screws provided added cohesion around any internal defects within the wood section, promoting the formation of row shear failure over splitting. Brittle failure modes also occurred along the line of the top row of bolts where the beams were under compressive stresses from the applied moment. However, failure in this zone was characterized by a splitting in the wood between the first bolt and the end of the beam at the column side, followed by row shear in the wood section between the bolts. Figures 4.18 (a) and (b) show these failure modes in Test 1S and 3S, both connected with four bolts, strengthened with STS and having four and five-times bolt diameter end distances, respectively. As highlighted by Figures 4.18(a) and (b), no splitting failure occurred at the interface between the wood fibres under compression and those under tension when the top row of bolts in the strengthened connections was mobilized to resist the gradually increased beam rotations, as was also previously observed in the unstrengthened connections.



(a) Brittle failure modes in Test 1S with four bolts and four-times bolt diameter end distance.



b) Brittle failure modes in Test 3S with four bolts and five-times bolt diameter end distance

Figure 4.18 Typical failure modes for strengthened connections with four bolts

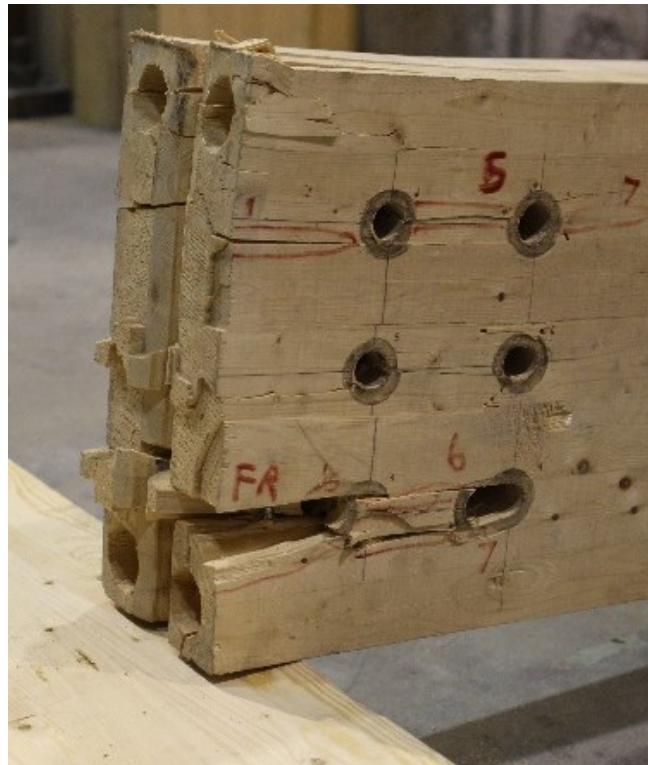
Failure in the connections with six bolts was preceded by row shear-out of the wood section along the middle row of bolts after the bottom row of bolts had already failed in row shear, or by splitting above the top row of bolts. Figures 4.19 (a) and (b) show the failure modes of the wood section in Tests 2S and 4S, both with six bolts and having four and five-times bolt diameter end distances, respectively.

Based on these failure modes, it can be difficult to effectively estimate the capacity of the STS-strengthened connections, as other sections of the beam may be carrying the load not just the bearing surface of the bolts and the wood surface resisting row shear out. As observed by the splitting at the compression flange, the beam was bearing against the column and the actions of the bolts worked at an angle that lies somewhere between the parallel and perpendicular axes relative to the wood grain. Additionally, it was observed that increasing the number of bolts from four in two rows to six in three rows resulted in more splitting and row shear, as well as more pronounced failure modes once the STS yielded. Even though the connections initial failure mode is ductile; however, strengthened connections eventually experienced more destructive and severe failure compared to unstrengthened connections. This can be interpreted as evidence that the STS first ensure that splitting does not occur before row shear; however, once row shear can occur, the STS resists the applied load until it yields. Once the strengthening yields, the wood is undergoing loading substantially over its capacity, causing rapid brittle failure to propagate through the wood section.

In summary, failure of the glulam beam-to-column connections would initially occur by splitting or row shear in unstrengthened connections, as splitting is indicative of deformities in the wood section that cause splitting to occur before row shear. Also, when the connection is strengthened, the STS effectively reduced the effects of any deformities in the wood, and ultimately prevented splitting. The failure in the strengthened connections then occurred once enough force was applied to cause row shear of the entire wood stress block resisting the applied moment which then transferred the load to the STS strengthening. The connection was able to sustain a greater applied moment until the STS strengthening yielded within the beam, causing the previously sheared rows of wood to shift and undergo row shear.



(a) Brittle failure modes in Test 2S with six bolts and four-times bolt diameter end distance.



(b) Brittle failure modes in Test 4S with six bolts and five-times bolt diameter end distance.

Figure 4.19 Typical failure modes for strengthened connections with six bolts.

Chapter 5 Fire Resistance Experimental Testing Results

As the test assemblies underwent exposure to a standard fire, the vertical displacements measured from the three draw-wire displacement sensors were used to calculate the gradual change in the angle of rotations of the glulam beam-to-column wood-steel-wood connections. The temperature of the wood section halfway between the steel plate and the external char layer were measured by thermocouples TC 3 through TC 8 that were placed in locations that corresponded to center of the wood sections resisting row shear out in the bolt rows exposed to either compressive or tensile forces and those along the neutral axis, Figure 3.12. Thermocouples TC 9 to TC 14 were used to measure the temperatures of the concealed steel plates along tensile and compressive planes, at the first column of bolts, at the fillet weld of the connection and of two of the bolt heads; one in the compression row and the other in the tension row. The rotation values for both test assembly's sides were found to be in good agreement, and the majority of the temperatures recorded by the thermocouples were found to be in good agreement within each test group and over all between the tests. In general, increasing the number of bolts increased the beam-to-column fire resistance time by a greater increment than that observed when increasing the end distance from four to five-times bolt diameter. Also, reinforcing the connection using STS resulted in an increased fire resistance time and a reduction in the occurrence of brittle failure modes. Table 5.1 provides a summary of the fire resistance experimental testing results for the sixteen beam-to-column connection samples, represented in eight fire resistance test groups. The test assembly was deemed to have failed once the connection failed to hold the applied load or its angle of rotation with the column became greater than 0.12 radians. A rotation of 0.12 radians was selected as this is approximately ten times greater than the rotation of Test 1 connection at ambient temperature failure. For the purpose of designing for fire resistance, it is understood that rotations and deflections can be much greater than that permissible at ambient temperature, as the main objective of safe fire resistance design is to avoid structural collapse rather than fulfilling any serviceability condition, such as limiting deflections and rotations. The unstrengthened connections failed by the chosen rotation failure criterion. While the strengthened connections mostly failed at much lower rotations, at about 0.06 radians, once the connection could no longer maintain the load. This is shown in the graphs as an extremely sudden increase in rotation values with an almost completely vertical line at the end of the time domain between 0.06 and 0.12 radians of rotation.

Table 5.1 Summary of fire resistance experimental testing results.

Assembly No.	End Distance	No. of Bolts	STS	Fire Resistance Time	
				Seconds	Minutes
1F	4 <i>d</i>	4	No	817.0	13.62
1FS	4 <i>d</i>	4	Yes	1020.0	17.00
2F	4 <i>d</i>	6	No	969.0	16.15
2FS	4 <i>d</i>	6	Yes	1092.0	18.20
3F	5 <i>d</i>	4	No	921.0	15.35
3FS	5 <i>d</i>	4	Yes	1028.0	17.13
4F	5 <i>d</i>	6	No	1050.0	17.50
4FS	5 <i>d</i>	6	Yes	1140.0	19.00

5.1 Effect of Bolt's End Distance

It was observed that the test assemblies underwent two different trends of increased rotations with time in all four tests. The connection rotation values slightly increased in a linear trend during the initial testing time (about 3 to 5 minutes); however, once enough time elapsed and the standard fire temperature elevated, the rotations increased exponentially over time until failure. As shown in Figure 5.1, increasing the bolt's end distance from four to five-times bolt diameter in the four-bolt connections incrementally increased the connection fire resistance time by a slightly greater margin than that seen when increasing the end distance in the six-bolt connections (Figure 5.2). For the four-bolt connections, increasing the end distance from four to five-times bolt diameter increased the fire resistance time by about 100 seconds. While for the six-bolt connections, increasing the bolt's end distance increased the fire resistance time by about 70 seconds. It was also observed that increasing the end distance did not change the rate at which rotations increased with time during failure, but it delayed the time at which more rapid failure would begin to occur in the connections.

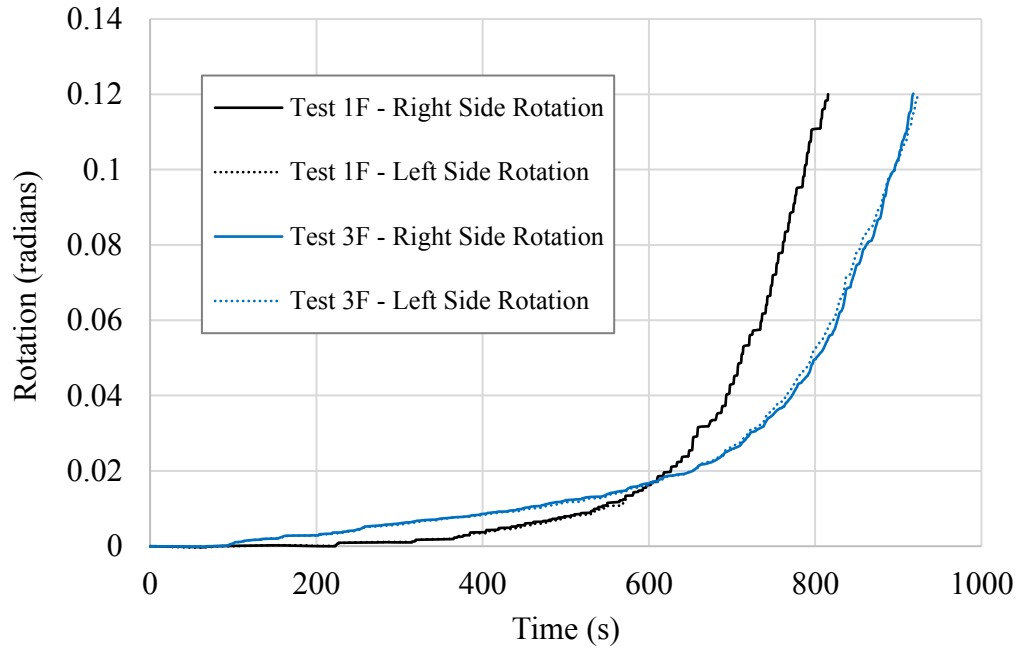


Figure 5.1 Time-rotation relationships developed to illustrate the effect of changing the bolt end distance in fire resistance Tests 1F and 3F, both with four bolts.

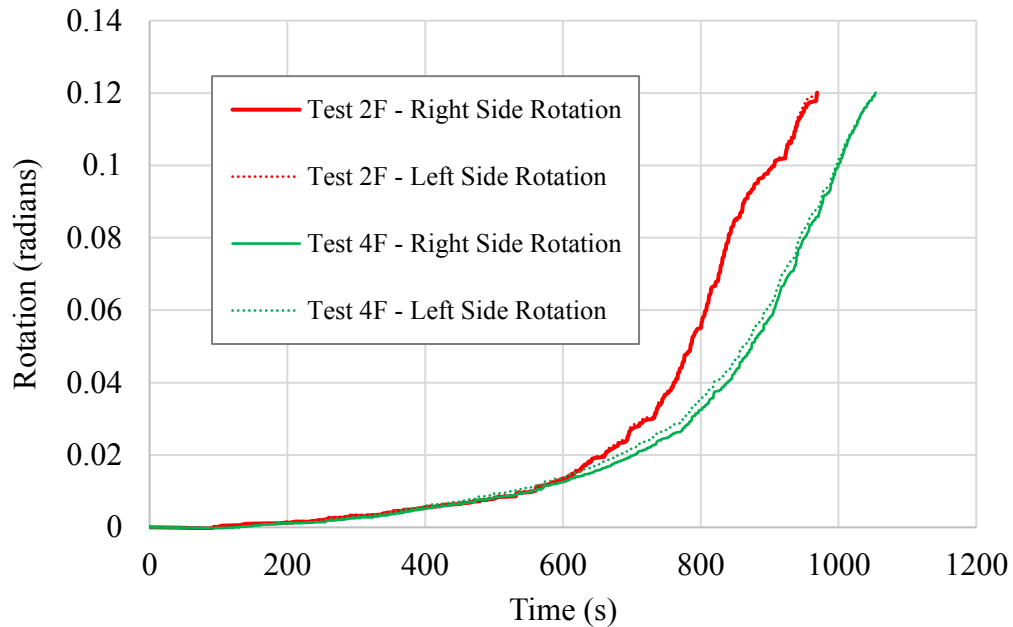


Figure 5.2 Time-rotation relationships developed to illustrate the effect of changing the bolt's end distance in fire resistance Tests 2F and 4F, both with six bolts.

For the STS-strengthened connections, increasing the bolt's end distance from four to five-times bolt diameter increased the fire resistance time by a lesser increment in the four-bolt connections than in the six-bolt connections (Figure 5.3 and Figure 5.4, respectively). However, increasing the bolt's end distance provided no additional fire resistance time for the strengthened four-bolt connections, while an increase in the bolt's end distance for the six-bolt connections increased the fire resistance time by about 80 seconds. Changing the bolt's end distance was not observed to impact the rate at which rotations increased with time during failure; however, in the case of six-bolt connections, it delayed the time at which more rapid failure would begin to occur in the strengthened connection.

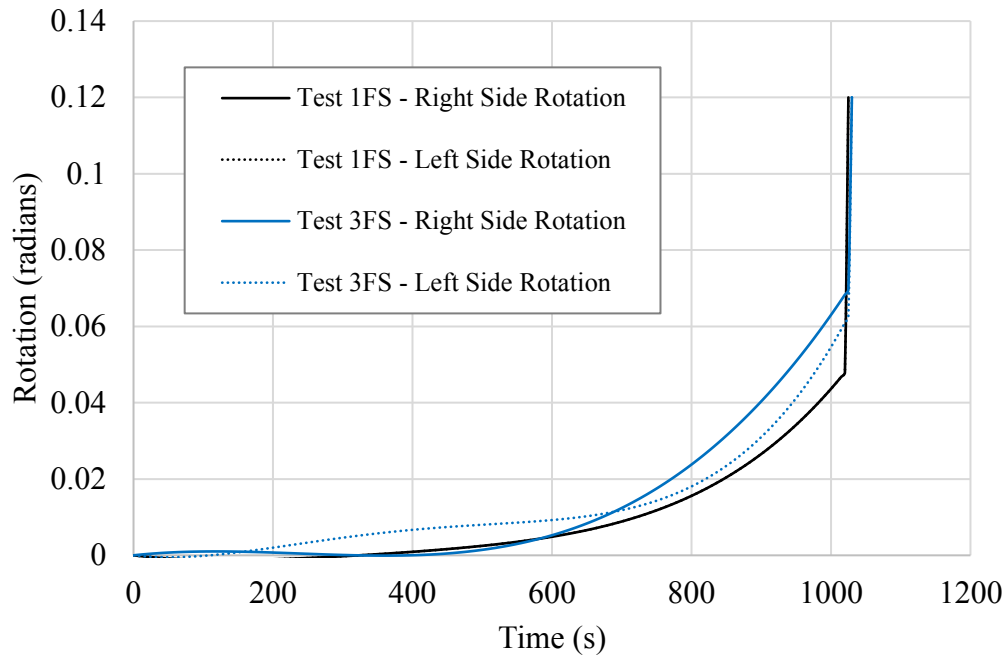


Figure 5.3 Time-rotation relationships developed to illustrate the effect of changing the bolt's end distance in fire resistance Tests 1FS and 3FS, both with four bolts.

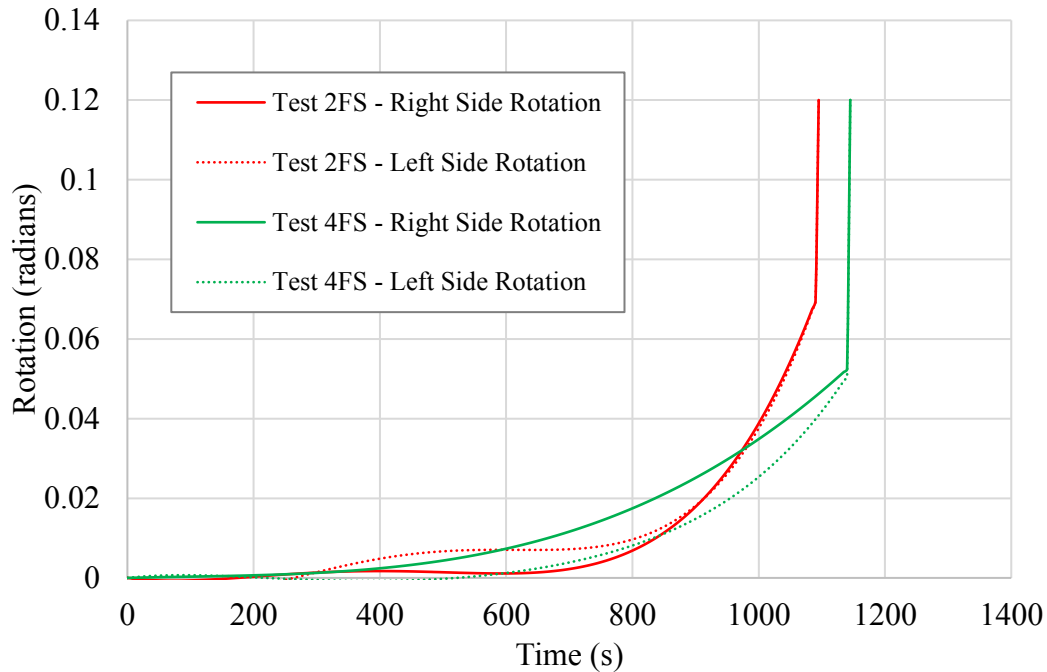


Figure 5.4 Time-rotation relationships developed to illustrate the effect of changing the bolt's end distance in fire resistance Tests 2FS and 4FS, both with six bolts.

5.2 Effect of Number of Bolts

Figures 5.5 and 5.6 illustrate the effect of changing the number of bolts from four bolts in two rows to six bolts in three rows for four and five-times bolt diameter end distance connection assemblies on the connection rotations and fire resistance, respectively. For the connections with four-times bolt diameter end distance, increasing the number of bolts from four to six increased the assembly fire resistance by about 165 seconds; while in the five-times bolt diameter end distance connections, changing the number of bolts increased the assembly fire resistance by about 135 seconds. The marginal increase in the fire performance of the different beam-to-column assemblies was more pronounced in the connection with an end distance of four-times bolt diameter when compared to the results of the connections with an end distance of five-times bolt diameter. Additionally, it was observed that increasing the number of bolts from four to six, increased the stiffness of the connections, which is highlighted in Figures 5.5 and 5.6 where the slope of the connection time-rotation relationship curves for the six-bolt connections during failure at elevated temperatures is reduced when compared to the assemblies connected with four bolts in two rows.

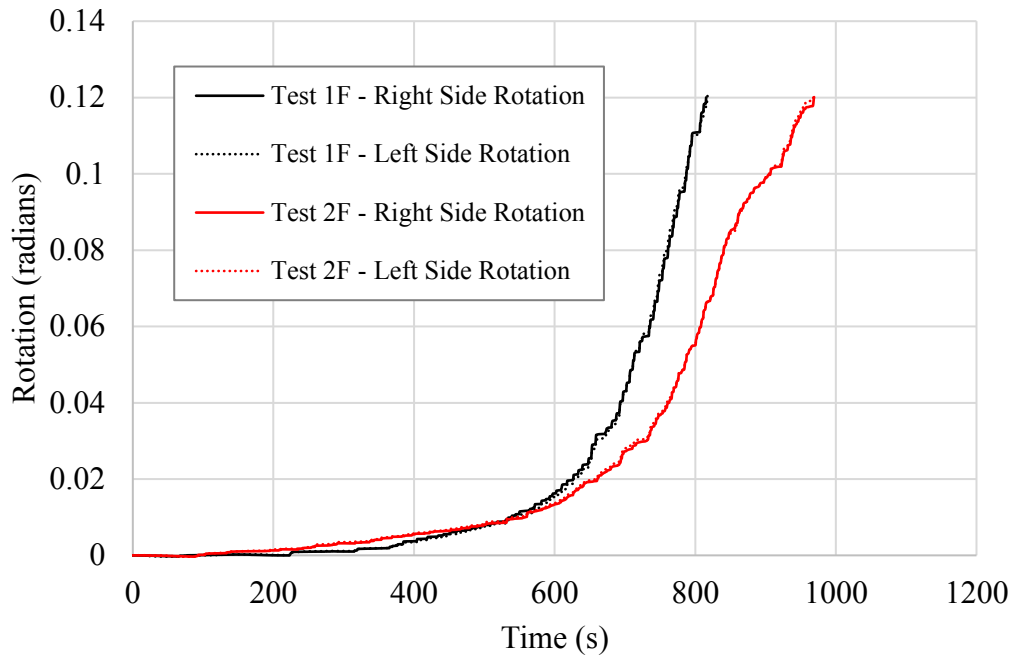


Figure 5.5 Time-rotation relationships developed to illustrate the effect of changing the number of bolts in fire resistance Tests 1F and 2F, both with four-times bolt end distance.

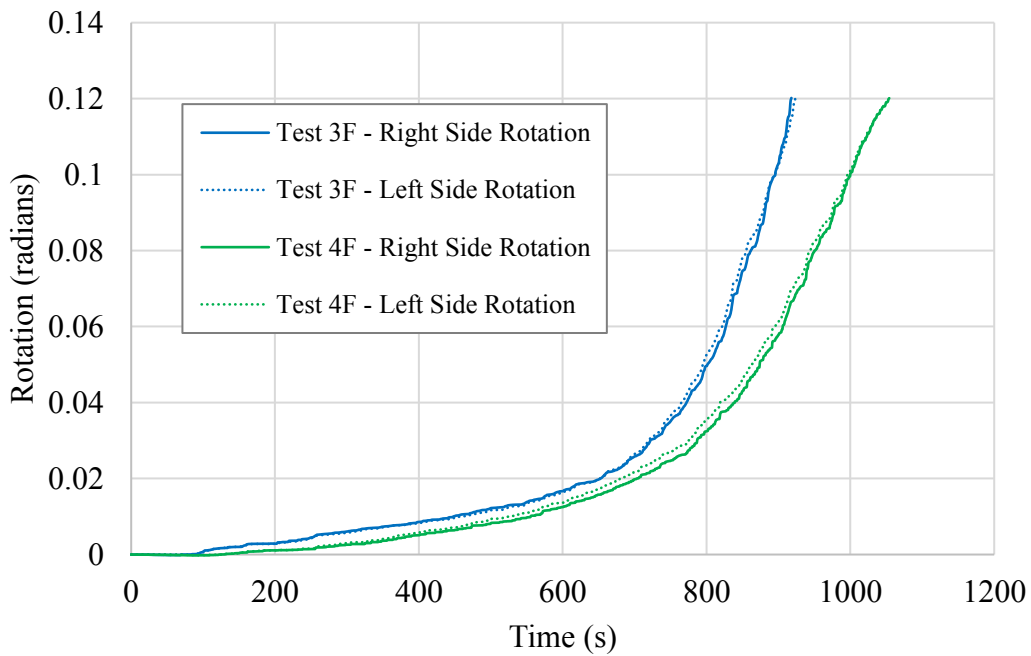


Figure 5.6 Time-rotation relationships developed to illustrate the effect of changing the number of bolts in fire resistance Tests 3F and 4F, both with five-times bolt end distance

For the STS-strengthened connections, Figure 5.7 and 5.8 showcase the effect of increasing the number of bolts from four in two rows to six bolts in three rows on the rotation and fire resistance of the connections featuring four and five-times bolt diameter end distance, respectively. For connections with four-times bolt diameter end distance, changing the number of bolts from four to six increased the fire resistance by about 72 seconds; while for the five-times bolt diameter end distance connections, introducing two additional bolts increased the fire resistance by about 155 seconds. The marginal increase in the fire performance of the different beam-to-column assemblies due to increased number of bolts was more pronounced in the connection with an end distance of five-times bolt diameter when compared to the results of those with an end distance of four-times bolt diameter. Furthermore, it was observed that the connections having six bolts instead of four were stiffer, as highlighted in Figures 5.7 and 5.8, where the slope of the connection’s time-rotation curves for the six-bolt connections during failure at elevated temperatures is reduced when compared to the assemblies connected with four bolts in two rows.

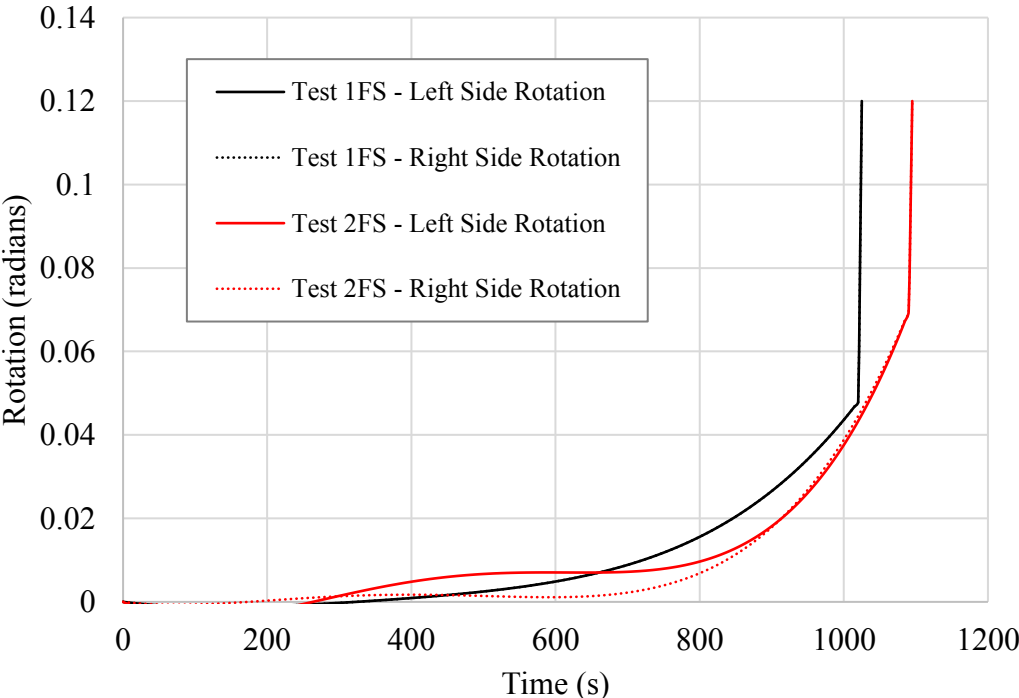


Figure 5.7 Time-rotation relationships developed to illustrate the effect of changing the number of bolts in fire resistance Tests 1FS and 2FS, both with four-times bolt end distance.

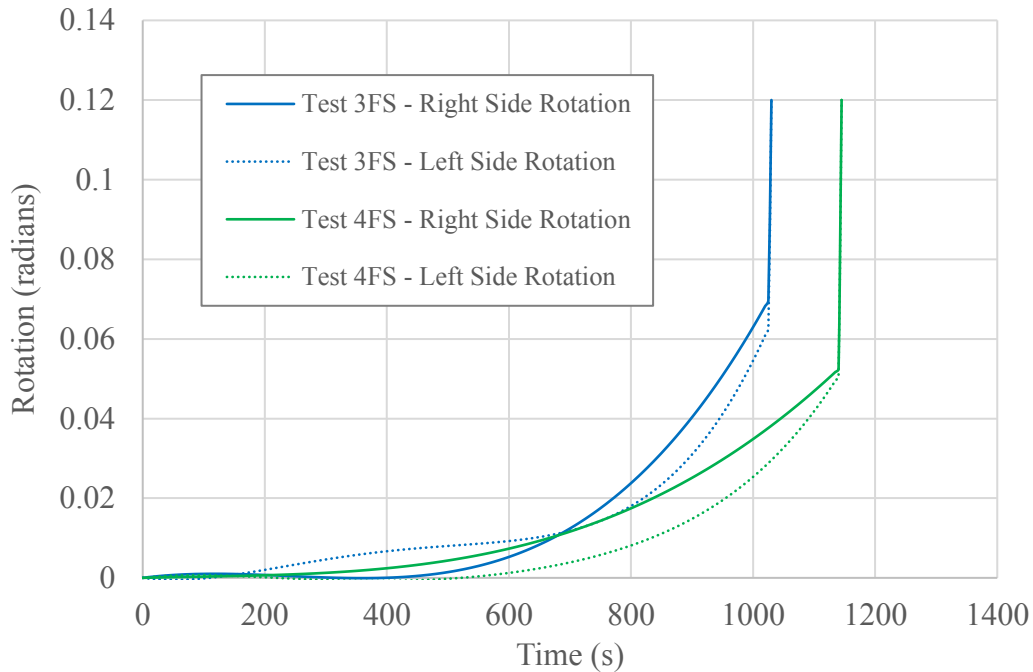


Figure 5.8 Time-rotation relationships developed to illustrate the effect of changing the number of bolts in fire resistance Tests 3FS and 4FS, both with five-times bolt end distance.

5.3 Effect of STS Strengthening

Figures 5.9 through 5.12 illustrate the effect of self-tapping screws (STS) strengthening on the behaviour of concealed beam-to-column connections. For all four connection configurations, the introduction of perpendicular-to-the-grain strengthening increased the connection's fire resistance by a greater increment than that observed by increasing the bolt's end distance or number of bolts in both strengthened and unstrengthened connections. As shown in Figure 5.9, the increment was most pronounced in connections with four-times bolt diameter end distance and four bolts in two rows, gaining an additional 200 seconds in fire resistance. Reinforcing the six-bolt connection with four-times bolt diameter end distance increased the connection's fire resistance by an increment of about 104 seconds, Figure 5.10. As highlighted in Figures 5.11 and 5.12, reinforcing four or six-bolt connections with a five-times bolt diameter end distance increased their fire resistance by about 96 and 115 seconds, respectively. In all four test groups, the connections with perpendicular-to-the-grain strengthening experienced a reduced rate of linear

rotation and a significant delay in time until the exponential rotation trend was observed over the failure time.

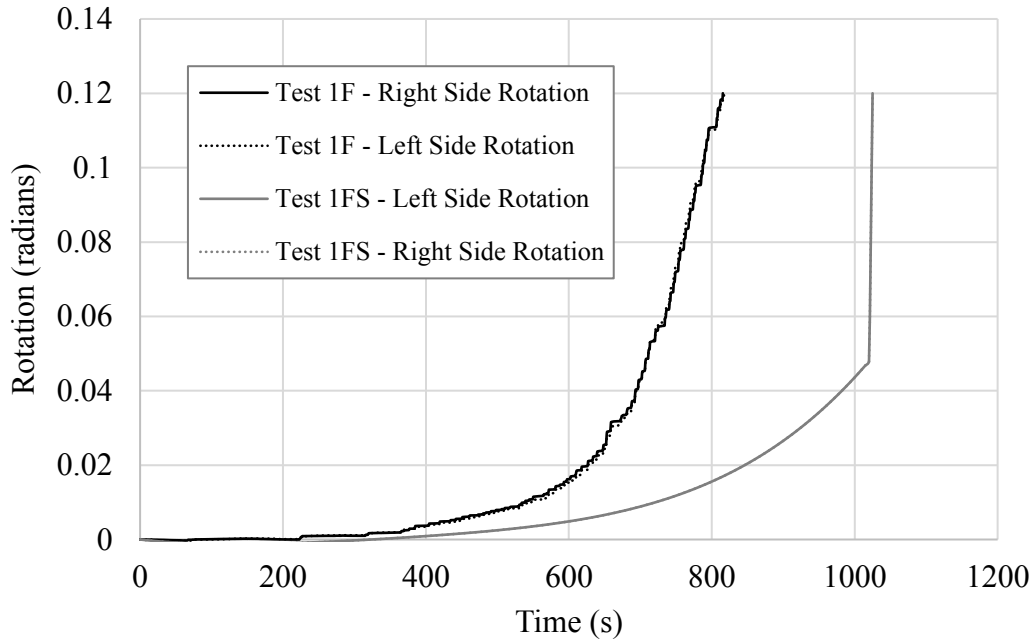


Figure 5.9 Time-rotation relationship showing the effect of perpendicular STS strengthening on the rotational resistance of connections with four bolts and four-times bolt end distance.

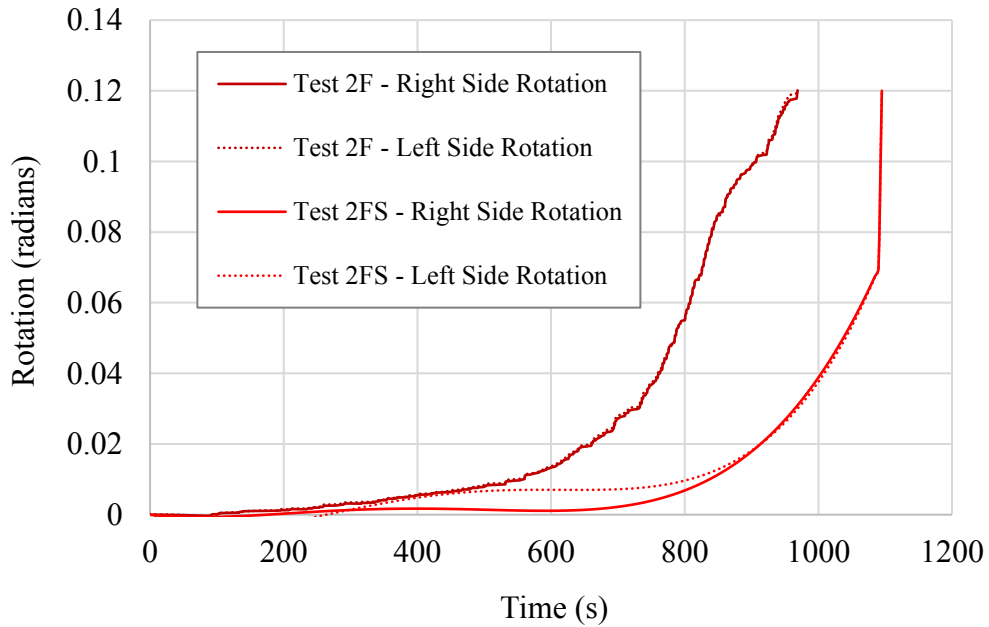


Figure 5.10 Time-rotation relationship showing the effect of perpendicular STS strengthening on the rotational resistance of connections with six bolts and four-times bolt end distance.

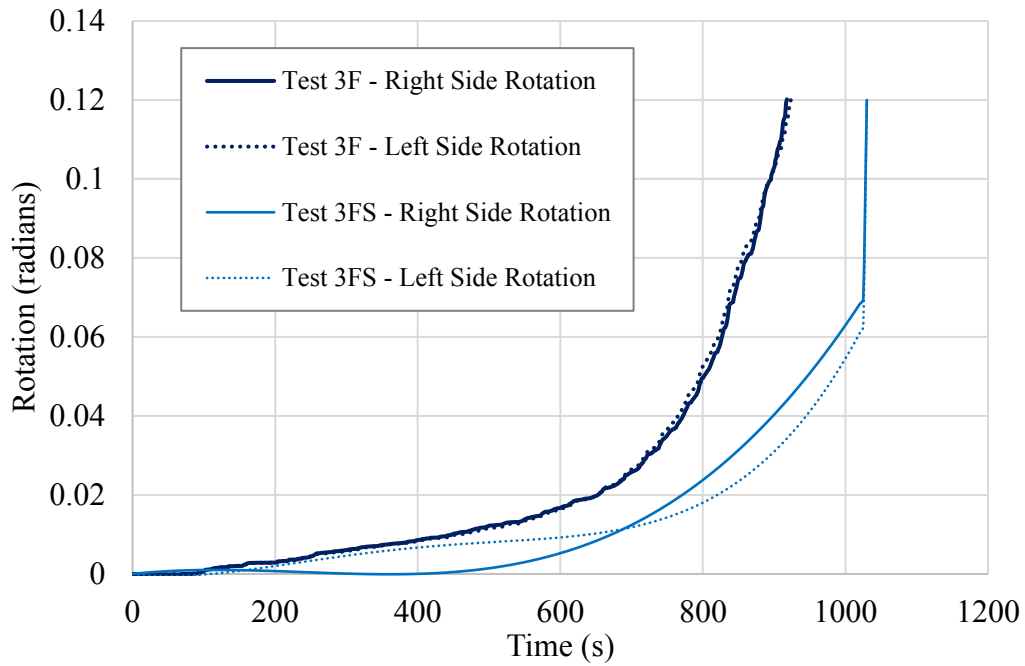


Figure 5.11 Time-rotation relationships showing the effect of perpendicular STS strengthening on the rotational resistance of connections with four bolts and five-times bolt end distance.

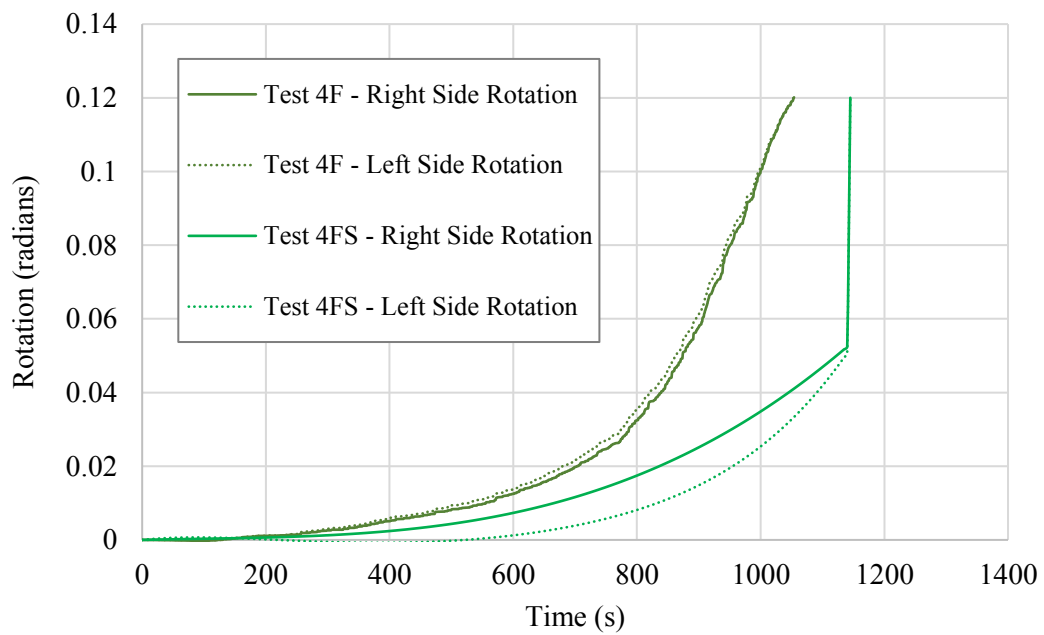
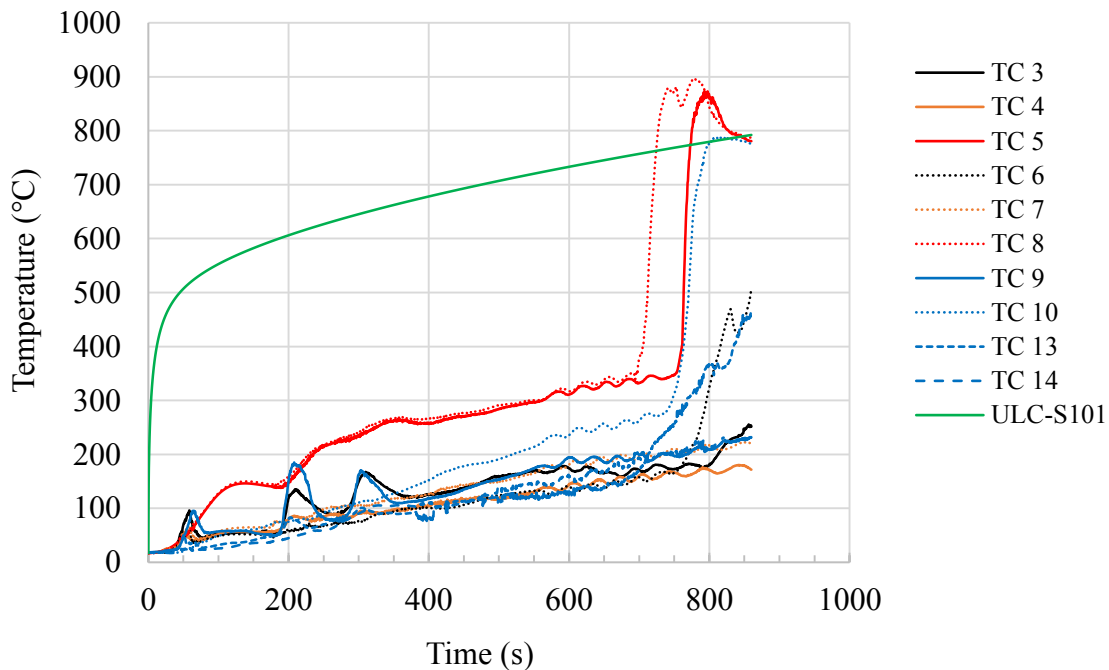


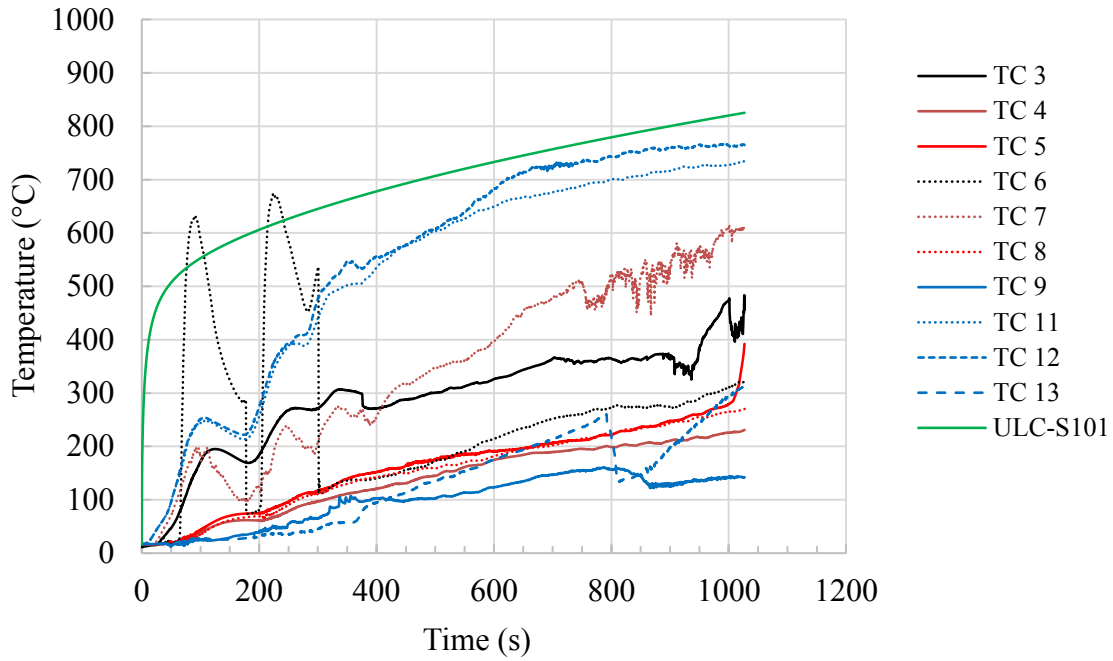
Figure 5.12 Time-rotation relationships showing the effect of perpendicular STS strengthening on the rotational resistance of connections with six bolts and five-times bolt end distance.

5.4 Time-temperature Curves

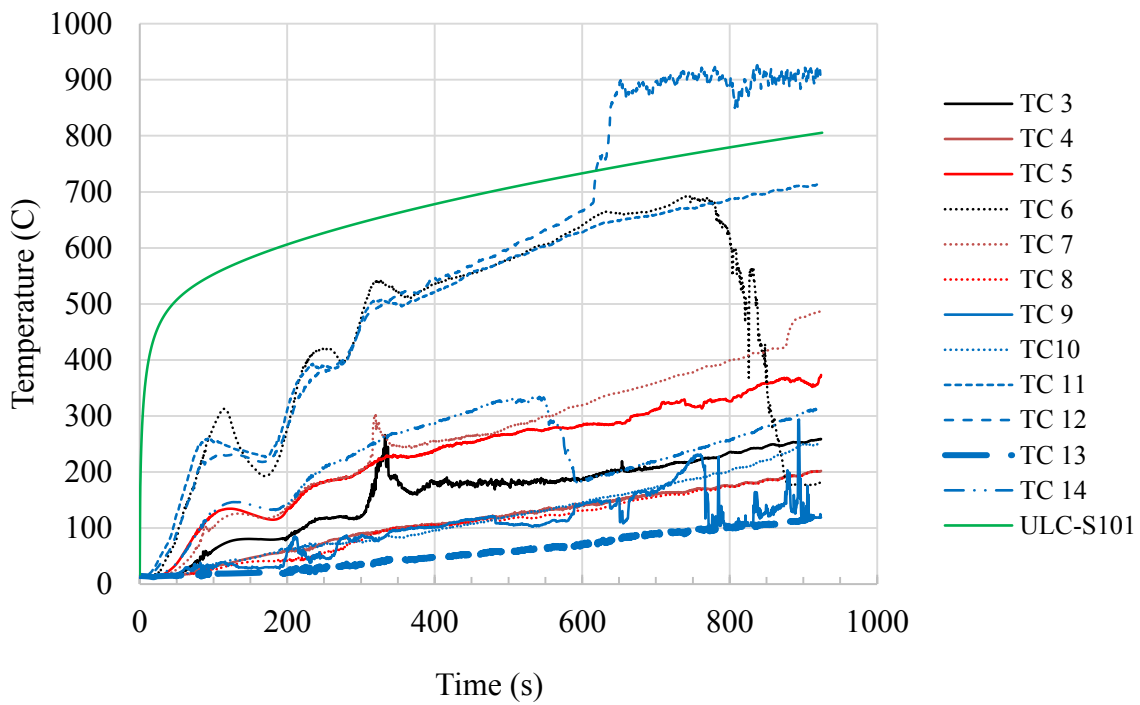
Represented in Figures 5.13 (a) through (d) are the time-temperature curves of Tests 1F through 4F, respectively. Generally, it was noticed that the internal temperatures of the wood sections and the temperatures of the steel components were much lower than the environment temperature inside the fire testing furnace. It was also observed that rapid rotations began to occur in the connections when the temperatures inside the middle of the wood section resisting row shear-out in the bottom row reached about 200°C, a state where the wood mechanical properties started to deteriorate rapidly prior to charring. The time-temperature curves developed in all four fire resistance tests were found to be in good agreement with each other. A hydrothermal relationship was observed to occur on the concealed steel plates in all four tests as shown by the relatively straight curves at about 100°C for TCs 9, 10, 13 and 14 before continuing to follow an upward trend.



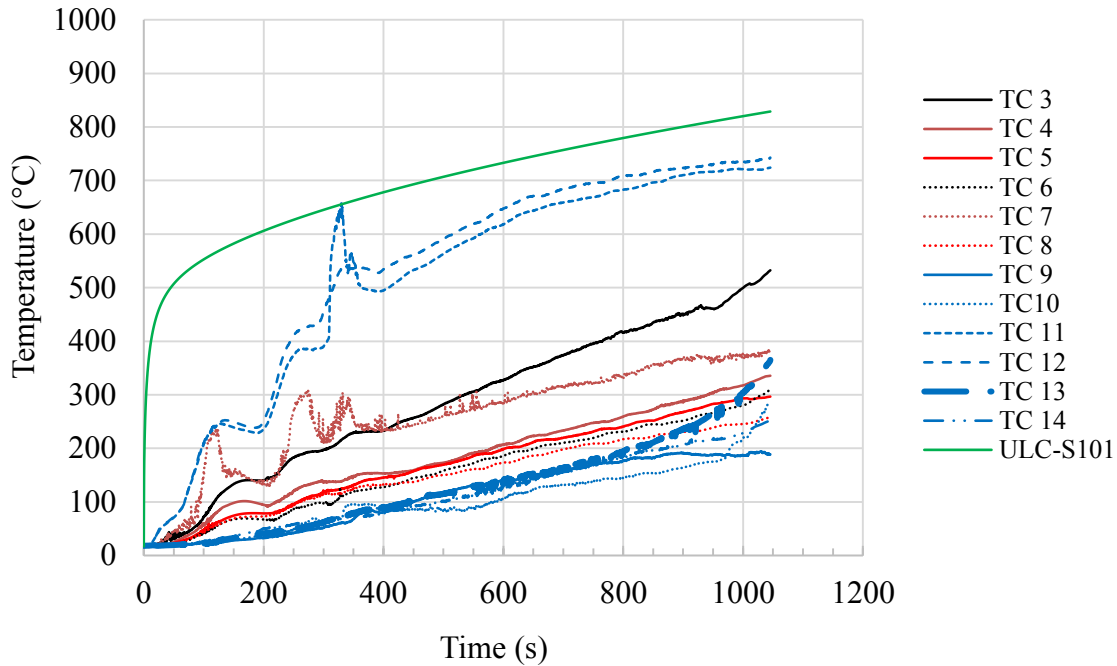
(a) Test 1F (four-bolt connection with four-times bolt diameter end distance).



(b) Test 2F (six-bolt connection with four-times bolt diameter end distance).



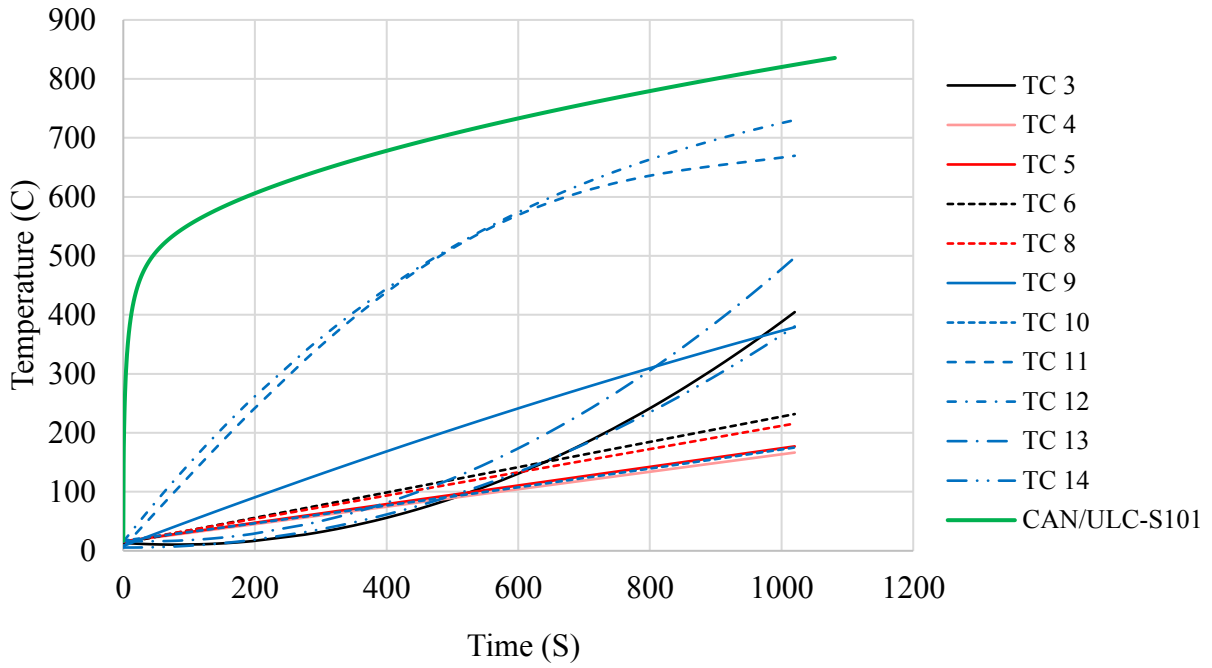
(c) Test 3F (four-bolt connection with five-times bolt diameter end distance).



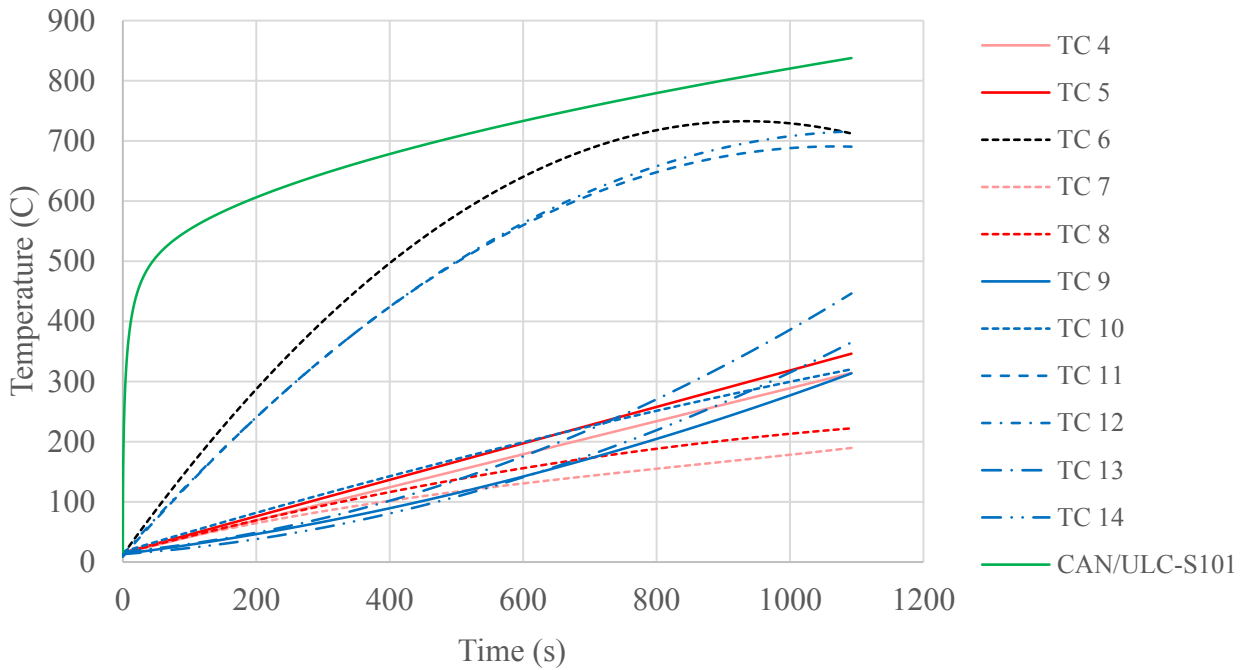
(d) Test 4F (six-bolt connection with five-times bolt diameter end distance).

Figure 5.13 Actual time-temperature curves of all thermal measurements taken in fire resistance Tests 1F through 4F.

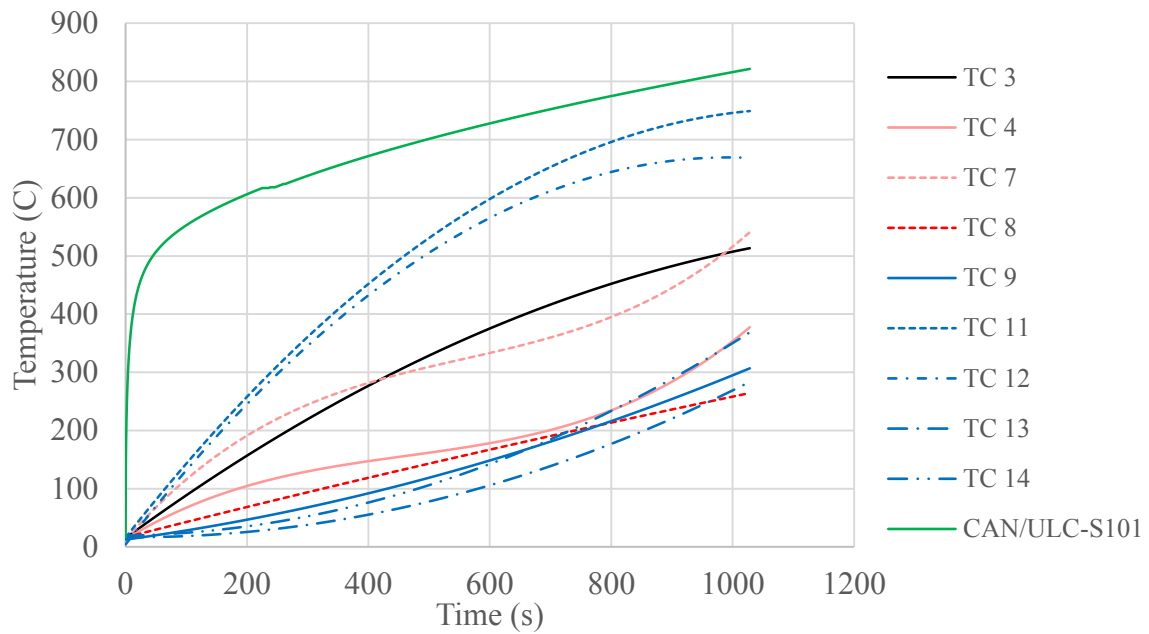
Figures 5.14 (a) through (d) illustrate the time-temperature curves for Tests 1FS to 4FS, respectively. Overall, it was noticed that the internal temperatures of the wood sections and the temperatures of the concealed steel components were much lower than the environment temperature inside the furnace. Based on the collected thermal data, it was observed that rapid rotations began to occur in the beam-to-column connections when the temperatures of the wood section midway between the char and steel plate located in the lower bolts row resisting shear out reached approximately 200°C. At this temperature, wood mechanical properties begin to deteriorate rapidly prior to complete charring. All four time-temperature curves were found to be in good agreement with each other. In addition, a hydrothermal relationship was observed to occur on the concealed steel plates in all four tests.



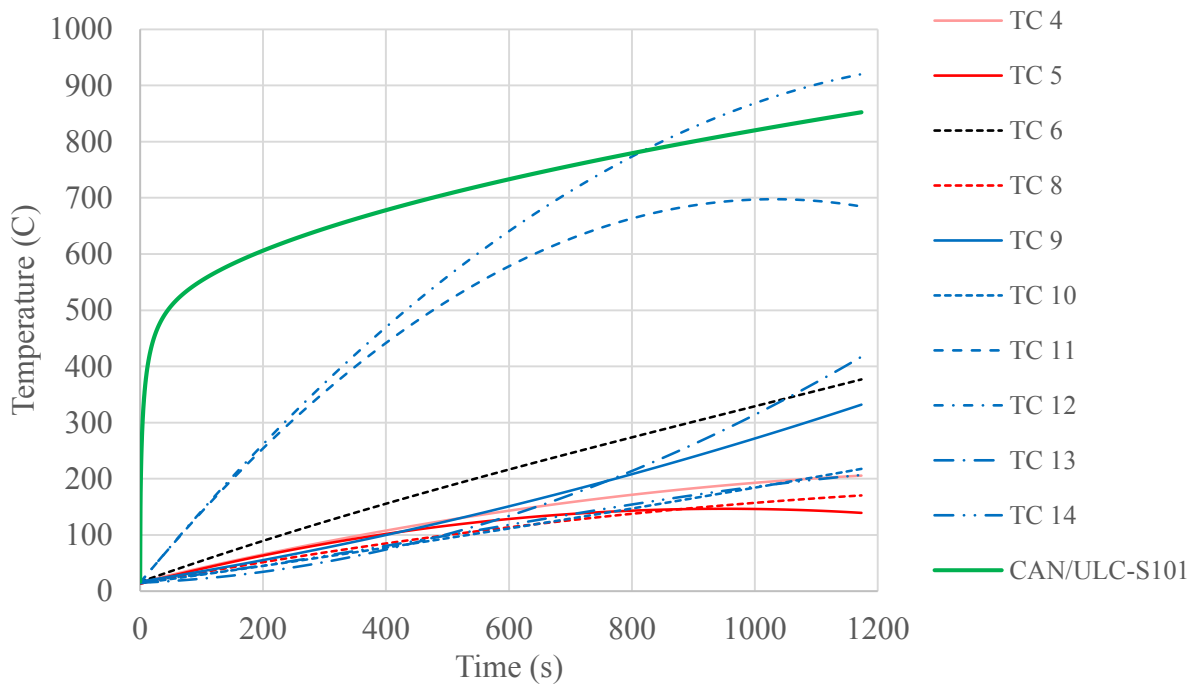
(a) Test 1FS (four-bolt strengthened connection with four-times bolt diameter end distance).



(b) Test 2FS (six-bolt strengthened connection with four-times bolt diameter end distance).



(c) Test 3FS (four-bolt strengthened connection with five-times bolt diameter end distance).



(d) Test 4FS (six-bolt strengthened connection with five-times bolt diameter end distance).

Figure 5.14 Actual time-temperature curves of all thermal measurements taken from test assemblies 1FS through 4FS.

Figure 5.15 shows the hydrostatic behaviour captured by thermocouples attached to the concealed steel plates. This thermal behaviour is characterized by the condensation of water on the concealed steel plates, where water continues to condense and insulate the steel until the temperatures are high enough for this process to stop. Water condenses on the steel plate as it is evaporating from the wood due to the heat of the fire applied to the external surfaces of the glulam members.

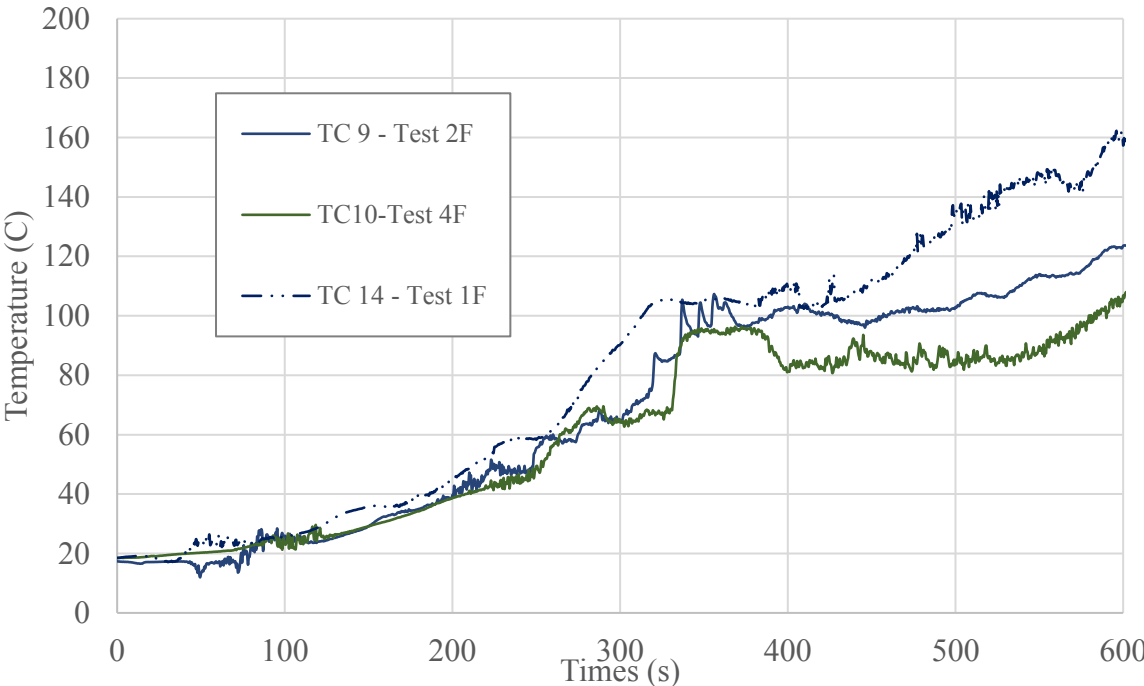


Figure 5.15 Hydrostatic behaviour on steel concealed plates.

5.5 Observed Failure Modes

For both unstrengthened and strengthened beam-to-column connections, brittle failure modes such as, row shear-out and splitting, as well as hole elongation were observed all test assemblies at the bottom bolts' row.

5.5.1 Unstrengthened Connections

For unstrengthened connections, Figure 5.16, shows the glulam beams of Test 1F with four bolts and four-times bolt diameter end distance. The same figure highlights the hole elongation mostly presented in the bolt holes at the lower row exposed to tensile stresses. This suggests that the rapid increase in the connection rotations preceding failure from fire exposure was mainly caused by the high temperatures transferred in the steel bolts, and thus caused excessive charring of the wood around the bolt holes that led to hole elongation in a direction opposite to the tensile force direction at the connection bottom side and a rapid loss in the connection stiffness. Most interestingly, the inside of the slotted cuts was found to be thermally degraded but with no noticeable char layer formed nearby the concealed steel plates.



Figure 5.16 Glulam beam sections with the char layer removed, Test 1F

In addition, the wood around the connections was found to have very little residual strength with several connections snapping apart by hand while removing them from the furnace and during cleaning after the fire resistance tests. The unstrengthened connections experienced similar failure

modes at elevated temperatures as the comparable connections did at normal temperatures, as highlighted in Figure 5.17.



Figure 5.17 Row shear-out and splitting failure modes experienced in Test 1 and Test 1F assemblies at ambient and elevated temperatures, respectively

Moreover, the concealed steel connectors experienced minor thermal damage and minimum yielding in all four fire resistance tests; however, a few steel bolts experienced some thermal deformation and yielding in all test assemblies. The yielding of the connection steel components can be assumed to have occurred when the steel began to reach temperatures above 400°C to 500°C, which coincided with a rapid increase in the connection rotations in the fire resistance tests. For all connections, failure was first observed to occur along the line of the bottom row of bolts. Failure along this row resulted in splitting or shear pull-out of the wood between the end of the beam and the first bolt, then between the first bolt and second bolt in the row. This failure typically continued to propagate past the bolt farthest from the end of the beam as a split in the wood section propagated. This is a similar failure mode to that undergone by the comparable connections loaded to failure at ambient temperatures, as illustrated by the comparison in Figure 5.17. Also, it was noticed that hole elongation occurred around the bolts farthest from the column-beam interface where the wood did not undergo brittle failure in the form of splitting, row shear-out or crushing.

5.5.2 Strengthened Connections

Brittle failure modes such as, row shear-out and splitting, were not observed in the glulam beam section near the connections for all strengthened test assemblies. The primary modes of failure were extreme hole elongation or complete combustion of the wood section between the first column of bolts and the contact surface between the beam and column. Figure 5.18 shows one of the glulam beams of Test 1FS with four bolts and four-times bolts diameter end distance after being subjected to monotonic load and standard fire exposure.



Figure 5.18 Failure modes observed in STS-strengthened connection with four bolts and five-times bolt diameter end distance (hole elongation, reduced brittle failure modes and complete combustion of almost all wood between the face and the first column of bolts)

In the strengthened connections, almost no brittle failure modes, such as splitting, cracking or row shear out, were observed; however, hole elongation was substantially more pronounced as highlighted in Figure 5.19 for Test 2FS.



Figure 5.19 Failure modes observed in STS-strengthened connection with six bolts and four-times bolt diameter end distance (increased hole elongation and reduced brittle failure modes)

The strengthening provided by STS substantially reduced the formation of brittle failure modes at elevated temperatures, and was observed to promote a more ductile failure mode as evidenced by the increase in hole elongation of the strengthened connections. The inside of the slotted cuts was found to be thermally degraded, but no noticeable char layer had formed where the wood contacted the concealed steel plates. Figure 5.20 shows Test 4FS beam-to-column assembly which underwent the longest fire exposure time of all tested assemblies. However, some thermal degradation had occurred in that connection along the wood inside the slotted cut due to the prolonged contact with the heated steel plate. As seen by the cut on the right side of Figure 5.20, there is a minimal amount of browning on the inside of the wood side members cross section, when compared to the thermally degraded layer presented beneath the removed char on the outside of the wood member that was directly exposed to fire.



Figure 5.20 Thermally degraded cross section of the concealed slot cut of the strengthened connection with six bolts and five-times bolt diameter end distance,

The wood was found to have very little residual strength around the connection's bolts with several connections snapping apart by hand while removing them from the furnace and during cleaning after the fire resistance tests. Most interestingly, in all strengthened connections the wood between the first strengthening screw and beam end and along the bottom row resisting row shear from tension forces was completely charred with the STS screw exposed or embedded and holding together charred material. This caused some of the strengthening screws closest to the beam face at the column to be exposed to fire near the end of the test, and were found to have undergone some thermal degradation after failure occurred. Strengthened connections, which primarily failed due to hole elongation in the wood and yielding in the steel components, were able to sustain greater loads as the strengthening screws stopped brittle failure modes from occurring in the wood and even kept wood that had been charred. This is highlighted in Figures 5.21 (a) through (d), showing the observed failure modes in strengthened connections with the char layer removed for Tests 1FS through 4FS, respectively. For connections with a reduced end distance, with both four and six bolts, it was found that the entire wood section between the column and the first column of bolts had been consumed in the fire, highlighted in Figures 5.21 (a) and (b). For connections

with five-times bolt diameter end distance, both four and six bolt connections had some or most of the wood present, as shown in Figures 5.21 (c) and (d). Connections with six bolts also experienced more extreme hole elongation in the connection as highlighted by Figures 5.21 (b) and (d).



(a) Charred layer removed from Test 1FS assembly (four-bolt strengthened connections with four-times bolt diameter end distance).



(b) Charred layer removed from Test 2FS assembly (six-bolt strengthened connections with four-times bolt diameter end distance).



(c) Charred layer removed from Test 3FS assembly (four-bolt strengthened connections with five-times bolt diameter end distance).



(d) Charred layer removed from Test 4FS assembly (six-bolt strengthened connections with five-times bolt diameter end distance).

Figure 5.21 Strengthened connection test assemblies with charred layer removed.

5.6 Charring Rate

The charring rates of the different glulam beam-to-column test assemblies have been summarized below in Table 5.2. Due to the relatively short fire resistance test durations, the charring rates for the samples were higher than the published values of 0.64 mm/min, which are determined from tests lasting longer than thirty minutes. However, it was shown that the charring rate was reduced for the strengthened connections, as the STS strengthening prevented the formation of splits or cracks which can significantly increase the charring rate and number of surfaces on which the charring is occurring. It was also found that the concealed connections only experienced charring on the sides directly exposed to the fire; however, significant corner rounding occurred in all tests at the wood section between the first column of bolts and end of the beam section. Charring rates for the connections were determined based on the residual cross section left between the two columns of bolts. The charring rates were taken from the reduction in width of the cross section, as this was the controlling area of wood with respect to row shear resistance of the connection. Generally, the trends in Table 5.2 show that increasing the bolt's end distance resulted in a minor decrease in the charring rate for all cases, and the presence of STS strengthening reduced the charring rate by even greater increments.

Table 5.2 Charring rates of all tested connections.

Test No.	End Distance	No. of Bolts	STS Strengthening	Fire Resistance (minutes)	Average Char Depth (mm)	Charring Rate (mm/min)
1F	4D	4	No	13.72	17.0	1.23
1FS	4D	4	Yes	17.00	17.0	1.0
2F	4D	6	No	16.47	19.0	1.15
2FS	4D	6	Yes	18.20	17.0	0.93
3F	5D	4	No	15.40	19.0	1.23
3FS	5D	4	Yes	17.00	19.0	1.12
4F	5D	6	No	17.63	22.0	1.25
4FS	5D	6	Yes	19.55	22.0	1.12

Chapter 6 Conclusions and Recommendations for Future Work

In order to address the growing interest in using glulam and other mass timber products as the primary building material for medium and tall buildings, a greater understanding needs to be acquired for the design of moment-resisting connections at both ambient and elevated temperatures. This thesis purposefully focused on experimentally examining the current minimum code specifications for wood connections to design a moment-resisting connection that was designed to fail mainly in brittle row shear. The number of bolts, bolt's end distance and STS strengthening were three variables that were examined for their impact on the failure modes and moment-resisting capacity and strength of the glulam beam-to-column connection at both ambient and elevated temperatures. The experimental data gathered and the analyses performed afterwards led to a number of relevant conclusions and recommendations that can be adopted to further enhance the design of mass timber moment-resisting connections.

6.1 At Ambient Temperature

For connections tested at ambient temperature, the outcomes of using either the code specified four or five-times bolt diameter bolt's end distance, increasing the number of bolts from four to six and the addition of perpendicular-to-the-grain STS strengthening on the strength and behaviour of the glulam beam-to-column connections have driven the following conclusions;

1. Increasing the number of bolts in the strengthened connections increased the moment-resisting capacity of the connection with both four and five-times bolt diameter end distances, as the connections saw the moment capacity increase by a factor of about 1.15;
2. The moment-resisting capacity increase was more pronounced in unstrengthened connections which saw increases in capacity by a factor of 1.35 and 1.5 for connections with four and five-times bolt diameter end distances, respectively;
3. In the unstrengthened connections, increasing the end distance from four to five-times bolt diameter resulted in a marginal increase in the connection's moment-resisting capacity, with an increase factor of about 1.15 for connections that had four bolts and 1.25 for those with six bolts. In the connections with STS strengthening, increasing the end distance from four to five-times bolt diameter resulted in a noticeable increase in the connection's moment-

resisting capacity, with an increase factor of 1.5 regardless of whether the connection had four or six bolts;

4. All test assemblies experienced brittle failure modes in the wood sections, with minimal deformations in the connecting steel bolts, and almost no deformations in the steel T-stub connectors. Also, in the unstrengthened connections, the primary brittle failure was splitting through the wood resisting row shear. The brittle failure modes in the wood of the strengthened connections occurred once the STS strengthening had yielded, allowing the formation of row shear to occur;
5. STS strengthening of the connections was found to greatly increase the moment-resisting capacity of all connections and reduce premature splitting or row shear failure. The effect was less pronounced in the six-bolt connections, which experienced a relatively lower increase than the connections with four-times bolt diameter end distances, a factor of 1.3 to 1.5 compared to a factor of 2.0 to 2.4, respectively;
6. The glulam beam-to-column connection's moment-resisting capacity was primarily governed by the glulam resisting the row shear by the stresses developed at the wood-bolt interface;
7. All connections exhibited some degree of brittle failure modes in the wood and sudden reductions in their moment-resisting capacities; however, the STS-strengthened connections featuring six bolts in three rows were observed to be following a mixed failure mode, with yielding occurring in the STS strengthening first followed by row shear in the glulam section. However, in the unstrengthened connections, six bolt connections with the increased end distance of five-times bolt diameter end distance also exhibited a mixed failure mode before complete brittle failure occurred in the wood section.

6.2 At Elevated Temperatures

In general, increasing the number of bolts increased the beam-to-column fire resistance by a greater increment than that observed when increasing the bolt's end distance from four to five-times bolt diameter. Also, reinforcing the connections resulted in an increased fire resistance and a reduction in the brittle failure modes. Based on the above observed experimental outcomes and

the analyses of the fire resistance tests' outcomes conducted afterwards, the following conclusions have been developed;

1. Increasing the number of bolts from four bolts in two rows to six bolts in three rows increased the fire resistance of the glulam beam-to-column connections by a greater increment than that observed by increasing the bolt's end distance from four to five-times bolt diameter. This was valid for both unstrengthened and strengthened connections;
2. The incremental increase in the connection's fire resistance from a greater bolt's end distance was marginally more effective in the connections with two rows of bolts in comparison to those using three rows of steel bolts. Comparatively, it was observed that in the strengthened connections the incremental increase in the fire resistance from a greater bolt's end distance was marginally more effective in the connections with three rows of bolts in comparison to the connections using two rows of bolts;
3. All test assemblies experienced substantial brittle failure modes, with some deformations in the connecting steel bolts. Also, in cases of more pronounced brittle failure modes, the wood stress block resisting row shear-out was charred completely through;
4. The glulam beam-to-column connection's fire resistance was primarily governed by the shear resistance of the wood section resisting row pull-out driven by the force applied by the steel bolts through side bearing;
5. The primary concern for this wood-steel-wood connection configuration at elevated temperatures was shown to be the reduction in the cross-sectional area of the wood resisting row shear-out;
6. Perpendicular-to-the-grain strengthening using STS substantially improved the fire resistance of all connections. This also reduced the formation of brittle failure modes, such as row shear out, splitting and cracking and promoted the formation of ductile failure modes, such as yielding in the steel connecting components or hole elongation;
7. The wood side sections in contact with the concealed steel plate did not undergo charring, where the wood in these regions was browned but not charred;

8. The strengthened glulam beam-to-column connection's fire resistance was primarily governed by temperature of the steel connectors, self-tapping strengthening screws and the shear resistance of the wood sections strengthened with STS;
9. The strengthened connections with four-times bolt diameter end distance saw all the wood between the first column of bolts and the column consumed in the fire. However, increasing the bolt's end distance, ensured that there was still a residual wood cross section for the STS strengthening to bind to, and increased the performance of the connections.

6.3 Recommendations for Future Work

Utilizing the experimental and analytical outcomes of this thesis, it is recommended that for the application of glulam moment-resisting connections, a greater end distance than the minimum specified in CSA 086-14 standard is required to prevent or at least minimize the brittle failure modes. It is also recommended that a larger bolt's end distance, such as seven-times bolt diameter end distance that was adapted in the previous versions of CSA 086-14 standard to be adopted as the minimum of both end distance and spacing between columns of bolts to reduce the formation of splitting and other brittle failure modes before the connection's capacity is fully developed. It is also advised that installing strengthening screws can reduce the formation of brittle failure modes, and strengthen the wood around any knots or other deformities that reduce the capacity of the connection, this is particularly important when using either four or five-times bolt diameter end distance, which saw premature splitting occur in the unstrengthened connections before full row shear was developed.

According to this thesis' experimental outcomes it was shown that perpendicular-to-the-grain strengthening with self-tapping screws (STS) is a relatively simple and cost-effective method to eliminate splitting in wood and to develop a ductile failure mode before brittle row shear failure. This strengthening can be applied to both axially-loaded connections and those resisting an applied moment. STS strengthening could also be used to retrofit existing wood structures to provide a source of increased moment-resisting capacity, strengthen the wood if any splitting has occurred over the buildings service life or allow for a potential increase in loading. Additionally, the STS strengthening added ductility and energy dissipation to the wood-steel-wood connections that suggests these connections could be successfully utilized in the construction of tall wood buildings;

where moment resistance is crucial in sustaining lateral design loads, such as wind and earthquakes forces, in case of lateral bracing system is lacking, for example.

Future research work should be expanded to investigate the following variables;

1. Using a bolt's end distance of seven-times bolt diameter, as per Eurocode 5 and the previous versions of CSA-086-14 standard;
2. The introduction of additional column(s) of bolts with greater spacing between them to eliminate brittle failure in the wood;
3. T-stub connectors that can be attached to the glulam beam without having cylindrical notches cut into the beam sections;
4. Applying reduced design loads until a fire resistance rating of 45 minutes is achieved without failure in the wood section;
5. Testing other strengthening techniques to eliminate or at least minimize brittle failure modes in the wood sections at elevated temperatures;
6. The effect of defects in the wood, e.g., glue lines between lamina and finger joints, on the moment-resisting capacity of the concealed glulam beam-to-column connections;
7. Utilizing the experimental outcomes of this thesis' research project to validate newly-developed computer models to simulate the structural behaviour of such wood-steel-wood bolted glulam concealed connections under the effect of other parameters.

References

- Andreolli, M., Piazza, M., Tomasi, R. and Zandonini, R. (2011). Ductile moment-resistant steel-timber connections. *Proceedings of the Institution of Civil Engineers-Structures and Buildings*, 164(2): 65-78.
- Audebert, M., Dhima, D., Taazount, M., and Bouchaïr, A. (2012). Behavior of dowelled and bolted steel to-timber connections exposed to fire. *Engineering Structures*, 39: 116-125.
- Audebert, M., Dhima, D., Taazount, M., and Bouchaïr, A. (2014). Experimental and numerical analysis of timber connections in tension perpendicular to grain in fire. *Fire Safety Journal*, 63: 125-137.
- Bailey, C. G. (2006). Advances in fire engineering design of steel structures. *Structures & Buildings*, 159(1): 21-35.
- Bisby, L., Gales, J., and Maluk, C. (2013). A contemporary review of large-scale non-standard structural fire testing. *Fire Science Reviews*, 2(1): 1-27.
- Bustos, C., Beauregard, R., Mohammad, M., and Hernandez, R. E. (2003). Structural performance of finger-jointed black spruce lumber with different joint configurations. *Forest products journal*, 53(9): 72.
- Canadian Commission on Building and Fire Codes (2015). National Building Code of Canada, 14th Edition, Canadian Commission on Building and Fire Codes, National Research Council of Canada, Ottawa, Ontario, Canada.
- Canadian Wood Council (2015). Wood Design Manual. Nepean, Canada.
- CCMC (2014). Evaluation Report: SWG ASSY VG Plus and SWG ASSY 3.0 Self-Tapping Wood Screws. Canadian Construction Materials Centre Report No. CCMC 13677-R.
- CCMC (2014). Evaluation Report: Nordic Lam. Canadian Construction Materials Centre Report No. CCMC 13216-R.
- CSA (Canadian Standards Association) (2014). *Engineering design in wood*. CSA O86-14, Toronto.
- European Committee for Standardization and British Standards Institution (1995). *Eurocode 5: Design of timber structure*. Brussels: BSI.
- Frangi, A., Fontana, M., and Mischler, A. (2004). Shear behaviour of bond lines in glued laminated timber beams at high temperatures. *Wood science and technology*, 38(2): 119-126.

- Fryer, Janet L. (2014). *Picea mariana*. In: Fire Effects Information System, [Online]. U.S. Department of Agriculture, Forest Service, Rocky Mountain Research Station, Fire Sciences Laboratory (Producer). Available: <http://www.fs.fed.us/database/feis/> [2016, April 25]
- Gattesco, N., and Toffolo, I. (2004). Experimental study on multiple-bolt steel-to-timber tension joints. *Materials and structures*, 37(2): 129-138.
- Gehloff, M., Cloßen, M., and Lam, F. (2010). Reduced edge distances in bolted timber moment connections with perpendicular to grain strengthenings. In *Proceeding of the World Conference on Timber Engineering (Vol. 230)*.
- Hampson, J. A., Prion, H. G., and Lam, F. (2003). The effect of end distance on the moment resistance of timber rivet connections. *Canadian Journal of Civil Engineering*, 30(5): 945-948.
- Hadjisophocleous, G. V., and Benichou, N. (1999). Performance criteria used in fire safety design. *Automation In Construction*, 8(4): 489-501.
- Humbert J., Lee S.J., Park J.S., and Park M.J. (2014). Moment resistance of post-and-beam joints with concealed metallic connectors. In *Proceedings of the 13th World Conference on Timber Engineering, WCTE2014*, Quebec, Canada.
- Jessome, A.P. (2000). Strength and Related Properties of Woods Grown in Canada. Forintek Canada Corporation.
- J.Y. Richard, L. (2004). Performance Based Fire Safety Design of Structures - A Multi-dimensional Integration. *Advances In Structural Engineering*, 7(4): 311-333.
- Klippel, M., Frangi, A., and Hugi, E. (2013). Experimental Analysis of the Fire Behavior of Finger-Jointed Timber Members. *Journal of Structural Engineering*, 140(3).
- Lam, F., and N. Mohadevan. (2007). Development of New Construction of Glulam Beams in Canada. In *Proceedings of the International Council for Building Research and Innovation in Building and Construction: Working Commission W18-Timber Structures*, Bled, Slovenia. CIB-W18/40-12-1. pp10.
- Lam, F., Schulte-Wrede, M., Yao, C. C., and Gu, J. J. (2008). Moment resistance of bolted timber connections with perpendicular to grain strengthenings. In *10th World Conference of Timber Engineering WCTE2008*, Miyazaki, Japan.
- Lamont, S., Lane, B., Flint, G., and Usmani, A. (2006). Behavior of structures in fire and real design--a case study. *Journal of Fire Protection Engineering*, 16(1): 5-35.

- Les Chantiers Chibougamau Ltée. Black Spruce's Unique Fiber. (n.d.). Retrieved April 25, 2016, from <http://chibou.com/en/the-resource/black-spruce>
- LeVan, Susan L., and Winandy, J. E. (2007). Effects of fire retardant treatments on wood strength: a review. *Wood and Fiber Science* 22(1): 113-131.
- Martin, Z., and Tingley, D. A. (2000). Fire resistance of FRP strengthened glulam beams. In *World Conference on Timber Engineering, Whistler Resort, British Columbia, Canada*
- Mohammad, M., and Quenneville, J. H. (2001). Bolted wood steel and wood steel wood connections: verification of a new design approach. *Canadian journal of civil engineering*, 28(2), 254-263.
- Murty, B., Asiz, A., and Smith, I. (2008). Wood and engineered wood product connections using small steel tube fasteners: An experimental study. *Journal of the Institute of Wood Science*, 18(2), 59-67.
- Nordic Wood Structures Inc. (2015). Design Properties, Nordic Lam. Technical Note S01.
- Peng, L., Hadjisophocleous, G., Mehaffey, J., and Mohammad, M. (2010). Fire resistance performance of unprotected wood–wood–wood and wood–steel–wood connections: A literature review and new data correlations. *Fire Safety Journal*, 45(6): 392-399.
- Peng, L., Hadjisophocleous, G., Mehaffey, J., and Mohammad, M. (2011). Predicting the fire resistance of wood–steel–wood timber connections. *Fire technology*, 47(4):1101-1119
- Peng, L., Hadjisophocleous, G., Mehaffey, J., and Mohammad, M. (2012). Fire Performance of Timber Connections, Part 1: Fire Resistance Tests on Bolted Wood-Steel-Wood and Steel-Wood-Steel Connections. *Journal of Structural Fire Engineering*, 3(2), 107-132.
- Peng, L., Hadjisophocleous, G., Mehaffey, J., and Mohammad, M. (2012). Fire performance of timber connections, Part 2: thermal and structural modelling. *Journal of Structural Fire Engineering*, 3(2), 133-154.
- Pirvu, Ciprian, (2006). Final Report: Opportunities For Glued Wood Products. FPI Innovations. N.p., 2006. Web. 27 Mar. 2016.
- Racher, P., Laplanche, K., Dhima, D., and Bouchaïr, A. (2010). Thermo-mechanical analysis of the fire performance of dowelled timber connection. *Engineering Structures*, 32(4): 1148-1157.

- Rossi, S., Cairo, E., Krause, C., & Deslauriers, A. (2015). Growth and basic wood properties of black spruce along an alti-latitudinal gradient in Quebec, Canada. *Annals of forest science*, 72(1): 77-87.
- Scheibmair, F., & Quenneville, P. (2012). Moment Connection for Quick Assembly of Timber Portal Frame Buildings: Theory and Validation. *Journal of Structural Engineering*, 140(1).
- Song, X., Jiang, Y., Gu, X., & Wu, Y. (2017). Load-Carrying Capacity of Lengthwise Cracked Wood Beams Retrofitted by Self-Tapping Screws. *Journal of Structural Engineering*, 143(6).
- Spatacean, C. A. (2008). Propriétés Du Bois Et Qualité Des Sciages Dans Les Pessières Noires de Seconde Venue Issues de Coupe Et de Feu (Doctoral dissertation, Université Laval).
- Timusk, P. C. (1997). Experimental evaluation of the ULAG glulam beam simulation program (Doctoral dissertation, The University of Toronto).
- Tong, Q.J., Fleming, R.L., Tanguay, F., and Zhang, S.Y. (2009). Wood and lumber properties from unthinned and precommercially thinned black spruce plantations. *Wood Fiber Science* 41: 168–179
- Torquato, L. P., Auty, D., Hernández, R. E., Duchesne, I., Pothier, D., and Achim, A. (2013). Black spruce trees from fire-origin stands have higher wood mechanical properties than those from older, irregular stands. *Canadian Journal of Forest Research*, 44(2): 118-127.
- Weckendorf, J., Kiwelu, H.M., and Smith, I. (2015). Critical reaction forces of glulam members with tension-side notches at end supports. *Canadian Journal of Civil Engineering* 42(10): 779-786.
- Xiong, H., and Liu, Y. (2014). Experimental study of the lateral resistance of bolted Glulam Timber Post and Beam Structural systems. *Journal of Structural Engineering*, 142(4).
- Xu, B. H., Bouchaïr, A., and Racher, P. (2015). Mechanical behavior and modeling of dowelled steel-to-timber moment-resisting connections. *Journal of Structural Engineering*, 141(6).
- Yang, T. H., Wang, S. Y., Tsai, M. J., and Lin, C. Y. (2009). Temperature distribution within glued laminated timber during a standard fire exposure test. *Materials & Design*, 30(3), 518-525.
- Zarnani P., and Quenneville P. (2014). Design method for coupled-splice timber moment connections. In *Proceedings of the 13th World Conference on Timber Engineering*, WCTE2014, Quebec.